

Wisdom-volkano: A novel tool based on open GIS and time-series to analyse and share volcanic data



Fulgencio Sanmartín

2016
Department of
Physical Geography and Ecosystem Science
Centre for Geographical Information Systems
Lund University
Sölvegatan 12
S-223 62 Lund
Sweden



Fulgencio Sanmartín (2016). Wisdom-volkano: A novel tool based on open GIS and time-series to analyse and share volcanic data

Master degree thesis, 30/ credits in Master in Geographical Information Science

Department of Physical Geography and Ecosystem Science, Lund University

Wisdom-volkano: A novel tool based on open GIS and time-series to analyse and share volcanic data

Fulgencio Sanmartín
Master Thesis, 30 credits, in Geographical Information Science

Supervisors:

Dr Harry Lankreijer (Lund University)

Dr Nicolas d'Oreye (European Centre for Geodynamics and Seismology)

This page intentionally left blank.

Abstract

Active volcanoes threaten life around. In order to predict their eruptions earlier and mitigate their hazards, several variables must be observed and compared. Geographical information systems (GIS) combine different geospatial images from remote or local sensing. However, GIS often miss how maps change during the time. In this thesis Wisdom-volkano is presented, a web GIS based on open source standards that integrates time-series on data such as seismic events and ground deformation from interferograms and global navigation satellite system (GNSS). Based on the data from stations and remote sensing on two different volcanos, the implemented tool allows maps visualization and trend analysis over time, to help detecting changes and eventually leading to volcanic activity alert ahead of eruptions. Integrating the time dimension increases greatly the utility of a GIS, not only for monitoring volcanoes and prevent eventual losses caused by them, but also for detecting land use changes and other purposes with a big economic impact.

Résumé

Les volcans actifs menacent la vie aux environs. Pour prédire leurs éruptions plus en avance et atténuer les risques associés, plusieurs variables doivent être observées et comparées. Les systèmes d'information géographique (SIG) combinent différentes images géospatiales de détection locale ou à distance. Or, souvent ils leur manquent les changements au cours du temps. Dans cette thèse, Wisdom-volkano est présenté, un SIG web basé en standards open source qui intègre des séries chronologiques sur des données telles que des événements sismiques et la déformation du sol à partir des interférogrammes et des systèmes de navigation par satellite (GNSS). Sur base des données des stations et de télédétection sur deux volcans différents, l'outil mis en place permet la visualisation de cartes et l'analyse des tendances au fil du temps, pour détecter des changements et finalement alerter de l'activité volcanique avant les éruptions. L'intégration du temps comme une dimension permet d'augmenter considérablement l'utilité du SIG, pas seulement pour la surveillance des volcans et la prévention de pertes causées par leur activité, mais aussi pour la détection des changements d'utilisation des terres et autres fins avec un grand impact économique.

Keywords: Volcanic eruption, GIS, time-series, interferogram, seismology, GNSS.

This page intentionally left blank.

TABLE OF CONTENTS

TABLE OF CONTENTS	vii
LIST OF FIGURES	viii
LIST OF TABLES.....	ix
GLOSSARY	ix
CONVENTIONS AND LICENCE	xi
ACKNOWLEDGEMENTS.....	xi
1. INTRODUCTION	1
2. BACKGROUND	3
2.1. State of art of volcanic monitoring with GIS and time-series	3
2.2. State of art of web GIS and time-series development	4
2.2.1. Data repository and formats	5
2.2.2. GIS Server	6
2.2.3. Discovery layer, metadata	6
2.2.4. Client	7
2.2.5. Symbology	7
2.2.6. Time-series data and visualization tools.....	8
2.2.7. Wisdom-volkano initial application stack	8
2.3. Scope and study area	9
3. MATERIALS AND METHODS.....	11
3.1. Functional requirements and iterations	11
3.2. Data sources: interferograms and time-series.....	13
3.2.1. SAR products	13
3.2.2. SAR satellites	20
3.2.3. InSAR files.....	22
3.2.4. MSBAS time-series	24
3.3. Data sources: seismic events	26
3.3.1. Seismic stations	27
3.3.2. Seismic events localization.....	29
3.3.3. Seismic events counting time-series.....	30
3.4. Data sources: GNSS	31
3.4.1. GNSS receiver stations.....	31
3.4.2. GNSS data files	33
3.5. Functional analysis.....	33
3.6. Software architecture	37
3.6.1. Database and code source deliveries	38
3.6.2. Geospatial visualization with GeoServer and OpenLayers	40
3.6.3. Time-series visualization with Highcharts	42
3.6.3.1. MSBAS time-series ajax calls	43
3.6.3.2. Stations time-series.....	43
3.6.4. Detrending time-series	43
3.7. Coordinates	44
4. IMPLEMENTATION.....	47
4.1. Installation, security, back-end and front-end	47
4.2. Geospatial functional requirements and data	49
4.2.1. GeoServer workspaces, stores, layers and styles.....	49
4.2.2. Wisdom-volkano layers.....	51
4.3. Time-series FR and data.....	54
4.3.1. MSBAS time-series chart and favourites dataset	55
4.3.2. Histogram time-series chart.....	58
4.3.3. GNSS time-series chart	60
4.3.4. Detrending.....	60

4.4. Validation; test with new data	62
4.4.1. New InSAR and MSBAS data	62
4.4.2. New seismic data	64
4.4.3. New GNSS data	65
4.4.4. Validation summary	67
5. DISCUSSION	69
5.1. Web GIS and time-series	69
5.2. Limitations and opportunities	70
5.3. Recommendations for the future	70
6. CONCLUSIONS	73
REFERENCES	75
APPENDIX: Source codes	85
Series from Lund University	92

LIST OF FIGURES

Figure 1: Overview of relevant web GIS standards	5
Figure 2: High-level Wisdom-volkano software architecture	9
Figure 3: Map of lava flows around Nyiragongo and Nyamulagira volcanoes, and Goma City	10
Figure 4: SAR amplitude image from ENVISAT	14
Figure 5: (Left) InSAR geometry. (Right) How the fringes are created due to the baseline (Luzi 2010)	15
Figure 6: Example of differential interferogram wrapped on the shaded relief DEM of Nord-Kivu	16
Figure 7: Coherence of an ENVISAT InSAR	19
Figure 8: Unwrapping ground displacement coordinates	20
Figure 9: SAR on RADARSAT-1	22
Figure 10: Coordinate to pixel calculation	25
Figure 11: The 1906 San Francisco earthquake, detected in Gottingen (Germany), 9100 km away	27
Figure 12: Seismograph and GNSS stations network by ECGS/RMCA	29
Figure 13: GNSS localisation based on intersecting spheres	32
Figure 14: Mock-up of Wisdom-volkano	35
Figure 15: Simulation of the time-series calculation from the rasters stack	36
Figure 16: Flow diagram from a map point to displaying MSBAS time-series	37
Figure 17: Wisdom-volkano software architecture stack view	38
Figure 18: Entity - Relationship database diagram	39
Figure 19: GeoServer interfaces used in Wisdom-volkano	41
Figure 20: Overview of main screen of Wisdom-volkano	48
Figure 21: Colour ramp for complex interferograms, generated by the SLD and previewed in GeoServer	49
Figure 22: List of layers as shown in GeoServer	50
Figure 23: Create layer option in Wisdom-volkano	51
Figure 24: Option to reorder the loaded layers	52
Figure 25: Main screen of layers and map in Wisdom-volkano, with detail after selecting a point	53
Figure 26: Symbols for seismic localization events, generated by the SLD and previewed in GeoServer	54
Figure 27: Highcharts chart with only the events generated with Source code 11 and Source code 12	54
Figure 28: Options available when creating an MSBAS time-series	56
Figure 29: MSBAS time-series calculated from a raster stack of InSAR	57
Figure 30: Zoom detail on the MSBAS chart with detail information when hovering a point	57
Figure 31: Screen capture of the MSBAS time-series manage modal window	58
Figure 32: Favourite MSBAS points dataset	58
Figure 33: Screen capture from Wisdom-volkano on creating a time-series based on seismic stations	59
Figure 34: Seismic counting events of OVG station	59
Figure 35: Example of a GNSS time series as plotted in Wisdom-volkano	60
Figure 36: Detrend dialog for the GNSS chart in Figure 35	61
Figure 37: GNSS time-series from Figure 35, with the NS axis detrended	61

Figure 38: GNSS time-series from Figure 35, with the NS and EW axis detrended61
 Figure 39: List of detrended GNSS and MSBAS time-series62
 Figure 40: New complex interferogram (April 2011 - July 2012) wrapped on DEM shaded relief63
 Figure 41: GNSS chart of Rubavu station data, from the file in Table 2266
 Figure 42: Zoom around second half of 2012 of Figure 4167

LIST OF TABLES

Table 1: List of eruptions of Nyamuragira and Nyiragongo (Smithsonian Institution 2013)3
 Table 2: List of data sources of Wisdom-volkano, sorted by priority by ECGS/RMCA11
 Table 3: List of FR of Wisdom-volkano12
 Table 4: List of documentation of Wisdom-volkano12
 Table 5: List of SAR satellites used in Wisdom-volkano21
 Table 6: Parts within the file name of an InSAR image23
 Table 7: Content of an ENVI header file23
 Table 8: Detail on the map_info field from an ENVI header file24
 Table 9: Sample content of an MSBAS time-series file25
 Table 10: Sample content of a seismic localization events file30
 Table 11: Sample content of a seismic station on counting events file31
 Table 12: Sample content of a GNSS station file33
 Table 13: List of events near the volcanoes42
 Table 14: Coordinates example between the WGS 84 datum and the Web Mercator projection, with size of the pixel defined by the interferograms45
 Table 15: Content of the log (text) file generated by Source code 2547
 Table 16: New MSBAS header data, in meters64
 Table 17: Sample of the new seismic counting events file64
 Table 18: Improvements for the seismic counting values files65
 Table 19: Sample of the new seismic location file65
 Table 20: Sample of the new GNSS xyz data file66
 Table 21: Sample of the new GNSS UTM data file66
 Table 22: Resulting GNSS file from integrating Table 20 and Table 2166

GLOSSARY

ajax	Asynchronous JavaScript and XML
API	Application Program Interface
CSS	Cascade Style Sheets
CRS	Coordinate Reference System
CSA	Canadian Space Agency
CSV	Comma-Separated Values
DEM	Digital Elevation Model
DLR	<i>Deutsches Zentrum für Luft- und Raumfahrt</i> (German Space Agency)
ECGS	European Centre for Geodynamics and Seismology
ENVI	Environment for Visualizing Images
ESA	European Space Agency
EW	East-West axis ground displacement
FR	Functional Requirement
GB	Gigabytes or 1000 ³ bytes
GD	Geospatial Data
GDAL	Geospatial Data Abstraction Library
GeoTIFF	Georeferenced Tagged Image File Format

GIS	Geographical Information System
GLONASS	GLObal NAVigation Satellite System (Russian)
GML	Geographic Markup Language
GNSS	Global Navigation Satellite System (generic)
GPS	Global Positioning System
HTML	HyperText Markup Language
HTTP	Hypertext Transfer Protocol
InSAR	Interferometric Synthetic Aperture Radar
INSPIRE	Infrastructure for Spatial Information in the European Community
ISO	International Organization for Standardization
JAXA	Japan Aerospace Exploration Agency
JSON	JavaScript Object Notation
KML	Keyhole Markup Language
LP	Long-Period seismic events
MVC	Model View Controller
MSBAS	Multidimensional Small Baseline Subset
NASA	National Aeronautics and Space Administration
NS	North-South axis ground displacement
OGC	Open Geospatial Consortium
OSGeo	Open Source Geospatial Consortium
PHP	PHP Hypertext Preprocessor
PNG	Portable Network Graphics
RAM	Random Access Memory
REST	Representational State Interface
RMCA	Royal Museum for Central Africa
RS	Remote Sensing
SAR	Synthetic Aperture Radar
SLD	Styled Layer Descriptor
SP	Short-Period seismic events
SPIDER	System of Participatory Information, Decision support and Expert knowledge for irrigation River basin water management
SSD	Solid State Drive
TS	Time-series
TSV	Tab-Separated Values
UP	Up-Down axis ground displacement
URL	Uniform Resource Locator
USB	Universal Serial Bus
UTM	Universal Transverse Mercator projection
W3C	World Wide Web Consortium
WFS	Web Feature Service
WGS	World Geodetic System
WMS	Web Map Service
XML	Extensible Markup Language

CONVENTIONS AND LICENCE

Physical products will be cited as Product (manufacturer, city, country). Software and online products can be found in the References section, except where the copyright or license obliges to. Since web addresses or Uniform Resource Locators (URL) (W3C 2009) are usually anything but permanent, all have been checked and have at least one archived copy in the Wayback Machine (Internet Archive 2014). URLs are enclosed within angle brackets and the "http://www." is usually omitted. All references in the main text, both internal and external, are marked with brown text.

External software and product licences are beyond the objectives of this thesis and are not mentioned.

The license chosen for Wisdom-volkano software is the European Union Public Licence (European Commission 2015) because it allows free and open source code, and due to its legally binding translations to many European languages.

This thesis, figures included, and the Wisdom-volkano documentation are allowed to reuse under the terms of the license CC BY NC SA 4.0 (Creative Commons 2015) except otherwise stated.

Cover image: Virunga lava lakes by night; Nyiragongo (right) and Nyamuragira (left), by Nicolas d'Oreye (ECGS), 15th May 2015, from the website of Benoît Smets <bsmets.net>.

ACKNOWLEDGEMENTS

Above all, thanks to my dear wife Marina M. Mangado, for her love, support, patience and African passion. Long life to 2709 books.

Thanks to Nicolas d'Oreye for the opportunity, knowledge, explanations and time; to Harry Lankreijer for his useful comments; to Benoît Smets, François Kervyn, Halldor Geirsson and other researchers of the ECGS/RMCA for their support and amazing work; to the correctors yet still friends, Óscar Gómez, Joan Villespir and María J. Jerez; to the professors David Tanenbaum and Per-Ola Olsson for their useful comments; to Vicente Bodas for the inspiration.

It all started in Italy; thanks to John Van Aardenne, Suvi Monni and Valerio Pagliari, who discovered a cartographer in me, and a special *pensiero* to Lorenzo Orlandini, who arrived before I did and left before I will.

This page intentionally left blank.

1. INTRODUCTION

«We need to understand better what it means for a location to have not only space coordinates but also time coordinates.»
(Hägerstrand 1970)

Map visualization has always been useful, but already in 1970 and even more nowadays this is not enough, because it often lacks the *when* dimension to register change during time. Maps and time-series should be integrated and shown together. This will increase their value, their meaning, their utility.

Recent eruptions of Nyamulagira and Nyiragongo volcanoes in the Nord-Kivu province (Democratic Republic of the Congo) have been and still are a threat to the nearby population (Allard et al. 2003; Smets et al. 2010; Tedesco et al. 2007), although also an opportunity to collect more and better information on the different signals.

Data from seismic events and ground deformation, both from local stations and remote sensing (RS) interferometric synthetic aperture radar (InSAR) and ground sensing global navigation satellite system (GNSS), as well as gas emissions showed that there is a clear correlation between them and the eruptions (Smets et al. 2013).

With a multivariate analysis, the researchers of the European Centre for Geodynamics and Seismology (ECGS) and the Royal Museum for Central Africa (RMCA) found a posteriori some pre-eruptive signals up to 3 weeks prior to the 2010 eruption at the volcano Nyamulagira. Each signal on its own was not significant enough; they went unnoticed until a subsequent re-analysis of the InSAR data with a new methodology, Multidimensional Small Baseline Subset (MSBAS) (Samsonov et al. 2012), triggered the finding. However, these signals contrast with the precursor activity commonly recognized before an eruption at Nyamulagira, namely an increase of the seismicity few hours prior the lava outburst.

Using Geographic Information Systems (GIS) to monitor volcanos is useful (Vicari et al. 2011) and even mandatory for large amounts of data, but not always better than manual handling (Carrara et al. 2000): as in any information system, it actually depends of the quality of data. In this particular case, even with an information system, the human interpretation of data is indispensable. Same happens when adding the time dimension to produce time-series (Colditz et al. 2008). In order to assess and improve the quality of GIS time-series data, both should be built and tested together, a feature often missing in this kind of tools (Wright et al. 2003).

The main objective of this thesis is help identifying correlations and precursor activity to recognize pre-eruptive indicators. Identifying precursor activity of passed eruptions (Murphy et al. 2011; Rusangiza et al. 2012) may help detecting potential new events that were maybe unrecognized yet, and eventually recognize a priori potential pre-eruptive activity in the area.

In order to do so, it should implement adequately the functional requirements:

1. Show many georeferenced images and time-series collections, some to be calculated automatically.
2. Allow several users spread over the world to use the tool, or to run it in a laptop on the field.
3. Follow standards to integrate and reuse the tool within existing and future projects, so the source code shall ideally be open and available for all scientific community, except where explicitly requested by the ECGS/RMCA (European Centre for Geodynamics and Seismology, and Royal Museum for Centre Africa).
4. Integrate analytical functionalities like detrending.

The tool's name is Wisdom-volkano, what is an acronym of Web Interface for Sharing Data on Monitoring, while *volkano* is the Swahili (the language spoken in the area) word for volcano, from the Portuguese *volcão*.

2. BACKGROUND

2.1. State of art of volcanic monitoring with GIS and time-series

Though volcanic eruptions in the North-Kivu have been registered often (Wauthier et al. 2015) and for a long time (Smets et al. 2015) (see Table 1 for a list), data has been scarce due to the difficult maintenance of ground stations in the Nord-Kivu politic environment (Kisangani 2012). Given the current period of stability, the ECGS/RMCA has been able to install new equipment in ground stations (Geirsson et al. 2016). This is already generating such a big volume of data that, in order to be analysed, it will need to be shared.

Previous research focused on statistical analysis of volcanic hazard (Tonini et al. 2015) while other analysed stakeholders (such us volcano scientists, hazard analysts, GIS specialists and developers) knowledge in order to get the functional requirements, leaving the web GIS to a later step (Le Cozannet et al. 2014). A European initiative put heat, volcanic emissions and ground deformation maps into a single project called Evoss (Bernal-Carrera 2014; Tait and Ferrucci 2013), foreseen to continue after its funding was over in 2013, though no external or published tool seems to be available and the project websites are not working anymore.

The National Aeronautics and Space Administration (NASA) produced and maintains a web GIS tool called QuakeSIM simulating earthquakes from InSAR images integrated with Google Maps (Google 2016a; Parker et al. 2015). Google Maps is also used for showing points in order to model magnetic, gravitational and deformation data with a genetic algorithm (Currenti et al. 2014). Another effort on showing satellite images with a specific model to accelerate the processing is Lav@hazard (Vicari et al. 2011).

Research has linked time-series with interferograms and GNSS data, though not with a specific tool (Peltier et al. 2010). Others have used time-series but without GIS, either for statistically estimated prediction of eruptions (Mendoza-Rosas and De la Cruz-Reyna 2008), SO₂ or heat emissions (Galle et al. 2003; Wooster and Rothery 1997), seismic data in real time (Endo and Murray 1991), seismic prediction (Romero et al. 2016) or InSAR data (Sansosti et al. 2010).

Table 1: List of eruptions of Nyamuragira and Nyiragongo (Smithsonian Institution 2013)
Background colour alternates by decade. Nyiragongo eruptions in brown text, Nyamuragira in black.

Volcano	Eruption started	Eruption ended
Nyamuragira	2011 Nov 6	2012 Mar 16 (?)
Nyamuragira	2010 Jan 2	2010 Jan 29
Nyamuragira	2006 Nov 27	2006 Dec 5 (?)
Nyamuragira	2004 May 8	2004 May 28 ± 3 days
Nyamuragira	2002 Jul 25	2002 Sep (?)
Nyiragongo	2002 May 17 (?)	2016 Mar 1 (continuing)
Nyiragongo	2002 Jan 17	2002 Feb 3 (in or after)
Nyamuragira	2001 Feb 6	2001 Apr 5 ± 4 days
Nyamuragira	2000 Jan 27	2000 Feb 10 (in or after)
Nyamuragira	1998 Oct 17	1998 Oct 25 (in or after)
Nyamuragira	1996 Dec 1	1996 Dec 5 (in or after)
Nyamuragira	1994 Jul 4	1994 Aug 25 (in or after)
Nyiragongo	1994 Jun 23	1996 Mar (?)

Volcano	Eruption started	Eruption ended
Nyamuragira	1991 Sep 20	1993 Feb 8
Nyamuragira	1989 Apr 24	1989 Aug 15 ± 5 days
Nyamuragira	1987 Dec 30	1988 Jan 4
Nyamuragira	1986 Jul 16	1986 Aug 20
Nyamuragira	1984 Feb 23	1984 Mar 14
Nyiragongo	1982 Jun 21	1982 Oct 17 ± 15 days
Nyamuragira	1981 Dec 25	1982 Jan 14
Nyamuragira	1980 Jan 30	1980 Feb 24
Nyiragongo	1977 Jan 10	1977 Jan 10
Nyamuragira	1976 Dec 23	1977 Jun 15 ± 5 days
Nyamuragira	1971 Mar 24	1971 May 5 ± 4 days
Nyamuragira	1967 Apr 23	1967 May 9
Nyamuragira	1958 Aug 7	1958 Nov 21
Nyamuragira	1956 Nov 17	1956 Nov 18
Nyamuragira	1954 Feb 21	1954 May 28
Nyamuragira	1951 Nov 16	1952 Jan 16
Nyamuragira	1951 Jul 25	1951 Jul 28
Nyamuragira	1948 Mar 1	1948 Jul 15 ± 5 days
Nyamuragira	1938 Jan 28	1940 Jun 25 ± 5 days
Nyiragongo	1927 Mar	1977 Jan 10
Nyiragongo	1920	1921
Nyiragongo	1918	Unknown
Nyamuragira	1912 Dec 3	1913 Apr
Nyiragongo	1911 Aug	1911 Oct
Nyamuragira	1909 May	1909 May
Nyamuragira	1907 Nov 7	1907 Dec 5
Nyamuragira	1907 Apr	1907 May
Nyiragongo	1906	Unknown
Nyiragongo	1905	Unknown
Nyamuragira	1905 Jul 22	1905 Sep 25 (in or after)
Nyamuragira	1904 Apr	1904 May 16 (?)
Nyiragongo	1902	Unknown
Nyamuragira	1901	Unknown
Nyiragongo	1901	Unknown
Nyiragongo	1900	Unknown
Nyiragongo	1899	Unknown
Nyamuragira	1899 Feb	Unknown
Nyiragongo	1898	Unknown
Nyamuragira	1896	Unknown
Nyiragongo	1894	Unknown
Nyamuragira	1894 Jun	Unknown

2.2. State of art of web GIS and time-series development

In order to develop Wisdom-volkano, a web-based application is chosen over a client-server one, to facilitate the development while avoiding the need to code server connections: many users will not be in an intranet but all over the world, accessing gigabytes (GB) of data files. A secondary objective is that clients (browsers) are lighter and readily updated. Furthermore, a number of web-oriented, open source libraries will be used in order to ease the development and comply with current GIS standards, increasing Wisdom-volkano interoperability.

Geospatial standards are mostly defined by the Open Geospatial Consortium (OGC) or the International Organization for Standardization (ISO). Some of them were first defined by the OGC and then adopted by ISO. OGC must not be confounded with Open Source Geospatial

Foundation (OSGeo), which maintains open source GIS tools (OGC and OSGeo 2011). These standards can be classified in layers (Steiniger and Hunter 2012); the relevant ones for this study are shown in Figure 1.

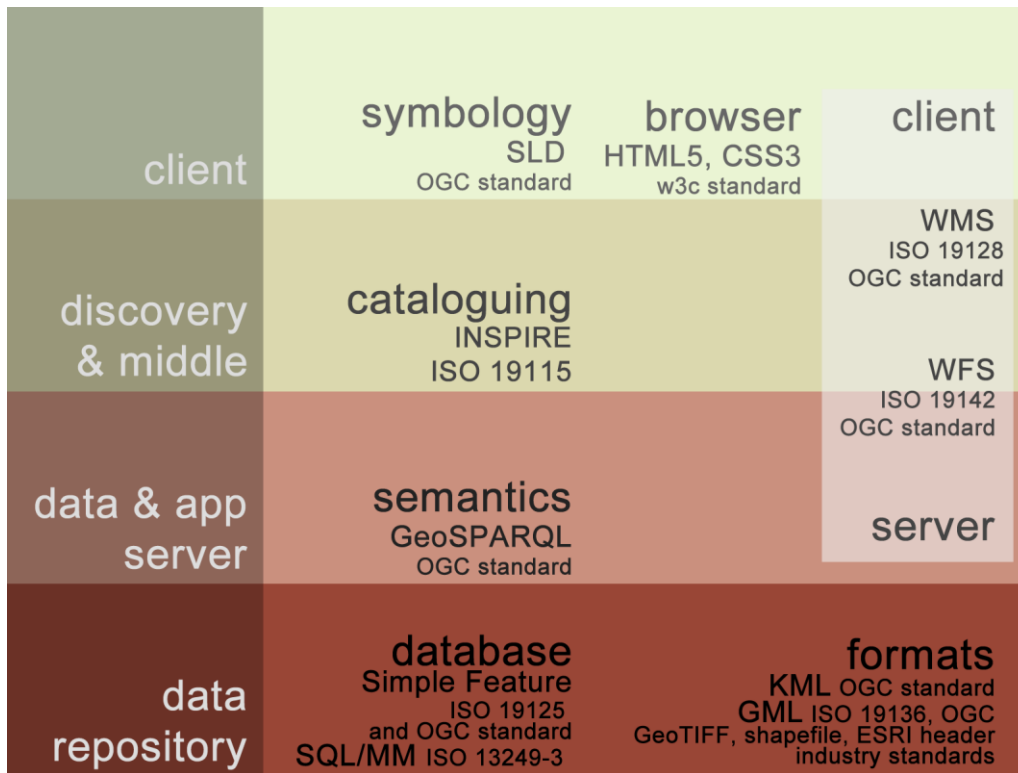


Figure 1: Overview of relevant web GIS standards

2.2.1. Data repository and formats

The data side has two parts. First, the spatial data repository or database shall follow the ISO 13249, called SQL/MM (International Organization for Standardization 2009), extension of the Simple Feature standard from OGC, also ISO 19125 (International Organization for Standardization 2005). Coverage of both is better (Stolze 2003) done by PostGIS (Refractions Research 2016) on PostgreSQL (Kandawasvika 2009; Steiniger and Hunter 2012; The PostgreSQL Global Development Group 2016) than by MySQL (Oracle 2016); all three open source software. Other proprietary solutions like Oracle database (Oracle 2015) or SQL Server (Microsoft 2016a) were not considered. PostGIS was therefore chosen for Wisdom-volkano.

The other part on data concerns formats. Two OGC standards are Keyhole Markup Language (KML) (Open Geospatial Consortium 2016a) and Geographic Markup Language (GML) (Open Geospatial Consortium 2016b), also ISO 19136 (International Organization for Standardization 2015) though only the former is being used by Wisdom-volkano; the latter is suggested for the future. Other formats used, all industry standards, are Georeferenced Tagged Image File Format (GeoTIFF) (Open Source Geospatial Foundation 2016a), also an OSGeo standard, Shapefile (ESRI 1998) and Environment for Visualizing Images (ENVI) Header (Harris Geospatial Solutions 2016).

2.2.2. GIS Server

Web Map Service (WMS) and Web Feature Service (WFS) are standard protocols for map viewing services over internet, were developed by the OGC and also adopted by ISO (de-la Beaujardiere 2006; Scharl and Tochtermann 2007). Both are exposed by the GIS server application, announced by the middle discovery layer, and run in the client. Almost all geospatial applications reviewed later in this section use them.

Two main software options are available for the server side:

- GeoServer (Open Source Geospatial Foundation 2014) open source software, the tool created and maintained by OSGeo, used by NASA for QuakeSIM (Parker et al. 2015).
- MapServer (Open Source Geospatial Foundation 2016b), also open source and used for example for visualizing maps from a database on greenhouse gases emissions (Bergamaschi et al. 2010; Janssens-Maenhout et al. 2012).

The features of both (Steiniger and Hunter 2012) were enough for Wisdom-volkano, while the performances were also similar (Anderson and Deoliveira 2007). GeoServer was chosen because of a better documentation, including many tutorials and examples, a Representational State Interface (REST) (Fielding and Taylor 2002), and a website to administer the layers.

Other available tools like ArcGIS (ESRI 2016a) were discarded due to having commercial, non-open source license. Google Earth Engine (Google 2015) is free and allows high performance GIS analysis and integrates Sentinel satellite Synthetic Aperture Radar (SAR) (Hanssen 2001) data; it even has a time lapse mode. But it is more of a video presentation than a point analysis tool, the application does not work offline and it is not open source.

Another standard that might be useful in the future lies within the interoperability of computers via a more abstract technology layer, also called semantic technologies. Here the OGC standard GeoSPARQL (Perry and Herring 2012) is already available, but others will certainly come.

2.2.3. Discovery layer, metadata

The catalogue or discovery layer involves the description of the data and services, that is, the metadata. They are beyond the topic, but nonetheless, the documentation delivered with Wisdom-volkano recommended the standard ISO 19115-1:2014 (ISO/TC 211 2014) and included a complete metadata template. GeoServer also provides natively forms to complete this.

A complementary and quite extended (in Europe) option is the Infrastructure for Spatial Information in the European Community (INSPIRE) Directive 2007/2/EC (European Parliament and Council of the European Union 2007). INSPIRE allows to combine data and discover datasets and services, which can be afterwards exposed via OGC web services.

Other services not covered in this study are download and transformation, though they may be implemented in the future. Licensing for sharing is far more complicated, as there are

many open source licences which may be incompatible in certain combinations; this alone deserves a complete thesis.

2.2.4. Client

The web GIS client side is itself a pair of different applications: it must include a web browser and the applications or libraries to connect to the server via the WMS and WFS standards and show the result in screen to the user. Concerning the browser, since the visualization of Wisdom-volkano must be rendered in any screen size or device, it must be compliant with World Wide Web Consortium (W3C) standards like HyperText Markup Language version 5 (HTML5) (W3C 2014) and Cascade Style Sheets version 3 (CSS3) (W3C 2016); Mozilla Firefox (Mozilla Foundation 2016) and Google Chrome (Google 2016b) are among the most used browsers (Frain 2012).

There are many libraries able to connect to WMS and WFS and to render the maps in the browsers mentioned. Usually they are open source and coded in JavaScript (ECMA International 2016). The choice was between OpenLayers (Open Source Geospatial Foundation 2016c) and Leaflet (Agafonkin 2015): both are actively maintained. The second is lighter and easier to implement with, but OpenLayers was chosen because it is more mature, robust and flexible, has more features (Lovelace 2014; Roth et al. 2013), and is widely used (Le Cozannet et al. 2014; Khattar 2014; Steiniger and Hunter 2012). Though OpenLayers is able to load maps without GeoServer, this caused a major problem with the visualization of points, solved in the third iteration of Wisdom-volkano.

2.2.5. Symbology

Symbols are the graphical parameters and fixed images that are used to provide information in a map. There are many ways to show a raster image map or features like points, lines and polygons: with different colours or just grey scales, symbols, size, choropleths, etc. (Slocum et al. 2010).

The OGC standard Styled Layer Descriptor (SLD) (Open Geospatial Consortium 2016c; Sae-Tang and Ertz 2007) is based on Extensive Markup Language (XML) (W3C 1998) and extends the WMS standard. Features and rasters can adopt symbols and colours defined by the user: each SLD file may have four sections, three for the features (points, lines and polygons) and one for the rasters.

In order to calculate thresholds between categories such as dates or magnitudes, QGIS (QGIS 2016) software has been used so the resultant classes are divided with natural breaks and enough data within each class (Slocum et al. 2010).

2.2.6. Time-series data and visualization tools

There are no standards for time-series other than the rather specific Water XML (WaterML) for hydrological time-series structures (Open Geospatial Consortium 2014), so the generic Tab-Separated Values (TSV) (Korpela 2005) format was used.

In order to visualize the time-series, a client application or library is needed; again a JavaScript one. There were several options: Highcharts (Highsoft AS 2016), Rickshaw (Shutterstock 2016), C3.js (Tanaka 2014), D3.js (Bostock 2013) and others (Johnson 2015; Patra 2014). Highcharts was considered despite of not being open source, yet free for non-commercial use. All the four libraries were included in a simple prototype and tested with time-series data and searched for documentation. Neither Rickshaw nor C3.js had enough features or community support. On the other hand, D3.js was so powerful and detailed that it would have need much more time and a whole team to include it properly. The tested prototype of Highcharts was found perfect for the project, with advanced and professional features.

Some other data visualization tools include maps as well as charts; they were discarded early due to having commercial license or their freemium model, that is, free for minimum requirements like one user and a few megabytes worth of data; and paying options for escalating in use or size, which was not suitable for Wisdom-volkano data requirements. Examples of this freemium model were CartoDB (Vizzuality 2016), MapBox (MapBox 2016) or Qlik (QlikTech International AB 2016). Tableau (Tableau Software 2016) is very powerful but does not provide a free version.

2.2.7. Wisdom-volkano initial application stack

An agile iterative development approach was chosen in order to deliver working prototypes early, to test functionalities and to be able to react to errors while adapting to changing requirements or priorities (Fowler and Highsmith 2001). Also, Wisdom-volkano is developed with the Model View Controller (MVC) in the PHP Hypertext Processor (PHP) (The PHP Group 2016) CodeIgniter (British Columbia Institute of Technology 2016) framework (Khattar 2014; Upton 2007). CodeIgniter has extensive and clear documentation, is small in size yet very performant (Janev et al. 2015; Samra 2015).

The main complete view of a whole web GIS and time-series application came from the System of Participatory Information, Decision support and Expert knowledge for irrigation River basin water management (SPIDER webGIS) (Moreno-Rivera et al. 2009), a widely used land-use web GIS created at the University of Castilla-La Mancha in Spain.

Given the above decisions, the high-level view of Wisdom-volkano software architecture is shown in Figure 2. The complete diagram is in Figure 17.

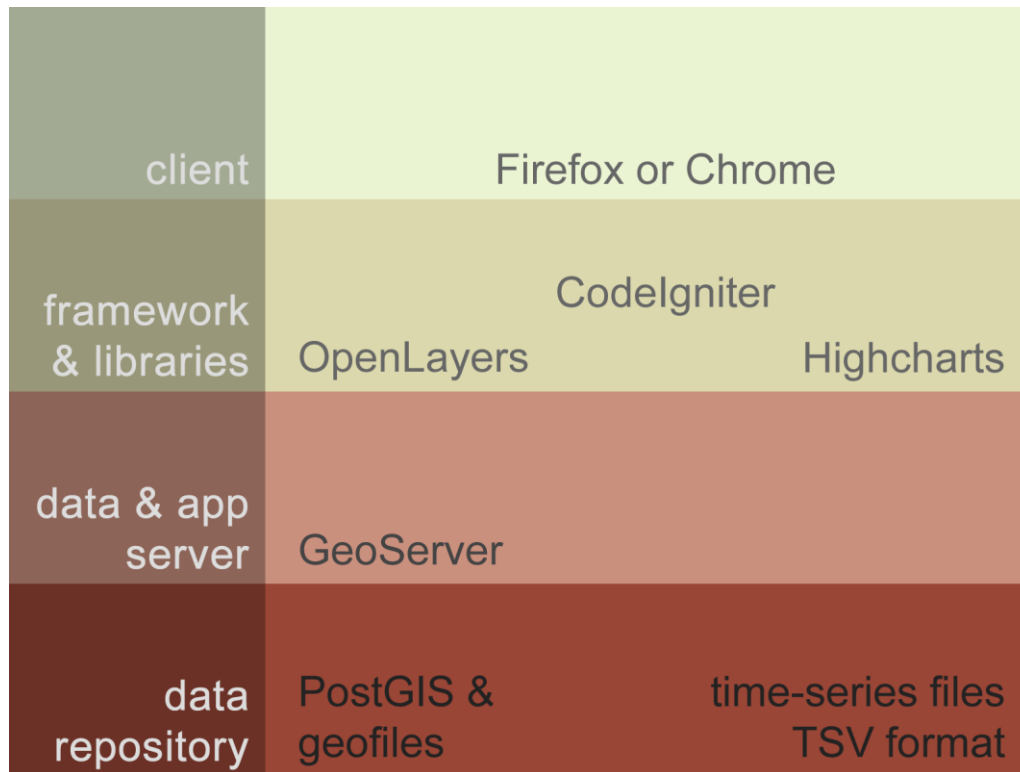


Figure 2: High-level Wisdom-volkano software architecture

2.3. Scope and study area

The data used to build and test Wisdom-volkano comes from the volcanoes Nyamulagira (or Nyamuragira), situated at 1.412° South 29.20° East, and Nyiragongo, at 1.523° South 29.25° East. Both volcanoes are in the North-Kivu province in the Democratic Republic of the Congo, and belong to the Virunga Mountain Range, which comprises six other volcanoes along the East African Rift and lies within three countries (the other two being Uganda and Rwanda).

Furthermore, the lava flows are spread in a wider region, at least between 1.15° and 1.7° South (Lake Kivu being the southern limit) and between 29.0° and 29.4° East (Smets, Wauthier, et al. 2010). The twin towns of Goma and Gisenyi belong to Democratic Republic of the Congo and Rwanda respectively, have a combined population of over 1.1 million people who live on or next to previous lava flows that may happen again. Figure 3 shows a map of the zone.

However, the real affected zone is somewhat bigger due to the spread of volcanic gases and other solid emissions, and certainly not restricted to the administrative boundary.

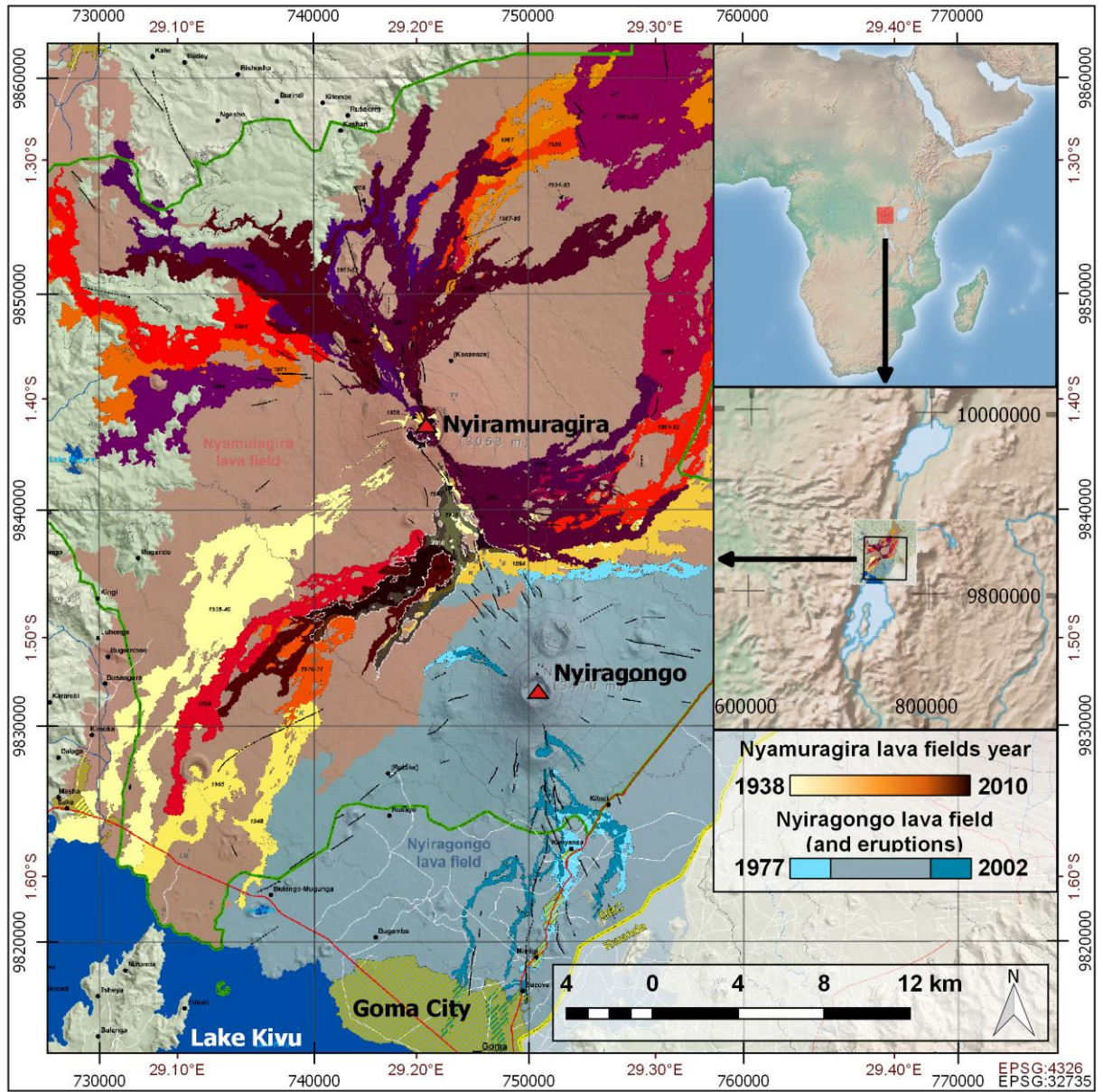


Figure 3: Map of lava flows around Nyiragongo and Nyamulagira volcanoes, and Goma City
Updated from (Smets, Wauthier, et al. 2010) by email from the author, Benoît Smets. Background overview from Natural Earth.

3. MATERIALS AND METHODS

3.1. Functional requirements and iterations

The original idea of this project was conceived after the findings of the ECGS/RMCA researchers of early precursor signals of eruptions (Smets et al. 2013). Some meetings were undertaken to decide the list and priority of data sources and functional requirements (FR). They are synthetized in Table 2 and Table 3 (codes are GD for geospatial data and TS for time-series). Furthermore, a number of supporting documents were to be delivered with the software. They were updated along the project and became the basis of this thesis; the list is in Table 4.

Two of the FR were classified as optional, meaning to be either considered later (FRO1) or dependent on external input (FRO2). Also, two other FR were external or not fully related to GIS: security of objects for administrators and stakeholders (FRE1), and a log audit of all administrative actions and errors performed in Wisdom-volkano (FRE2).

Given the stakeholders availability, an iterative model in three phases was suggested. At the beginning of each one, the author met the ECGS/RMCA researchers to decide the priority of the data sources and FR and at the end a working version (prototype) of Wisdom-volkano was presented with some of the data sources and FR implemented and the updated documentation. The meeting presenting the first iteration and the preparation of the second one were held together, and also for presenting the second iteration with the preparation of the third one.

Along with the second and third iterations, two videos showing the main functionalities were produced; they are available under request, intended as tutorials and feature presentations for both researchers and professors who were not able to attend in person the presentations at the ECGS/RMCA.

Table 2: List of data sources of Wisdom-volkano, sorted by priority by ECGS/RMCA
Not yet implemented data appear in brown text with the tag [future].

GD1: InSAR georeferenced images.
TS1: MSBAS time-series data from InSAR.
GD2: Seismic stations map.
TS2: Seismic counting events time-series (histogram) from stations.
GD3: Seismic location events map.
GD4: GNSS stations map.
TS3: GNSS time-series from stations.
GD5: GNSS displacement map [future].
TS4: SO ₂ time-series from stations [future].
GD6: Heat maps [future].

Table 3: List of FR of Wisdom-volkano

Not yet implemented ones appear in brown text with the tag [future].

- FR1 : Basic map interface, with zoom or pan, background from Google Maps or similar, opacity adjustable, layers (features: points, lines, polygons) and rasters (bitmap images).
- FR2 : Select point on the map.
- FR3 : Load time-series of a given coordinate from FR2.
- FR4 : Configuration of time-series.
- FR5 : Add points to dataset.
- FR6 : Show z-elevations profiles between two points [future].
- FR7 : Allow multi-looking (calculate also surrounding data, not just one point) on time-series [future].
- FR8 : Remove detrending: given a time-series (FR3) and a time range (FR4), the user might decide that the slope of the time-series is due to normal deformation of the land, and want to remove it to better analyse the time-series.
- FR9 : Save time-series pixel values, which might need to be calculated (FR13) before.
- FR10 : Add layers and rasters.
- FR11 : Keep configuration and view.
- FR12 : Modify order of layers.
- FR13 : Calculate time-series of a coordinate across a stack of layers.
- FR14 : Show histogram and accumulates as a special type of time-series.
- FRO1 : Portability and sharing of the system.
- FRO2 : Time-series outliers and trend changes [future].
- FRE1 : Security of the system.
- FRE2 : Log audit.

Table 4: List of documentation of Wisdom-volkano

Not yet delivered documents (related to TS or GD in Table 2) appear in brown text with the tag [future].

- Functional requirements document.
- Software architecture document.
- User manual embedded into the application.
- InSAR MSBAS data documentation.
- Seismicity data documentation.
- GNSS data documentation.
- SO₂ data documentation [future].
- Heat data documentation [future].

3.2. Data sources: interferograms and time-series

3.2.1. SAR products

SAR is an RS instrument in a satellite producing its own radiation, which is reflected by earth and then captured back (Hanssen 2001; Lu 2007), allowing night & day observation. This radiation has microwave wavelength (order from millimetres to a few centimetres), which trespasses clouds. The acquired radiation by the sensor is a complex image, so it has two parts: amplitude, which measures the reflected power like an optic image, and phase, which allows deducing the distance. Therefore, SAR produces images with complex pixels, composed of these two parameters, amplitude and phase. In Figure 4 an SAR amplitude image is shown.

The phase alone looks like noise and does not say much in a single SAR image. It is not able to distinguish two objects situated at the same distance yet different angles, because it depends on the roughness of the terrain rather than on its chemical composition (Ferretti et al. 2007). In order to solve that, two SAR images shall be used, either from one receptor at different times, or from two receptors at the same time from different positions. However, they must be comparable or close enough: the wavelength must be a fraction of the pixel change. This is a geometric condition, principle of the interferometry, whose equation is (Massonnet and Feigl 1998) shown in equation 1.

$$2L(\sin\theta_1 - \sin\theta_2) < \lambda \quad (1)$$

- L: pixel resolution on the ground (depends on the satellite; around 20m for ERS-1).
- λ : wavelength (56 mm for ERS-1).
- θ_1 and θ_2 : vertical angles of incidence (look angle) of the first and second images taken, respectively.

For ERS-1 (see the complete list of SAR satellites in Table 5), the distance between the two points of view from which images are acquired (i.e., the baseline) should be less than around 1 km. A bigger distance would result in geometrical decorrelation. The satellite position should also be known at better than a few centimetres. Nowadays satellite orbits are precise enough to fulfil these conditions. Figure 5 shows the InSAR geometry and how fringes are created due to the distance (baseline) between the satellites.

The phase difference allows computing a digital elevation model (DEM) of the Earth surface and, if any, ground displacement in the satellite line of sight (i.e. change in distance from the satellite to a given point on the Earth surface). This is expressed by the equation 2 (Hanssen 2001; Lu 2007).

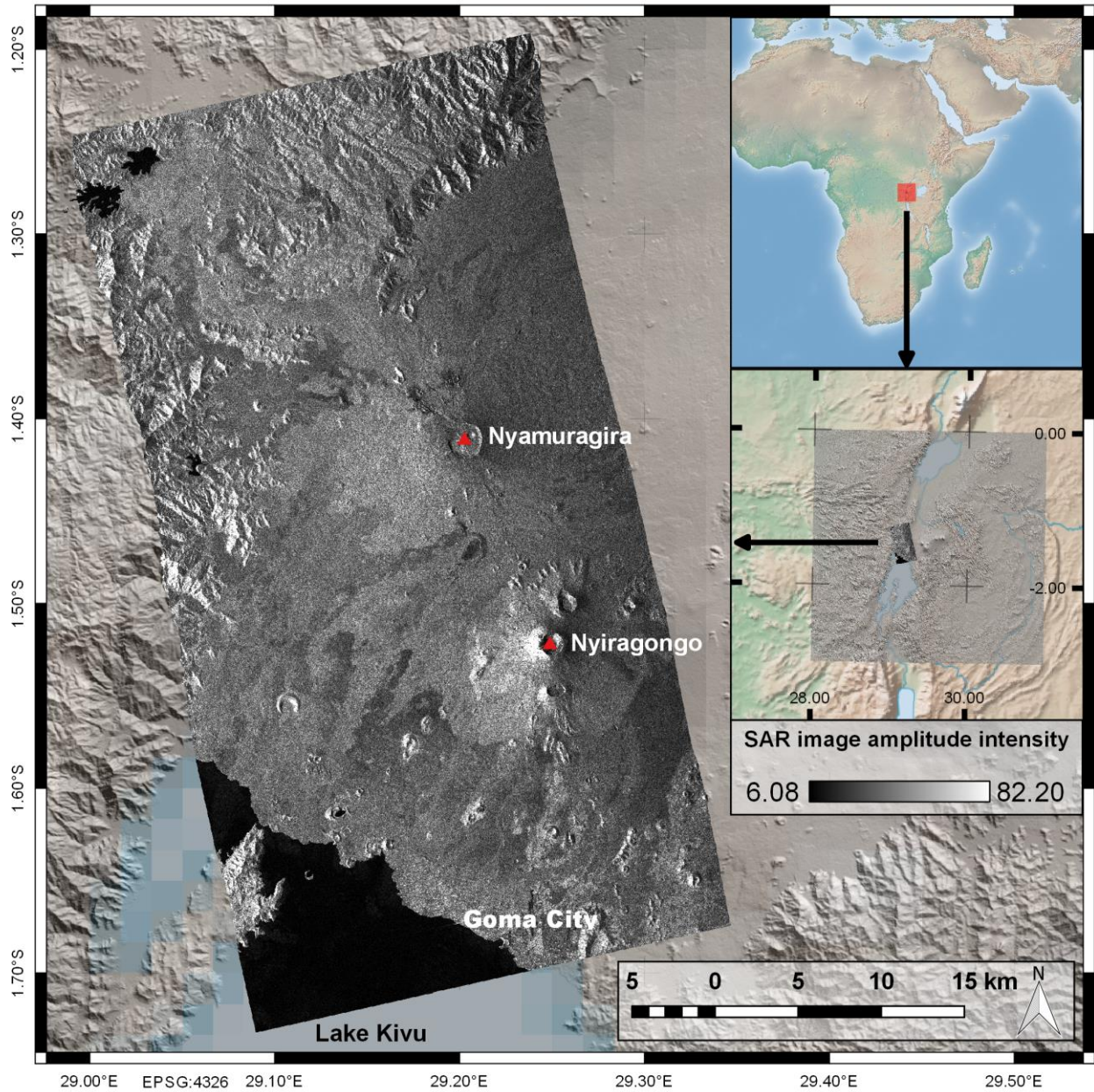


Figure 4: SAR amplitude image from ENVISAT

Image and DEM provided by ECGS/RMCA. Background in overview from Natural Earth.

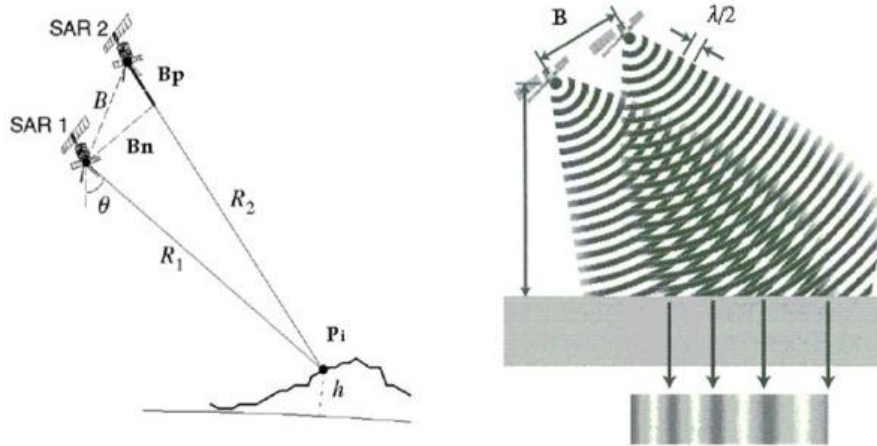


Figure 5: (Left) InSAR geometry. (Right) How the fringes are created due to the baseline (Luzi 2010)

$$\psi_P = \frac{-4\pi(R_1 - R_2)}{\lambda} \quad (2)$$

- ψ_P : interferometric phase of the point or pixel P; its value ranges from $-\pi$ to $+\pi$ (360°) or, translated to the wavelength of the satellite, from $-\lambda/2$ to $\lambda/2$.
- (R_1, R_2) : distances from the sensor to the ground target in the first and second image, respectively. The result of $(R_1 - R_2)$ usually has a range of some metres, but between neighbouring points (pixels in the images) just a few metres apart, the precision is below the wavelength, usually centimetres or less.
- 4π : due to the sinusoidal function of the wave (2π) times 2 because the signal goes and returns (Ferretti et al. 2007). The minus sign is explained in (Hanssen 2001).
- λ : wavelength.

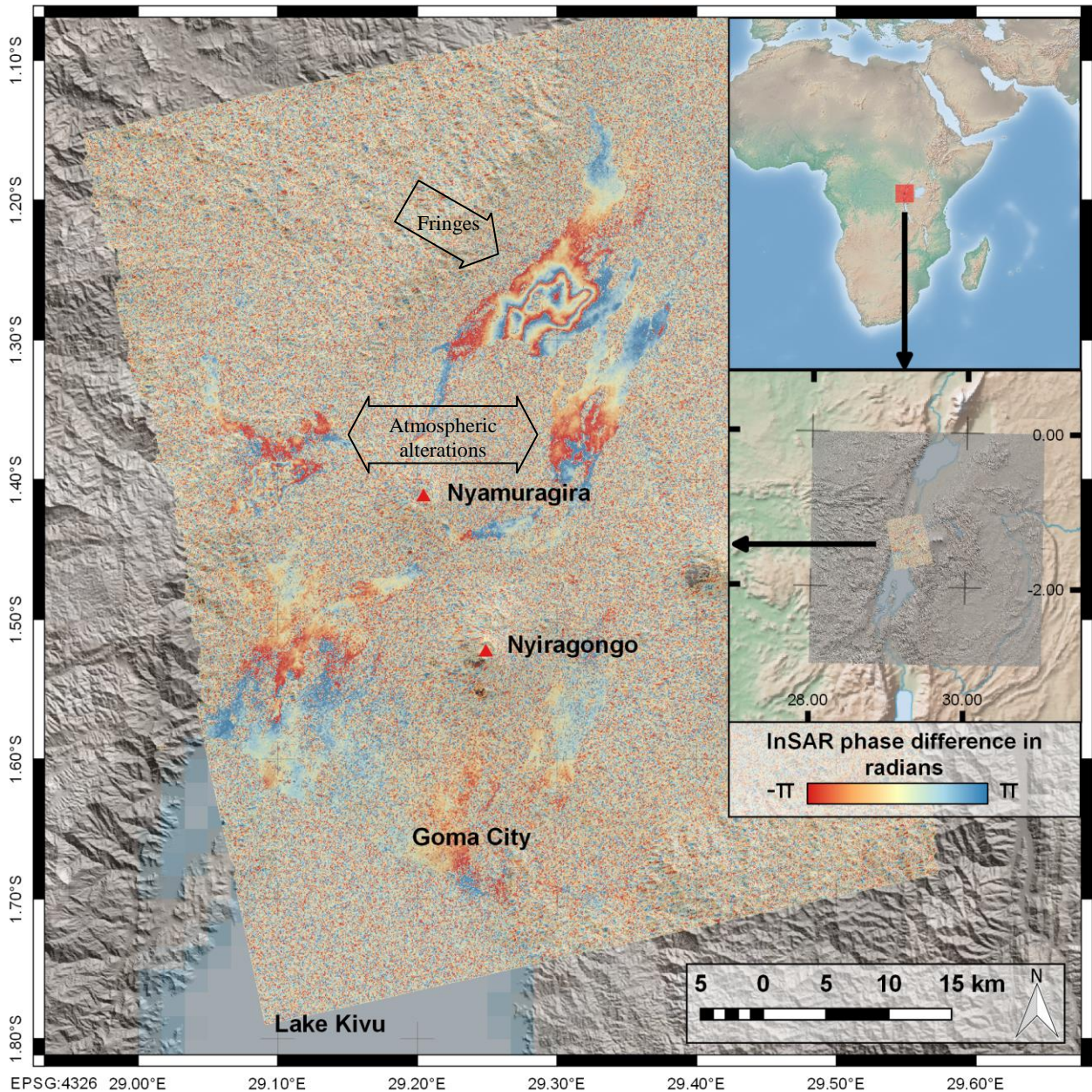


Figure 6: Example of differential interferogram wrapped on the shaded relief DEM of Nord-Kivu

The partially transparent interferogram was computed using two ERS satellite SAR images. It shows clear fringes produced by the compaction of old lava flows. Each colour cycle (or fringe, e.g., from red colour to next red colour) depicts a 2.8cm (half wavelength of SAR signal) ground displacement in the satellite line of sight. InSAR image and DEM provided by ECGS/RMCA. Background in overview from Natural Earth.

After differencing the two SAR images in a process called differential interferometry, the result is an interferogram with fringes, where the colours cycle from $-\pi$ to $+\pi$. Therefore, in Figure 6, every time that the same colour appears in a next fringe, there is a ground displacement of half the wavelength (2.8 cm for ERS-1) in the direction of the satellite point of view. An interferogram can be read like a topological map: quick colour changes would mean a steep difference in the phase.

Fringes may be due to four reasons:

- Different geometries such as the satellite orbital trajectories, the wavelength, the SAR antenna position, etc.
- Topography.
- Atmospheric alterations.
- Ground displacements.

The first is overcome by comparing close enough images from the same satellite, or knowing with high detail the orbits and radar characteristics of the satellites.

Interferometry may be also used for calculating topographic DEMs, but for volcanic ground displacements the topographic fringes must be removed. It may be enough to subtract a DEM to the interferogram, but the DEM error shall be still taken into account. This DEM error is also known as altitude of ambiguity, which is the height difference corresponding to a topographic fringe and can be calculated from the interferometric parameters (Ferretti et al. 2007) as shown in equation 3.

$$h_a = \frac{\lambda R \sin \theta}{2B_n} \quad (3)$$

- h_a : altitude of ambiguity.
- λ : wavelength.
- R : distance from the sensor to the ground target (the satellite altitude).
- θ : vertical angle of incidence of the image taken.
- B_n : perpendicular baseline as shown in Figure 5.

There is no way to remove automatically the atmospheric alterations, but they can be interpreted. In Figure 6, there are two red areas south and west of the main fringe area; these were qualified as atmospheric alterations by the ECGS/RCMA researchers, not only because they do not look like ground displacements, but also because they do not appear in interferograms calculated from different dates.

In order to allow performing interferometry, back scattering properties of the ground must remain the same between the two images acquisition. In this case, the images are considered coherent. Elements that affect coherence (Lu 2007) are the radar temperature; the space or geometry dimension, which must be very accurate; and the time, because vegetation, weather or human intervention may change the scattering conditions. Therefore, coherence measures how similar are the conditions in which the SAR images were taken. When points in an interferogram have a continuity in fringes, they are considered correlated and have high coherence; but when they are separated by noise and there is no continuity (or coherence), they may be at any distance in $\pm n \lambda/2$, where n is any number of cycles.

Since the resolution of a ground cell is much greater than the wavelength, the scattering for single cells cannot be calculated. However, some assumptions can be made (Hanssen 2001):

- There is no dominant scatterer element (of land use).
- The phase of every scatterer is distributed uniformly between $-\pi$ and $+\pi$.
- The scatterers' amplitude and phase are uncorrelated.

Given them, the coherence must be known to interpret the interferograms. An example is given in Figure 7.

Counting the fringes is how we can establish the ground displacement between points, but when there is no correlation (i.e., when the coherence is very low), the phase is not preserved and the interpretation is compromised. Furthermore, across a river or the Lake Kivu, no underwater information can be discovered (Wauthier et al. 2012).

An automatic procedure can translate from the original fringes interferogram, called wrapped or complex, to an unwrapped one. Graphic profile examples of both are in Figure 8.

The slope of the unwrapped interferogram is the same of the wrapped, but it accumulates values to show a kind of topography of the ground displacements. However, this still does not work where the correlation is interrupted. To avoid issues in the interpretation, these areas should be masked, though the process is still difficult to automate.

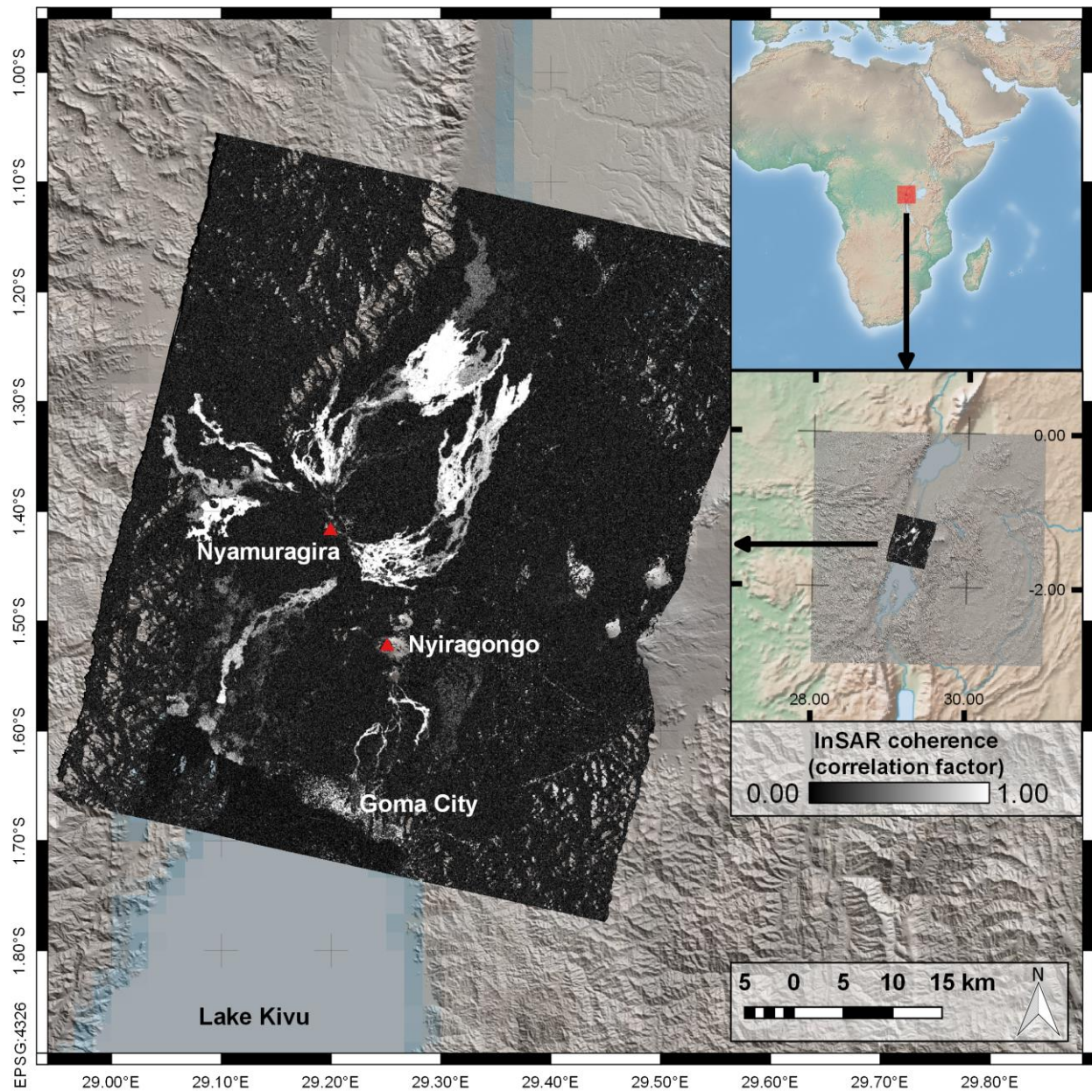


Figure 7: Coherence of an ENVISAT InSAR

The interferogram is more reliable when coherence is higher. Image and DEM provided by ECGS/RMCA, background overview from Natural Earth.

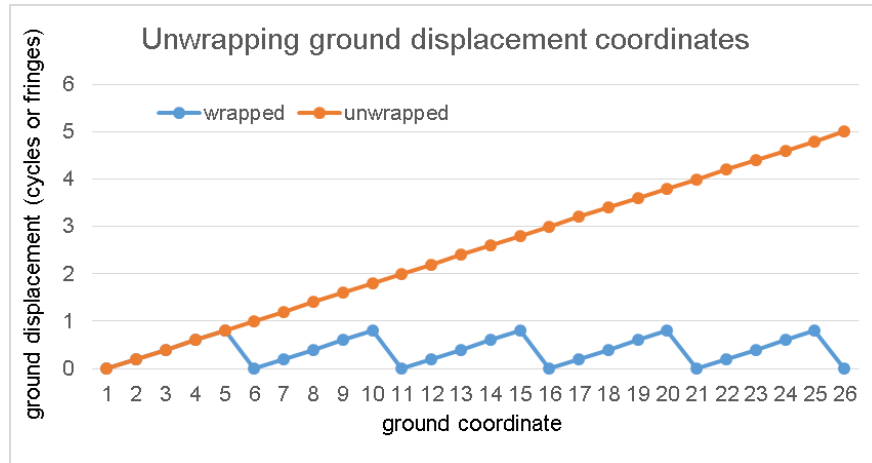


Figure 8: Unwrapping ground displacement coordinates
Based on (Massonnet and Feigl 1998).

3.2.2.SAR satellites

In Wisdom-volkano, the data from virtually any satellite SAR source may be used. The list in Table 5 includes the ones used by ECGS/RMCA, and their data are licensed by the different space agencies to their clients with more or less restriction. ECGS/RMCA retains the license of use and therefore no data is included in the software delivery except for minimal examples within this thesis. This satellite list will most likely be extended in the near future.

Some satellites can acquire images with different features like look angle, resolution, size of the footprint, polarisation... An example on how the RADARSAT-1 makes the swath and the different modes available is shown in Figure 9.

Table 5: List of SAR satellites used in Wisdom-volkano
 Wavelength = $C / \text{Frequency}$, where C is speed of light, 299,792,458 m/s (Baird et al. 1979).

Satellite, Agency	Years available	Band (wavelength)	Resolution	Swath	Revisit cycle	Satellite altitude
Envisat, European Space Agency (ESA)	2002 to 2012	C-band (5.6 cm or 5.331 GHz)	28-980 m	5-400 km	35 days	800 km
RADARSAT-1, Canadian Space Agency (CSA)	1995 to 2013	C-band (5.6 cm or 5.3 GHz)	8-100 m	45-500 km	24 days	793-821 km
RADARSAT-2, CSA	From 2007	C-band (5.5 cm or 5.405 GHz)	1-100 m	18-530 km	24 days (half an orbit difference from RADARSAT-1)	798 km
ALOS-1, Japan Aerospace Exploration Agency (JAXA)	2006-2011	L-band (23.62 cm or 1.269 GHz)	7-100 m	30-350 km	46 days (2 days for events)	692 km
ALOS-2, JAXA	From 2014	L-band (22.9 cm)	1-100 m	25-350 km	14 days	628 km
ERS-1, ESA	1991-2000	C-band (5.6 cm or 5.3 GHz)	10-30 m	5-100 km	35 days (3 days for events)	782-785 km
ERS-2, ESA	1995-2011	C-band (5.6 cm or 5.3 GHz)	10-30 m	5-100 km	Same as 1 with 35' delay (tandem)	780 km (mean)
TerraSAR-X, German Aerospace Centre (Deutsches Zentrum für Luft- und Raumfahrt, DLR)	From 2007	X-band (3.1 cm or 9.65 GHz)	1-16 m	5-100 km	11 days (4.5 days for events)	514 km
TanDEM-X, DLR	From 2010	X-band (3.1 cm or 9.65 GHz)	12 m	30 km (6 km overlap)	11 days (1 km from TerraSAR)	514 km
JERS-1, JAXA	1992-1998	L-band (23.5 cm or 1.275 GHz)	18 m	75 km	44 days	568 km
Cosmo SkyMed 4 satellites, Italian Space Agency, 2 nd generation planned for 2016	From 2007	X-band (3.1 cm or 9.6 GHz)	<1-110 m	10-200 km	16 days (<1 day for events)	619.6 km
Sentinel 1A, ESA, Sentinel 1B planned for April 2016	From 2014	C-band (5.55 cm or 5.405 GHz)	5-40 m	20-400 km	12 days (<3 h for events), 6 days with SENTINEL-1B	693 km

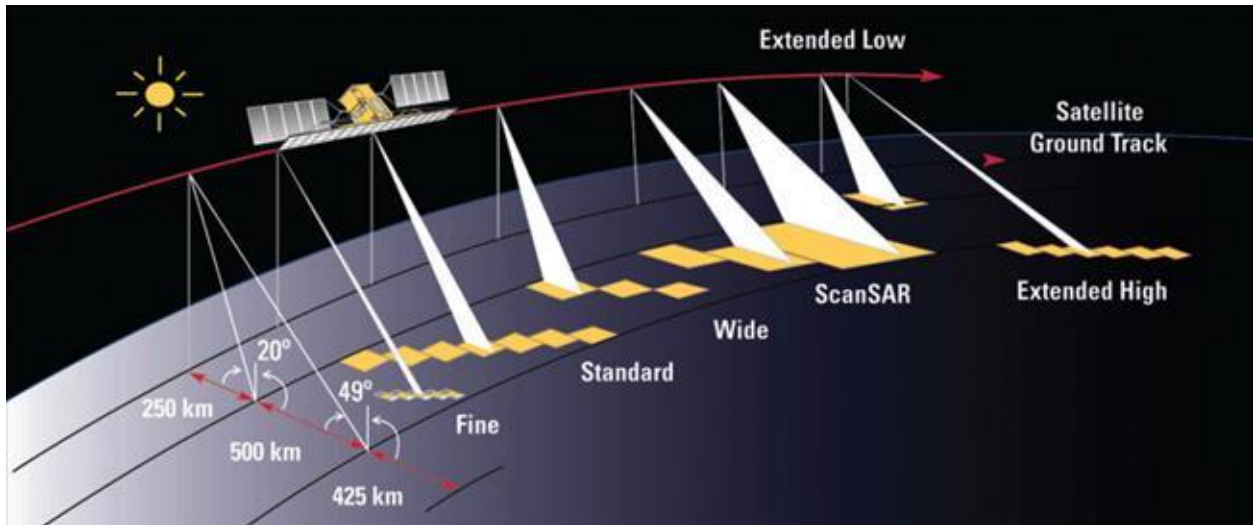


Figure 9: SAR on RADARSAT-1

© Canadian Space Agency, <<http://www.asc-csa.gc.ca/eng/search/images/watch.asp?id=460>>.

3.2.3. InSAR files

Sample files provided by ECGS/RMCA are organized in folders depending on their type: amplitude, complex interferogram (`cint`), coherence (`coh`), magnitude of the complex interferogram (`magcint`), unwrapped interferogram (`uint`) and `mask`, used for filtering out noise or other non-relevant information. The secondary folders inside each of these are organized per satellite from Table 5, while the third level is the orbit number and whether it is ascending (South to North) or descending (North to South).

This structure is not mandatory for Wisdom-volkano; is explained here as an example of how the InSAR products are available. For example, for `Asc42i5`, `Asc` means ascending orbit, `42` is the number of orbit, and `i5` is one of the possible incidence angles to which the satellite can be configured to send the SAR signal.

Inside each folder, the files are named depending on the collection; for amplitude files, it would be enough with the sequence number; for interferograms (difference between two SAR images), the naming is slightly more complicated. An example is:

```
\Cint\ENVISAT\Desc35i2\D35Nyiragongo4598_7103_AutoGEOC_LonLatCintFilt_Bp-77.4m_175days_Ha127.2m.nvi.
```

Each part is explained in Table 6.

The InSAR files given by ECGS/RMCA are in a binary format accompanied with an ASCII header file. That format is similar to the one used by ENVI, maintained by the company Harris Corporation, proprietary of the ENVI GIS software. Every image is presented in two files with the same name, but whose extensions are `.nvi` for the binary raster file, and `.hdr` for the header with the description. An example of content of the latter is in Table 7.

The first two lines describe the file. The third is `samples`, defines the number of pixels per image (columns). The `lines` defines the number of lines of pixels per each band. In this case there is only one band defined in `bands`, but if there would be more, they would be defined in

band_names. Next is header_offset, only used when the header is embedded in the raster file (not in this case). The file_type is the default ENVI, while the data_type expresses the precision of the representation; the value of 4 is a floating type, 32 bits. There are three types of interleave, bsq being the simplest: this means that lines in the same band are all sequential, and every band is stored separately. The sensor_type is here used and set arbitrarily as “Unknown”, like the final wavelength units; and the byte_order indicates that this file was generated for an Intel (Intel Corp. 2016) computer – all others, like for example Linux (Linux Kernel Organisation Inc. 2016), use a value of 0.

The map_info refers to the geographical information, and its contents are as shown in Table 8, always in the same order.

In order to read the ENVI header format, GeoServer needs a plugin called Geospatial Data Abstraction Library (GDAL) (Open Source Geospatial Foundation 2016d). However, GDAL for GeoServer has not been actively maintained since at least 2011, and though it worked in Windows (Microsoft 2016b), it did neither in Ubuntu (Canonical Ltd 2016) nor in Mac (Apple Inc 2016). Since GeoServer works natively with GeoTIFF, the files from ENVI header were converted to GeoTIFF format with QGIS. Once done, no further problems were found with GeoServer or the files.

Table 6: Parts within the file name of an InSAR image

- 4598: first SAR image, identified by the orbit number but it could be a date.
- 7103: second SAR image, from which the first is subtracted in order to get the interferogram.
- AutoGEOC: ECGS/RMCA calculation method.
- Bp-77.4m: perpendicular baseline between the two satellites points of view (see Figure 5).
- 175days: time difference between both images, taking into account that ENVISAT passes every 35 days, so it was 5 complete revisit cycles.
- Ha127.2m: altitude of ambiguity or fringe generated by DEM error.
- .nvi: format.

Table 7: Content of an ENVI header file

```
ENVI
description = {Header created auto from gridinfo (gmt) and
  LonLatMagMas.dat.grd.NoHdr on [ Fri Jan 8 13:27:02 CET 2010 ]}
samples = 601
lines = 781
bands = 1
header offset = 0
file type = ENVI Standard
data type = 4
interleave = bsq
sensor type = Unknown
byte order = 1
map info = {Geographic Lat/Lon, 1.0000, 1.0000, 29.00 , -1.1 , 0.000833333 ,
  0.000833333 , WGS-84, units=Degrees}
wavelength units = Unknown
```

Table 8: Detail on the `map_info` field from an ENVI header file

```

Projection name: Geographic Lat/Lon
Reference (tie point) pixel x location (in file coordinates): 1.0
Reference (tie point) pixel y location (in file coordinates): 1.0
Pixel easting: 29
Pixel northing: -1.1
x pixel size: 0.0008333
y pixel size: 0.0008333
Projection zone (UTM only)
North or South (UTM only)
Datum: WGS-84
Units: Degrees

```

3.2.4. MSBAS time-series

Each SAR satellite has its own orbital geometry and characteristics and acquires images with a precise revisiting period. SAR images acquired with different characteristics (mode, wavelengths, etc.) cannot be combined to produce interferograms. However, it is precisely useful combining interferograms acquired in different geometries to estimate ground displacement in horizontal and vertical components rather than only in satellite line of sight. The MSBAS methodology (Samsonov et al. 2012) was developed in order to integrate different InSAR images for producing a consistent time series of deformation. It allows integration of data with different wave-band, azimuth and incidence angles, different spatial and temporal sampling and resolution.

The data output of the MSBAS processing is a number of raster images, each showing the ground displacement in a date related to an initial date, in horizontal and in vertical direction. The stack of rasters allows calculating the displacement for each pixel in every date for the whole time-series. There is a file for each pixel; inside the file there is a list of dates, and for each, a value of displacement for the pixel for that date.

Every group of time-series has two folders (whose names are configurable, see section 3.6.1). Here `ts_name` would be `EW` or `UP`, for East-West or Up-Down ground displacement, respectively:

- `ts_name/RASTERS/`: stack of raster files in ENVI header format. The file name has the date formatted `YYYYMMDD`. Sample files are `20030116e.bin.hdr` - `20030116e.bin.nvi`.
- `ts_name/Time_Series/`: time series files with the calculation from the stack. Sample files for time series are `VVP_ML_1_Pixel_FullSerie_238_370test_EW.dat` and `VVP_ML_1_Pixel_FullSerie_238_370test_UP.dat`.

The pixel has the format `XXX_YYY` (238_370 in the example above), where `XXX` is the pixel X coordinate (longitude) and `YYY` is the pixel Y coordinate (latitude). These values are supposed to be:

- Always three characters, so all rasters must be images up to 999×999 pixels.
- Always positive values, so `001_001` corresponds to the top left pixel of the image.

Table 9 shows content from a time series file; the format is TSV. The first column is the decimal date: first comes the year followed by a point, while the rest is called a tick for the

moment during the year, where .00000 is the 1st January at 00:00:00, and .99999 is the 31st December at 23:59:59. The second value is the raster pixel value in the corresponding raster date file.

ECGS/RMCA provided some time-series already calculated, and expected Wisdom-volkano to calculate (FR13) and save (FR9) any other points. The pixel format was kept in the file naming, so coordinates must be transformed to pixels. In order to do so, the formulas in equations 4 and 5 must be applied; its graphic definition is in Figure 10.

$$\text{PixelX} = \text{round}(|\text{coordLongitude} - \text{PixelEasting}| / \text{xPixelSize}) \quad (4)$$

$$\text{PixelY} = \text{round}(|\text{coordLatitude} - \text{PixelNorthing}| / \text{yPixelSize}) \quad (5)$$

Table 9: Sample content of an MSBAS time-series file

2003.04110	0
2003.26849	0.085889235138893
2003.46027	1.1366897821426
2003.52055	0.95466285943985
...	

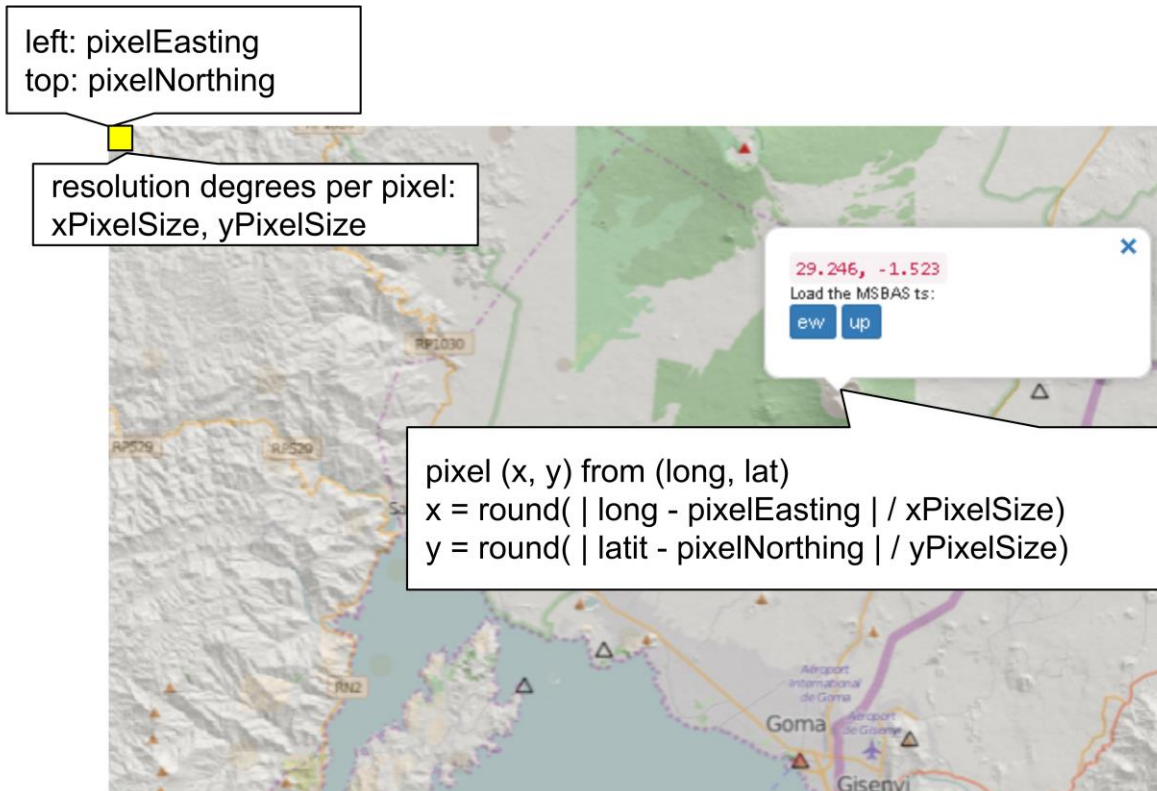


Figure 10: Coordinate to pixel calculation

Background from OpenStreetMap (OpenStreetMap 2016), DEM and stations from ECGS/RMCA. Screen capture from Wisdom-volkano.

The absolute value is used in the formula in order to convert any negative values from South or West coordinates to positive, because the pixels from the top left of the image are

always positive. The other values are found in the header of the first raster of the stack of ENVI header files.

The code for reading a pixel from an ENVI header raster file is in [Source code 1](#) (all pieces of source code can be found in the appendix). Lines 5 to 7 calculate the offset needed to reach the pixel in the file. After it is open (line 3), the file pointer is positioned at the correct place (line 8) and an amount of bytes corresponding to the data type is read (line 10). In case the files were generated in a little endian machine (calculated from 13 to 16), the bytes are then reversed (line 18). Finally, they are converted from binary to an array or unpacked in PHP (line 20) to get the second value (line 21), which is the pixel value.

For example, the coordinates shown in [Figure 10](#), 29.246°, -1.523° are actually 29.246° East 1.523° South; given the default values in the ENVI header file (see `map_info` in [Table 8](#) and equations 4 and 5 above), the calculation would be:

```
PixelEasting: 29
PixelNorthing: -1.1
xPixelSize: 0.00083333
yPixelSize: 0.00083333
PixelX = round( | 29.246 - 29 | / 0.00083333 ) = 295
PixelY = round( | -1.523 - (-1.1) | / 0.00083333 ) = 507
```

The pixel corresponding to that coordinate is found in column 295, row 507.

3.3. Data sources: seismic events

Volcanic tremor is a type of seismicity associated with active volcanoes, whose duration (up to days or even weeks) is longer than that of earthquakes ([McNutt 1992](#)). Also, the frequency is usually lower (1-9 Hz). Almost all eruptions have seismic activity associated, but not always the opposite. The consequence is that long, low frequency seisms usually indicate an active volcano ([Fehler and Chouet 1982](#)). Another characteristic of volcanic tremors is the amplitude, which varies several orders of magnitudes during time and must be normalized.

Volcanic seismic activity is measured with seismographs, which are placed inside the crater, near it or up to kilometres afar. For increased precision, also on where the tremor originated, a network of seismographs is needed.

A seismograph consists of an oscillating mass (pendulum) attached to a grounded base; during an earthquake, the base moves while the mass tends to stay still ([Graizer and Kalkan 2008](#)). The motion can be directly transcribed on paper, but nowadays it is usually digitally archived. A single pendulum only records one direction of the motion, so modern seismographs include at least three, covering the three dimensions of the space.

The result is called a seismogram, where the x-axis shows time, and the y-axis displacement. A straight line means no tremor, but when the pendulum starts balancing, there is a seismic wave arriving. First to come are the P-waves, which propagate in the same direction that particles move and travel through solid and liquid. P stands for pressure or primary, depending on the source. Some time later the S-waves (shear or secondary) come, perpendicular to the particle movement, and which do not travel through liquid, including magma. The S-waves are slower

than the P-waves, and the time gap between the two helps estimating the distance to the epicentre (T. Mavonga et al. 2010). An example is given in Figure 11.

These waves usually can be grouped in events, so we can separate them (Fehler and Chouet 1982; Tuluka Mavonga et al. 2006; McNutt 1992) in:

- Short-period (SP) events: differentiated P and S phases, with at least 5 seconds in between. They have high frequency, around 5 Hz. Similar to tectonic earthquakes, in volcanic context these are interpreted as breaking rocks due to magma pressure (Smets et al. 2013).
- Long-period (LP) events: weak or no P phase, low-frequency waveforms (1-3 Hz) and emergent or no S phases. LP earthquakes are interpreted as fluids moving (water, gas, magma) inside the volcano.

In Virunga mountain Range, LP events can precede eruptive episodes during months (Tuluka Mavonga et al. 2006; Smets et al. 2013). Sometimes significant changes are observed in LP and SP rate, and some of these changes may be related to upcoming eruptions.

1906 – NS component recorded at Gottingen, Germany

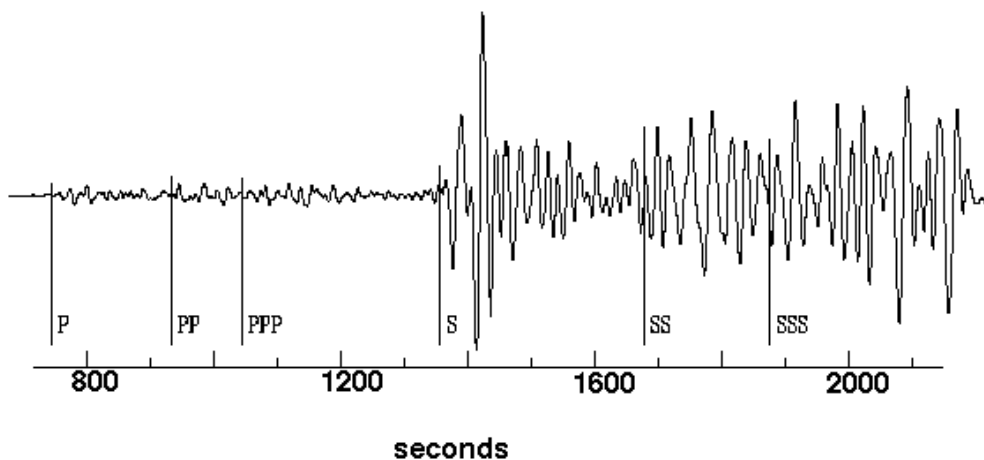


Figure 11: The 1906 San Francisco earthquake, detected in Gottingen (Germany), 9100 km away
 Detail of P- and S-waves, the latter arriving ~1350 seconds later. PP, PPP, SS and SSS are replicas of the original P- and S-waves after bouncing once or twice on the Earth surface. Image from USGS
http://earthquake.usgs.gov/regional/nca/1906/18april/got_seismogram.php.

3.3.1. Seismic stations

Data produced by the seismic stations are the property of Observatoire Volcanologique de Goma and therefore are not included in the software delivery. Only the minimal part needed to develop Wisdom-volkano was provided.

In 2013 (Smets et al. 2013), nine seismometers were installed in the zone, although not all of them were working:

- Five SS-1 Ranger seismometer from Kinematics (Pasadena CA, USA) (oscillation measuring up to 1 second).

- Three Lennartz (Tübingen, Germany) LE-3D/5s (low frequency sensitivity: up to 5 seconds).
- One Nanometrics (Kanata, Canada) Trillium 40 broadband (sensitivity up to 40 seconds).

The seismic counting data analysed only two stations (LBG and KBB), which were the only ones that had limited interruptions in data registering during the eruptions from November 2009 to February 2010.

Since 2015, the new network of seismograph stations maintained by ECGS, Kivu-S-Net, has replaced the whole seismic monitoring network with 13 broadband stations telemetered in real time, in the frame of the Resist project (Kervyn et al. 2015). The generated data will remain the property of ECGS/RCMA.

A list of seismic stations situation (points) was given by ECGS/RMCA in KML which are partially shown in Figure 12. This format is based in XML notation, and was established by a company acquired by Google, and then released as international standard of the OGC in 2008. Google Earth (Google 2016c) was the application to edit KML, though nowadays many GIS can work with it, including OpenLayers but not GeoServer.

The `Seismos.kmz` file was unpacked (KMZ is a ZIP-compressed KML) with 18 place marks, including seismic stations already installed, some to be, and some which are not emitting for different reasons, usually damaged. The stations extend into Rwanda.

OpenLayers loads natively KML files, so they were implemented directly in JavaScript and not read through the WMS from GeoServer like the other layers. However, during the presentation of the second iteration, the ECGS/RMCA spotted that stations supposed to be close enough (or in the same place) were shown apart by OpenLayers, no matter the zoom. GeoServer does not support KML files natively for features, so the KML was converted to Shapefile format (which is supported) with QGIS. They were then loaded in GeoServer and called with OpenLayers from Wisdom-volkano, what solved the issue.

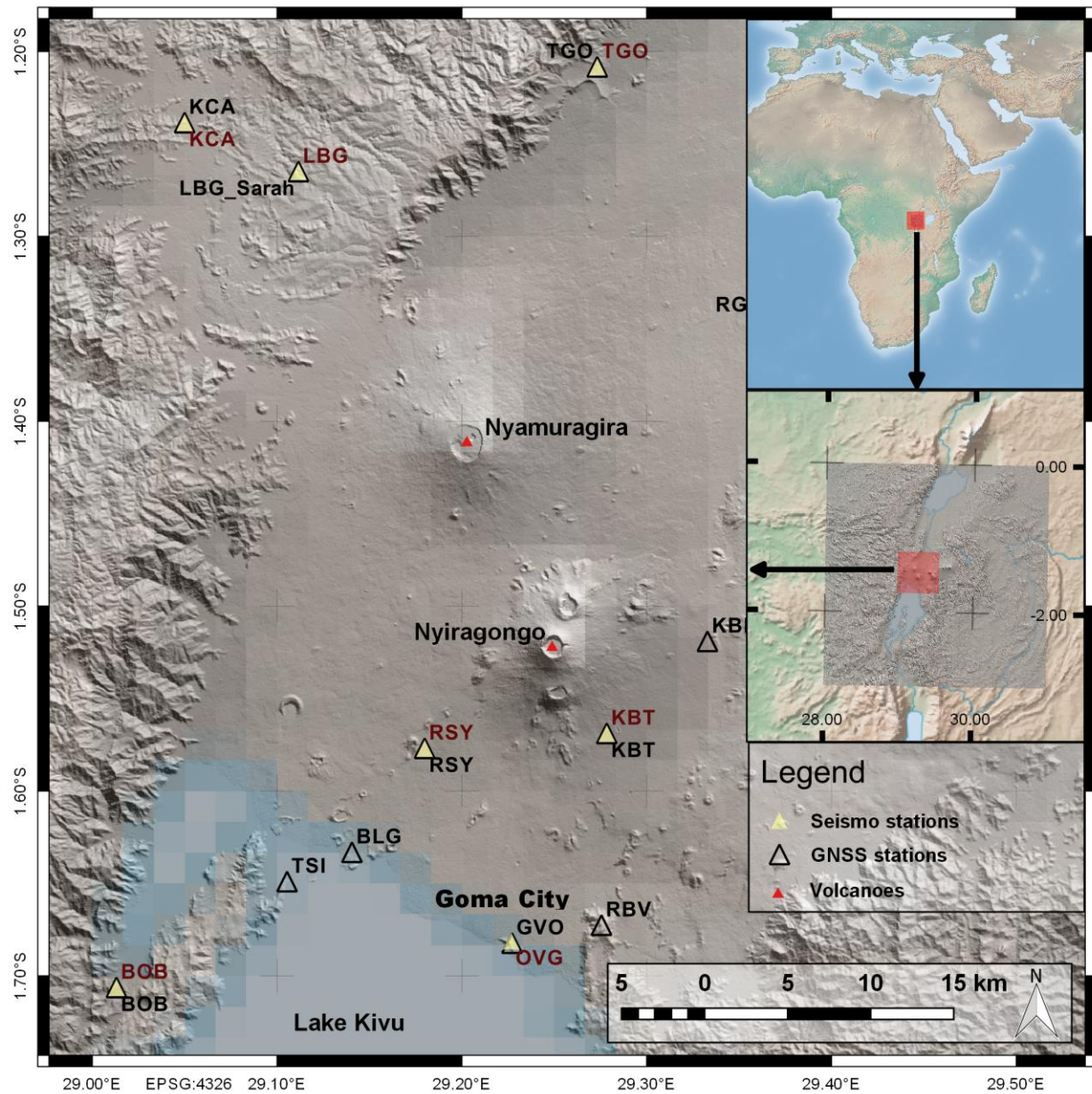


Figure 12: Seismograph and GNSS stations network by ECGS/RMCA
 Stations data and DEM provided by ECGS/RMCA, background overview from Natural Earth.

3.3.2. Seismic events localization

Sometimes before an eruption, and at the same time that the LP and/or SP occurrence varies, another seismic variable may be of importance: the hypocentres (place under the Earth surface where an earthquake or volcanic seismic event energy is first released) (Kukowski 2013) may become shallower (T. Mavonga et al. 2010; Smets et al. 2013), so it is relevant to know how deep they are and show their magnitude. The velocity of the waves allows calculating the top of of

the layer in kilometres and, as explained above, the distance between the S- and P-waves allows to calculate their distance and therefore, to know where their epicentres are.

Data about the localization of such seismic events hypocentres were sent from ECGS/RMCA as a comma-separated values (CSV) formatted file with the name `DataExtracted_300km_-2.73S+0.08N_28.5W30E_1973-2008_removed_mb-None.txt`. The content of the first lines has been formatted in Table 10 for improved readability.

Table 10: Sample content of a seismic localization events file

Year	Month	Day	Time UTC	mb	location	Long	Lat	Depth (km)	Depth (miles)
1977	12	29	11:50:38.00	5.4	LAKE EDWARD REGION	29.683	0.013	33	(20.5052 mi)
1977	1	6	18:33:43.50	5.3	LAC KIVU REGION	28.702	-2.509	21	(13.0488 mi)
1977	4	14	14:36:23.40	5.2	RWANDA	28.940	-2.456	33	(20.5052 mi)
Etc.									

The first line contains the titles. Dates had to be added to a single column in QGIS, and the whole text file be converted to a format understood by GeoServer. This was the process:

1. Load the CSV text file into QGIS, assuming projection “WGS84 EPSG:4326”.
2. Remove lines with magnitude (column “mb”) value “None”. They are not relevant to this exercise and prevent the column to be treated as numeric.
3. Convert to shapefile format. This allows to add columns.
4. Open attribute table, toggle edit mode, add column, name date, type date.
5. Open field calculator, update date column, formula:
`todatetime(concat("Year", '-',lpad("Month", 2,'0') , '-', lpad("Day",2,'0') , ' ',left("Time UTC",8))`
6. Save edit and toggle edit mode.

The shapefile is ready to be imported to GeoServer.

3.3.3. Seismic events counting time-series

Data on counting seismic events was made available by ECGS/RMCA in format `.xlsx`, an Office Open XML spreadsheet format developed and used by Microsoft. It was converted with Excel (Microsoft 2016c) (though this can be done with many other open or online tools) to a CSV format, a text file with a tabular structure similar to a spreadsheet. From CSV, any text editor will allow a quick replacement of all commas per tabs, so the file is converted to the TSV format used by Wisdom-volkano.

The file name is the acronym of the station, like `BOB.tsv`. Its content looks like Table 11.

Table 11: Sample content of a seismic station on counting events file

Date	LP	SP	LP-accumulated	SP-accumulated
01/01/2010	1	0	1	0
02/01/2010	2	1	3	1
03/01/2010	21	0	24	1
04/01/2010	36	0	60	1
etc.				

The first line contains the titles, and every value is tab-separated. There are 5 columns:

- Date: the file is ordered under this value, from the oldest to the most recent one.
- LP: long period earthquakes accounted in that station on that day.
- SP: short period earthquakes accounted in that station on that day.
- LP accumulated: all LP added up from previous days + those of the current day.
- SP accumulated: all SP added up from previous days + those of the current day.

3.4. Data sources: GNSS

3.4.1. GNSS receiver stations

The general term GNSS (Global Navigation Satellite System) is usually better known with the acronym GPS (Global Positioning System) (U.S. Air Force, Arlington County VA, USA), though the latter has been specifically developed in the United States. Other examples of GNSS are the European Galileo (ESA and European GNSS Agency, Prague, Czech Republic), the Russian "GLObal NAVigation Satellite System" (GLONASS) (Russian Aerospace Defence Forces, Moscow, Russia) or the Chinese BeiDou (China National Space Administration, Beijing, China). In every case, "system" means a set of satellites that emit signals that allow a user on the Earth (or in an airplane) to determine its position.

Basically, distance from the satellite is calculated with the time that takes the signal to travel to the receptor. But that distance could be any place on the surface of a sphere; thus, the position can only be calculated with three or more signals from different satellites at the same time, as shown in the [Figure 13](#). Four signals are the usual minimum for confidence.

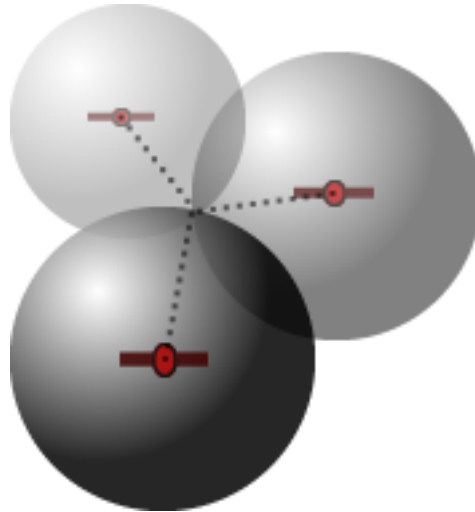


Figure 13: GNSS localisation based on intersecting spheres

The GNSS antennas and receivers form a network called Kivu-G-Net and is being developed and maintained constantly by ECGS (Geirsson et al. 2016). Data produced by receivers remain the property of ECGS/RMCA and therefore are not included in the software delivery. Only the minimal part needed to develop Wisdom-volkano was provided.

Three types of GNSS receivers/antennas are used:

- Leica (Leica Geosystems, Heerbrugg, Switzerland) GMX902GG receivers with Leica AX1202 antennas, able to connect to GPS and GLONASS. The GMX902 cannot store data, so it has to be permanently connected via its only serial port to the Universal Serial Bus (USB) connector of a tiny Raspberry Pi2 (Raspberry Pi Foundation, UK) computer, as well as sending the signal over radio to a dedicated computer in Goma city or sending the data via modem directly to Luxembourg by Internet.
- Leica GR10 receivers, able to connect to GPS and GLONASS. They have internal memory to store the data and are able to send data via modem directly to Luxembourg by Internet.
- Trimble (Sunnyvale CA, USA) NetRS receiver with Trimble Zephyr antenna, able to process GPS only. It also has internal memory to store the data and is able to send via modem directly to Luxembourg by Internet.

Receivers and antennas are mounted in so-called monuments in order to maximize the signal reception and minimize interferences.

Since the Democratic Republic of the Congo is politically and military unstable (Kisangani 2012), the places must be very carefully chosen in order to be protected. Moreover, the Kivu region is on top of two different and active tectonic plates, and its tropical climate is prone to lightnings, which makes it even more difficult to find potential places. Furthermore, proper bedrock is needed for the monuments.

As the Galileo satellite network and others are being completed, more data will be available. In addition, ECGS/RMCA is actively maintaining the stations with regular trips to Kivu. This will make the data flow more stable and therefore useful.

The list of GNSS stations situation (points) is given in KML format, and its integration is the same as the seism stations file in 3.3.1 and are shown in Figure 12.

Finally, the data source concerning ground displacement maps was not included in any delivery and has not yet been processed with Wisdom-volkano.

3.4.2. GNSS data files

The data is provided by the ECGS/RMCA in text files named like `station.enu` with content in rows as shown in Table 12.

Please note that the first column is separated from the rest with a tab character, while the remaining values are separated with spaces. There are no column titles, though they were explained by ECGS/RMCA:

- Date is in decimal format (explained in section 3.2.4).
- Next three values are the displacements in (x, y, z) or (longitude, latitude, elevation), measured in millimetres (they will be presented in centimetres in the chart). First row must be zero and is set at the station installation, so all displacements are measured from there.
- Last three values are the uncertainty of the displacements and are not used for this project, but they could for control purposes.

Table 12: Sample content of a GNSS station file

2009.33835616	0	0	0	0.499084	0.350243	6.31765
2009.34109589	1.6	2.3	-7.7	0.234611	0.181749	3.24396
2009.34383562	1.6	2.5	-3	0.288124	0.213118	3.60125
2009.34657534	0.4	4.8	-12.9	0.218981	0.178132	2.87382
2009.34931507	-0.7	5.2	-11.5	0.19963	0.151955	2.54887
...						

3.5. Functional analysis

After the FR were established a mock-up was produced (Figure 14), which shows the main distribution of Wisdom-volkano visualization elements in the web browser:

- An administration menu on the top.
- Layers on the left, collapsible to gain space, with background layers.
- A configuration panel for the time-series chart below the layer panel.

- The main map view occupying as much space as possible on the screen, with some points already selected.
- The chart for the time-series of the points selected in the map below it.
- The complete data tables for the time-series shown, space allowing and in case ECGS/RMCA would want to keep it.

When a point is clicked on the map, Wisdom-volkano announces the MSBAS time-series configured (in [Figure 15](#), the two blue buttons `ew` and `up`). As shown in [Figure 16](#), when one of them is chosen, the application performs a series of actions:

- i. Transforms the coordinate of the point to pixels.
- ii. Builds the file name with the pixel (column, row) information.
- iii. Checks the time-series folder to see if such a pixel has already been calculated.
- iv. If yes, nothing to be done, it goes directly to the two final steps.
- v. If not, it reads the folder with the raster files.
- vi. For each raster in the folder:
 - a. It extracts the date from the raster file name.
 - b. It opens the file to read the exact pixel value in it.
 - c. It writes date (from a.) and pixel value (from b.) into a new time-series file.
- vii. It writes the time-series file to the time-series folder.
- viii. Wisdom-volkano reads the time-series file point.
- ix. And finally shows the time-series in the chart.

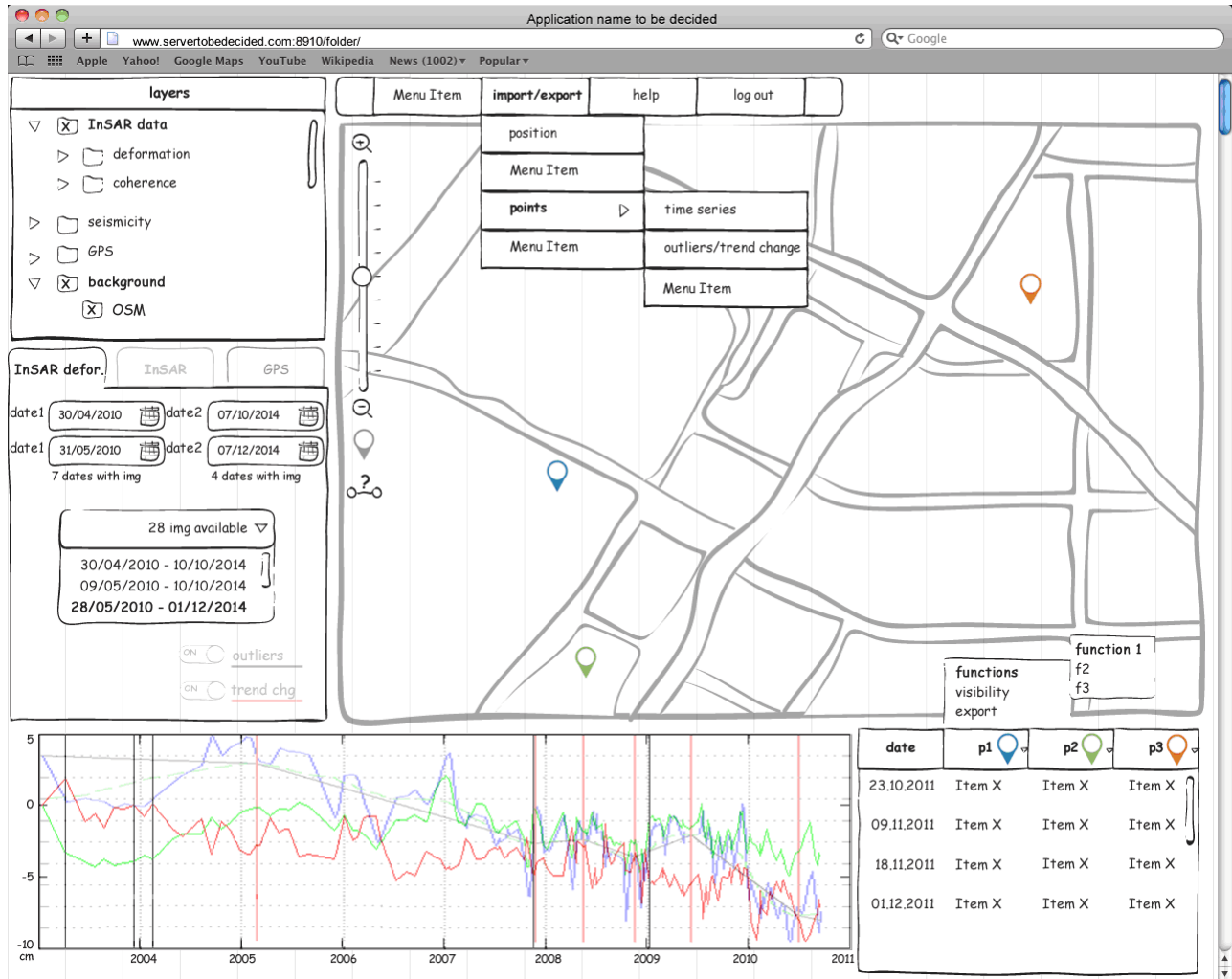


Figure 14: Mock-up of Wisdom-volkano

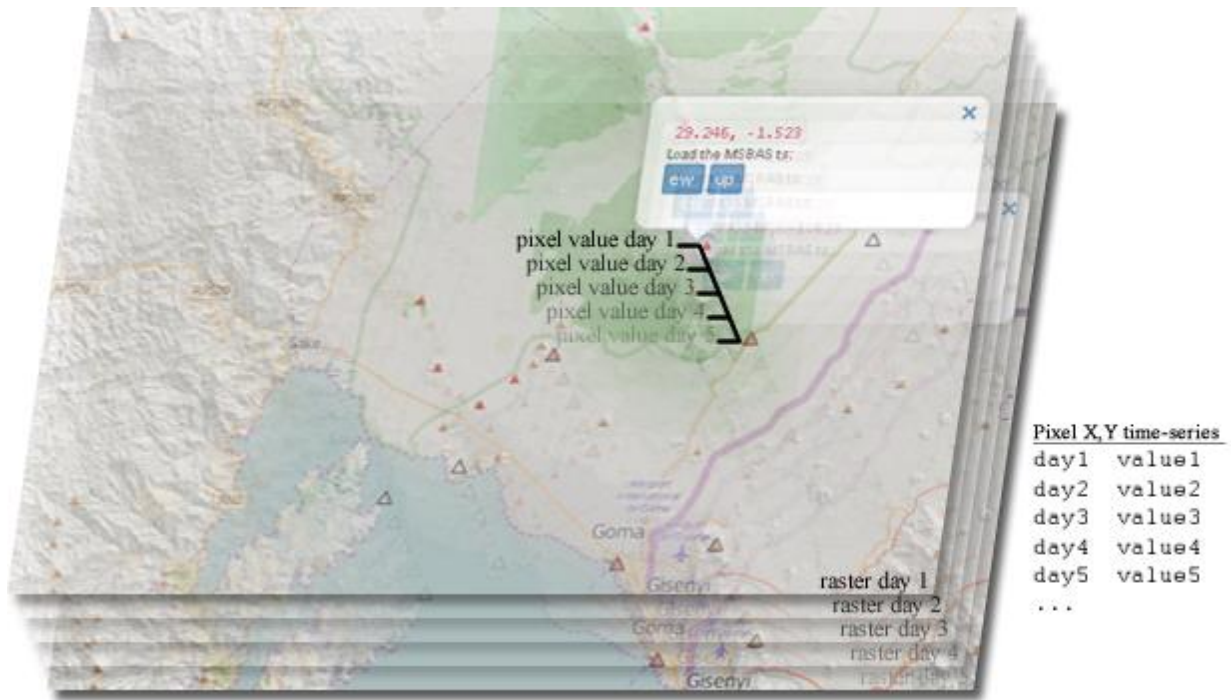


Figure 15: Simulation of the time-series calculation from the rasters stack
Background from OpenStreetMap; DEM and stations from ECGS/RMCA.

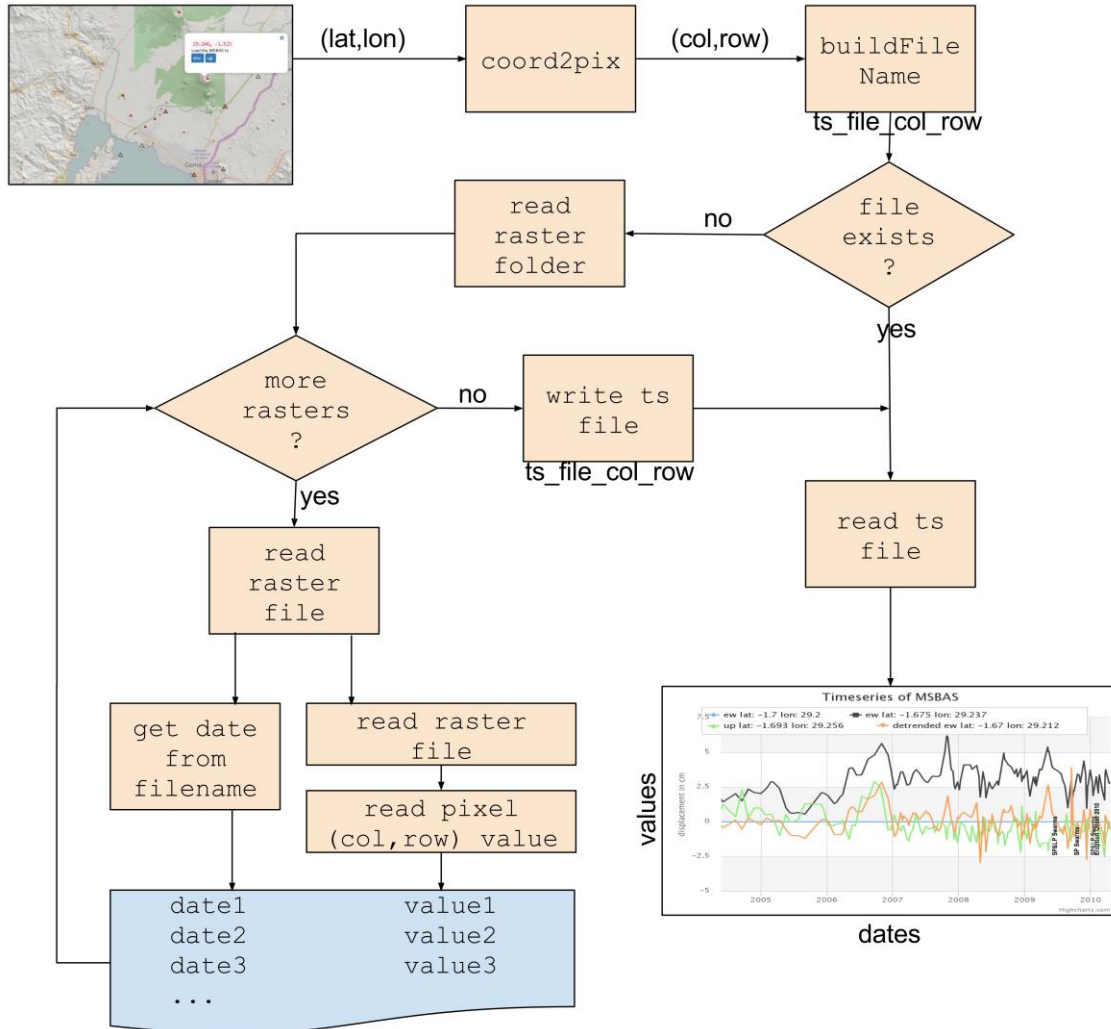


Figure 16: Flow diagram from a map point to displaying MSBAS time-series

3.6. Software architecture

The diagram in Figure 17 provides a high-level view of the system architecture with all the software components and technologies used to build and deploy the Wisdom-volkano.

As a web client server application, there are no special requirements for the Wisdom-volkano, other than a highly W3C standards compliant browser, such as Mozilla Firefox, Safari or Google Chrome. It is not shown in the above list of client software and technologies, but needed nonetheless.

OpenLayers		Highcharts	Bootstrap	HTML5	CSS3	Client	
Google Maps, OpenStreetMap	GeoServer [+GDAL]		Time- series files	CodeIgniter + Ion Auth + cURL		Framework	
	PostGIS	Geo files		Apache httpd		PHP	App server
					PostgreSQL		DB
Linux / Mac / Windows						System	

Figure 17: Wisdom-volkano software architecture stack view

For the client, a laptop with a standard browser is enough, though a screen with a fairly good resolution is advisable. For the server, it will depend on the common minimal requirements for running the software components specified in the next sections. The communication between server and client would be either through internet or an internal network.

In the case of portability, that is, when the server tier and the client are in the same computer (usually a laptop to bring to the terrain), then these minimal requirements may be critical and should be tested in advance. Neither GeoServer nor PostGIS, which are the most demanding applications, provide the list of their minimum requirements in their respective websites. However, upon experience of the author, a recent laptop with Linux, Mac or Windows, a quad-processor with at least 8 GB of Random Access Memory (RAM), and a Solid State Drive (SSD) hard disk big enough for the database and files, will be necessary.

The following sections develop the stack overview from Figure 17.

3.6.1. Database and code source deliveries

First, the database PostgreSQL and its geospatial complement PostGIS must be downloaded and installed. Tables needed were created following the well-known data normalization procedure of a database (Chen 1976; Yourdon 1989). The database or entity relationship diagram is shown in Figure 18. The complete scripts for creating the tables are delivered along with the source code of Wisdom-volkano.

The source code architecture is MVC, which separates the database part (model) from the user part (view) and the business rules (controller). Some functionalities of the client website are based on the Bootstrap (Bootstrap 2016) open source framework library and jQuery (Resig 2016) open source JavaScript library, which are cross-browser. None of them has to be downloaded; all are included in the source code delivered. Each release, together with installation instructions, has been uploaded to GitHub (GitHub Inc. 2016) under github.com/fulgen/Wisdom-volkano, announced to ECGS/RMCA by email and presented in person after each iteration.

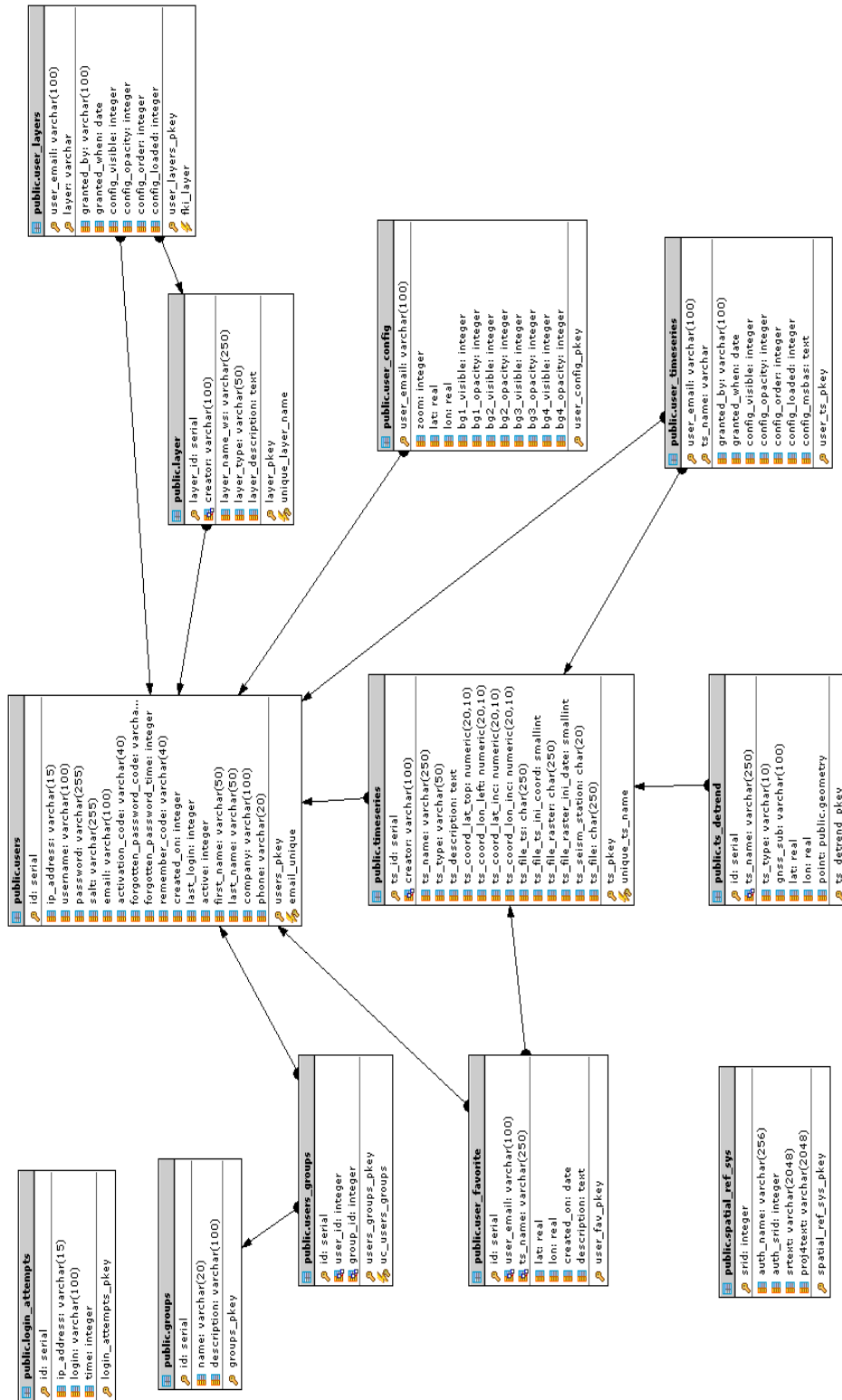


Figure 18: Entity – Relationship database diagram
 Created with PostgreSQL Maestro (SQL Maestro Group 2016).

3.6.2. Geospatial visualization with GeoServer and OpenLayers

The data source files provided by the ECGS/RMCA should be available in a local or mounted folder where they will be added in GeoServer. Although it is technically possible not to use it and show the maps directly through OpenLayers, it is highly recommended to install it as geographic middleware support for its performance, compatibility and functionalities (Theeten 2011). For Linux systems, GeoServer is distributed in web archive format, to be deployed in a servlet container like Tomcat (Iacovella 2014). Also, for some raster file formats like the ENVI-header, GeoServer needs the GDAL extension installed, but as explained, this can be overcome with a conversion to GeoTIFF or shapefile.

OpenLayers is a JavaScript library that allows loading and showing many raster and feature types of data sources on the browser and interact with them, with a number of features, such as the possibility to tile rasters in order to avoid the entire images to be loaded at once, instead splitting them into smaller pieces that are loaded and shown depending on the zoomed region.

Figure 19 shows the interfaces of GeoServer used by Wisdom-volkano. The list of available workspaces from GeoServer can be obtained via a REST interface, that is, via Hypertext Transfer Protocol (HTTP) (Fielding et al. 1999) as if GeoServer was administered via a web page. The access can be done with code PHP as shown in Source code 2, with the cURL (Stenberg 2016) free software. GeoServer replies in XML, which must then be parsed in order to obtain the workspace names. Line numbers are added and code is slightly adapted to highlight only the main parts.

Likewise, the list of rasters or layers for a given workspace can be obtained with a similar call, except for the line 4, which would become for raster and layers, respectively.

In Source code 3, the "cint" part is the workspace and is used as an example for complex interferograms. Any layer on this workspace would be called "cint:layer_name". This is not mandatory in GeoServer, where all layers may share the same workspace, but it helps classifying and maintaining with complex datasets like interferograms, where there are different products.

GeoServer maps, on the other side, can be accessed via its WMS; basically, a request similar to asking for a web page (via HTTP), though the returned content is a georeferenced image, for example in Portable Network Graphics (PNG) (Boutell 1997) format. The connection is done from the web page in JavaScript with the OpenLayers library in the way shown in Source code 4 (this can be done with several layers at the same time).

The seismologic and GNSS stations were added in the second iteration in KML format directly into OpenLayers, as can be seen in Source code 5.

However, as explained in section 3.3.1, KML files were converted with QGIS into shapefiles and added to GeoServer with the workspace and names, as shown in Source code 6. This corrected the error mentioned about the stations shown apart, and resulted in the correct map shown in Figure 12.

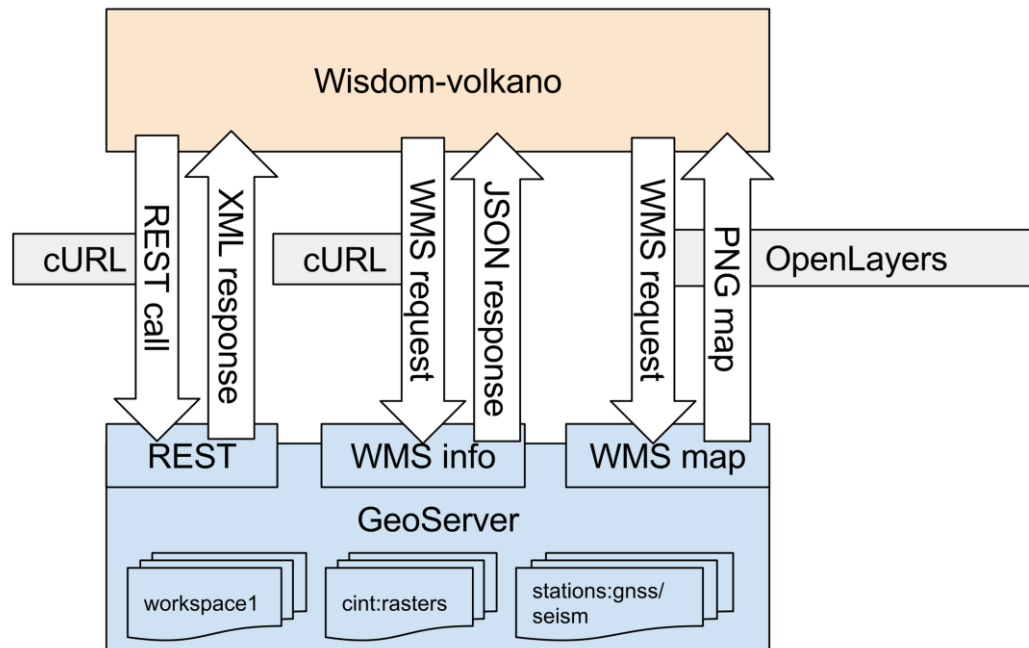


Figure 19: GeoServer interfaces used in Wisdom-volkano

At this point, the map is shown in Wisdom-volkano with as many layers as calls done as in Source code 4, plus the stations from Source code 6, plus the default background layers, Google Maps and OpenStreetMap, which are defined in a similar way (Source code 7).

But that is not enough to show a Google Maps layer. First, a personal Application Program Interface (API) key from its website must be created and written in the Wisdom-volkano configuration file. An additional library to connect Google Maps via OpenLayers is needed (Schivei Costa 2016), also included in the software code source.

For ordering layers in a list, the jQuery Sortable (von Andrian 2016) open source library plugin is used. Other functionalities are taken from the examples of OpenLayers, like the layer grouping, overlays, the scale or the permanent link to keep the status.

When clicking on the map, Wisdom-volkano carries out the following events (shown in Source code 8):

- When geographical coordinates are entered manually, they must be reprojected (line 1). See 3.7 for more information on coordinates.
- The main process can be done for one or several layers at the same time (lines 2-5 and line 13 can be repeated as many times as needed).

Then, Wisdom-volkano makes an asynchronous JavaScript and XML (ajax) (Garrett 2005) call to a CodeIgniter controller (Upton 2007), which will check which of the layers have information for the coordinate.

This call in the controller is done via cURL in a similar way (Source code 9) as Source code 2 though the JavaScript Object Notation (JSON) (Crockford 2006) format has been

specified. The URL query in `urlLayer1` (line 12) and `result` (line 15) in JSON, both from [Source code 8](#), are printed in [Source code 10](#).

Complex interferograms need a specific SLD description so the fringes may be shown properly ([Figure 6](#)), given its range of values: \pm half wavelength of the satellite, and since the value of both extremes equals to same distance, they shall have the same colour.

3.6.3. Time-series visualization with Highcharts

Highcharts is a JavaScript library used to handle and properly show time-series data. In order to use the import data feature and the image export, the corresponding modules must be downloaded as well. Highcharts also needs jQuery: all are included in the Wisdom-volkano delivery.

By default, Wisdom-volkano shows a single chart with events data. The list of events was provided by ECGS/RMCA by email and is shown in [Table 13](#) (“Unreliable” or “Swarms” are their annotations).

These events are loaded via a JavaScript array, with a date and a description ([Source code 11](#)); then it is loaded into a default empty Highcharts chart ([Source code 12](#)).

After selecting a position and the eventual time-series it will be loaded in the default chart via an ajax call.

Table 13: List of events near the volcanoes

```

Eruptions:
Onset 2011 : 2011, 11, 6
Second Cone 2011 : 2011, 11, 29
End 2011 : 2012, 4, 1 (* UNRELIABLE *)
Onsetr 2010 : 2010, 1, 2
End 2010 : 2010, 1, 27
Local Earthquakes
Lieu blabla : 2011, 9, 16
Lieu blabla : 2011, 2, 4
Kigali : 2011, 5, 23
Lieu blabla : 2015,08, 07
Lake Albert 1: 2013, 7, 2, 13h33m18s
Lake Albert 2 : 2013, 7, 3, 19h21m46s
Lake Albert 3 : 2013, 7, 3, 22h22m18s
LP Swarms
2012, 3, 14
SP Swarms
2009, 9, 15
SP&LP Swarms
2009, 5, 15
2009, 12, 15

```

3.6.3.1. MSBAS time-series ajax calls

An MSBAS time-series is related to the raster by its extent, by default. Please note that the latitude coordinates are negative (southern hemisphere) and this was hardcoded (as printed in [Source code 13](#) and [Source code 14](#)). This call will echo a JavaScript code ([Source code 12](#)) to load the time-series file ([Source code 15](#)).

This time-series load works as follows:

- Given a total number of MSBAS point time-series to be loaded ($\$totMsbas$), all their TSV files are loaded (lines 1 to 9).
- Then, they are read line by line (lines 20, 21).
- Split by the tab character (line 23).
- The date is parsed (line 24).
- Data are stored in an array (line 25).
- Title of the time-series is constructed (lines 30-31).
- The array data is assigned to the time-series (line 34).
- All this code is echoed (returned) back to be executed: this is done after reception of the ajax call in JavaScript ([Source code 16](#)).

This complete ajax call is actually very difficult to debug and maintain. The alternative would be reloading the whole page when adding or removing every time-series, which is not very user-friendly ([Kluge et al. 2007](#)).

3.6.3.2. Stations time-series

When there are station based time-series, either seismic or GNSS, they are called in the same way with ajax. Time-series are related with the station name as loaded from the KML file, shown in [Source code 17](#). They will use their own charts (one per each source data and station), which is done with JavaScript to create HTML `<div>` on the fly ([Source code 18](#)).

Also, to be able to remove the time-series `<div>` chart and unload it from memory, there is a snippet of code ([Source code 19](#)) added to each chart, after the [Source code 15](#).

3.6.4. Detrending time-series

Ground deformation may have trends due to tectonic or other natural (yet non-volcanic) movements ([Van Dam et al. 2001](#); [Samsonov et al. 2012](#)). In order to remove these trends (or regression lines) from MSBAS and GNSS time-series, a user may zoom into a section where the trend is more evident and select the detrend function, which will perform the algorithm of equations 6 and 7, based on the estimation through least squares ([Burt and Barber 1996](#)).

The implementation is as follows:

1. Calculation of linear regression based on the subset zoomed data (Source code 20).
2. Calculation of trend values for the whole time-series, based on the regression parameters from 1 (Source code 21).
3. Detrend the original, whole time-series, removing the trending (Source code 22). Offset is optional.

$$a = \frac{\sum_{i=1}^n Y_i}{n} - b \frac{\sum_{i=1}^n X_i}{n} \quad (6)$$

$$b = \frac{n \sum_{i=1}^n X_i Y_i - \sum_{i=1}^n X_i \sum_{i=1}^n Y_i}{n \sum_{i=1}^n X_i^2 - (\sum_{i=1}^n X_i)^2} \quad (7)$$

3.7. Coordinates

When publishing maps, coordinates are always an issue because of the projection used. In this section the basics of the problem are presented, and how they are treated in Wisdom-volkano, with the transformations done.

A projection is a procedure to transform a three-dimension reality (like the Earth) into a plane surface in paper or in screen (Van Sickle 2010), which depends on several variables, like the approach (cylindrical, conical, etc.) and the place of application of the bi-dimensional plane to it (Snyder 1997; van Wijk 2008). Already in the 16th century Mercator created one very useful to navigate in the far North, the use case needed at that time: it showed the angles between points. The projection bears its name and takes account of the Earth from a cylinder, with the same radius for the Equator and the Poles, which is not very accurate (Battersby et al. 2014; Slocum et al. 2010). Other projections are more suitable for working in GIS.

The mentioned three dimension reality is modelled with spheroids, that is, with ellipses rotating on an axis. Then, specific datums add local height variations to the spheroid in which they are based. Probably the most used datum is the World Geodetic System (WGS) WGS 84 (National Imagery and Mapping Agency (NIMA) 2000). By default, most GIS tools work with it, such as Google Earth and KML files. All coordinates shown in this thesis use this, except otherwise stated.

In many websites showing maps today, however, use a projection called Web Mercator or Spherical Mercator (Battersby et al. 2014). This is the one used by many online mapping services, including Google Maps, Bing Maps (Microsoft 2016d), ArcGIS online, OpenStreetMap and OpenLayers (Aitchinson 2011). However, since it is based on the original Mercator, it has one major problem: Canada, Norway, Antarctic and any region near the Poles have their size augmented.

The United States Departments are issuing recommendations not to use Web Mercator or at least know well the problems (Battersby et al. 2014; National Geospatial Intelligence Agency 2014). But it is hard to avoid it when working with online GIS mapping tools. Worth noting: Eurostat has chosen Lambert Azimuthal Equal Area projection for all the maps in the common GIS for the European Union (Annoni et al. 2001) (though this projection does not cover overseas territories).

A much better projection for the relatively small areas covered by the data sources used in Wisdom-volkano would be the Universal Transverse Mercator (UTM) 35S (Defense Mapping Agency 1989). It is situated in the southern hemisphere around the Virunga region: between 24° and 30° East, and -80° and 0° South. This projection is indeed used by the ECGS/RMCA in the newer interferogram products (see section 4.4.1).

So here there is a confusing issue in web GIS: querying GeoServer’s WMS from Open Layers (Source code 10) is done in meters of Web Mercator (a projection), as shown in `BBOX` parameters at the end of the URL. However, the response is given in decimal degrees of WGS 84 geographical coordinates (a datum).

The transformation between these two is easy in OpenLayers. Basically, all coordinates either at GeoServer or in Wisdom-volkano are shown in WGS 84, but the communication between GeoServer and OpenLayers is done in Web Mercator. To confirm so, the JavaScript Source code 23 is run every time that the main screen is loaded, which logs the projection to the console (the output is EPSG:3857, another name for Web Mercator).

Inside Wisdom-volkano, and in order to simplify the pixel calculation (see Figure 16), and visualization in the screen, just three decimals are kept from the degrees, as shown in Source code 24. This implies that each pixel is a square on the ground of around 111.3 meters per side at the Virunga latitude, as follows. The conversion from degrees in WGS 84 to meters in Web Mercator has been done with ArcGIS Geometry Server (ESRI 2016b) free online REST service and is shown in Table 14.

This three decimal limitation is only for displaying purposes. When saving into favourite points, for example, the limit is the database data type.

Table 14: Coordinates example between the WGS 84 datum and the Web Mercator projection, with size of the pixel defined by the interferograms

WGS 84		Web Mercator	
x coordinate	y coordinate	x coordinate	y coordinate
29.100°	-1.500°	3239397.18208426m	-166998.313752922m
29.101°	-1.501°	3239508.50157505m	-167109.671428654m
Dif: 0.001°	Dif: 0.001°	Dif: 111,31949079m	Dif: 111.357675732m

This page intentionally left blank.

4. IMPLEMENTATION

4.1. *Installation, security, back-end and front-end*

All components mentioned in the software architecture are available in Windows, Linux and Mac, so the whole stack can be installed in both a laptop and a server. The files (maps and time-series) are the only entities that would need to be copied from one installation to another. This is considered to be a solution for the `FRO1` requirement on portability and sharing of the system. Wisdom-volkano has been tested with Windows 8.1, Ubuntu Server 12.04 and Mac OSX.

Wisdom-volkano can only be accessed after authentication (`FRE1`) with a user and password given by the administrator(s). This was implemented with the Ion Auth (Edmunds 2010) open source library for CodeIgniter. The administration or back-end part of Wisdom-volkano, where layers and time-series may be created, is only accessible for administrators. They may grant layers and time-series to other users.

Concerning the log audit (`FRE2`), it was done with CodeIgniter own logging system as shown in [Source code 25](#), whose result is in [Table 15](#).

Table 15: Content of the log (text) file generated by Source code 25

```
INFO - 2016-02-24 00:17:59 --> [Wisdom-volkano] Layer test granted  
to test@test.com by admin@admin.com
```

The front-end in [Figure 20](#), on the other hand, shows how Wisdom-volkano evolved from the original mock-up in [Figure 14](#). There are some evident differences between them:

- The layers have now more features: not only they are grouped and can be disabled, but they also have opacity control.
- There is more than just one chart.
- As it was not needed (data files may be opened from the file system), there is no data table on the bottom right.
- The configuration of chart points (`FR4`) is done directly in the chart, the legend or in the handle (the square button on the top left corner of every chart).
- Z-elevations profiles (`FR6`) and outliers and trend changes (`FRO2`) vertical bars are not yet implemented.

Every modification on the screen, be it on the visualization of the layers or adding or removing time-series, is submitted to Wisdom-volkano immediately via an ajax call to be stored on the user profile in the database. Thus their configuration is kept when logging out and in Wisdom-volkano (`FR11`).

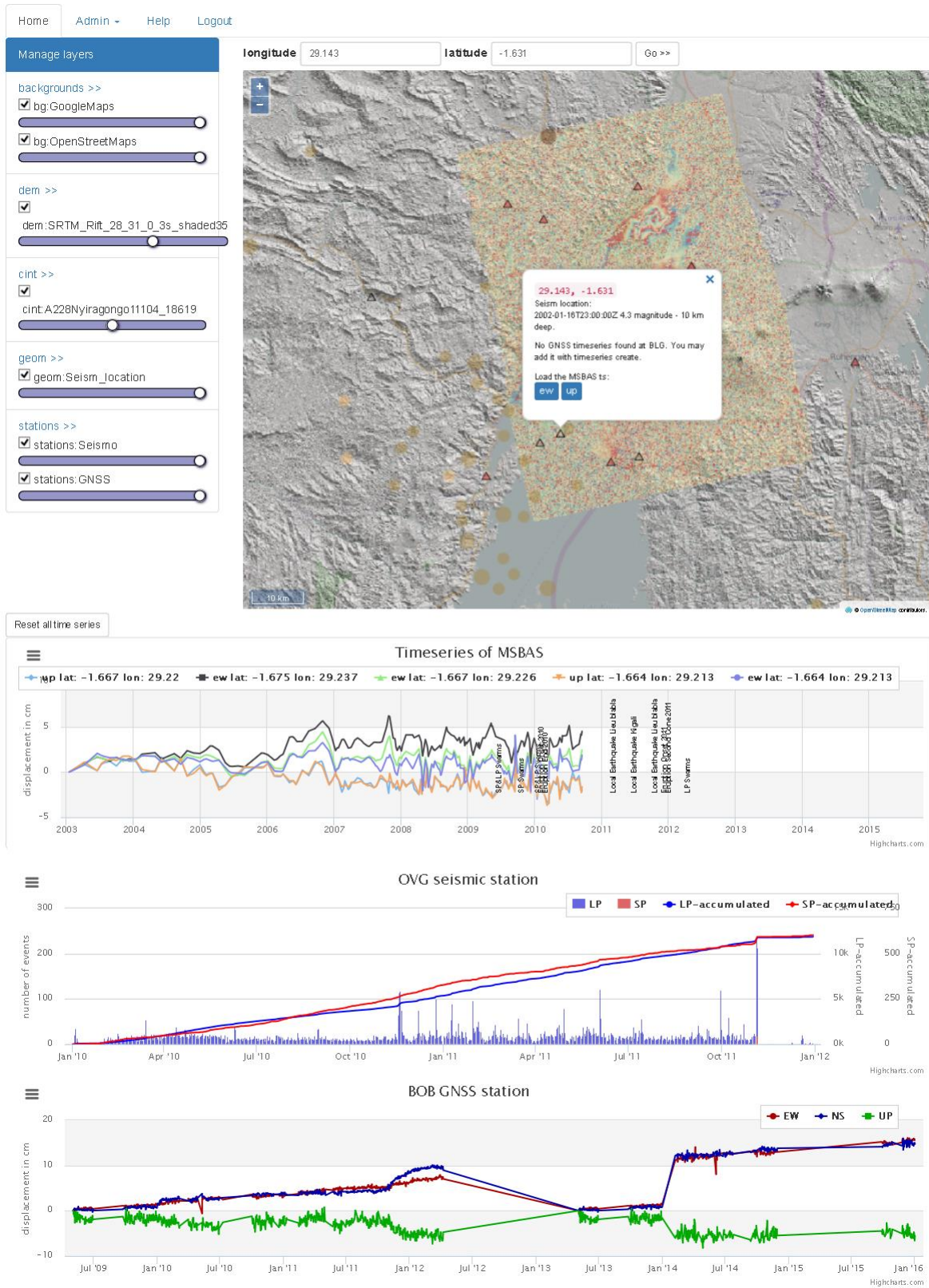


Figure 20: Overview of main screen of Wisdom-volcano

4.2. Geospatial functional requirements and data

4.2.1. GeoServer workspaces, stores, layers and styles

The foundation for working with geospatial data in Wisdom-volkano is GeoServer, where layers must be created and configured. Three levels are needed:

- Workspaces (or namespaces): though only one is needed and can be the default, it is highly recommended to have one for every group of layers. Their names are recommended to be short, e.g., `test`, `cint` or `dem`.
- Stores: one per file is needed. For features (e.g., shapefiles), they can have several layers in one file. For rasters, usually just one layer per file. In order to avoid errors, it is recommended that both names (store, layer) are the same.
- Layers: depending on the Store, see above. The resulting name will be `workspace:layername`.

An example of the resulting layers in GeoServer is shown in [Figure 22](#).

Another important step is configuring the correct style for each layer. In order to represent correctly the InSAR products (GD1), only the complex interferogram needs a specific SLD style: its extreme values shall have the same colour. An example of the complex interferogram with the style can be seen in [Figure 6](#). The style legend is shown in [Figure 21](#) as previewed in GeoServer; its SLD code is included in the source code delivery:

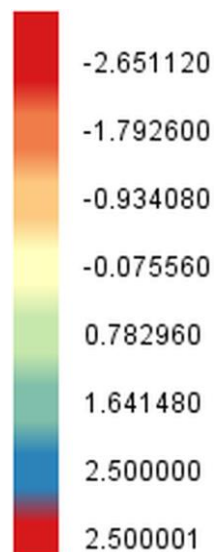


Figure 21: Colour ramp for complex interferograms, generated by the SLD and previewed in GeoServer

Layer Preview

List of all layers configured in GeoServer and provides previews in various formats for each.

<< < > >> Results 1 to 14 (out of 14 items)

Type	Name	Title
	amp:20110415.HH.mod.UTM.5x5	20110415.HH.mod.UTM.5x5
	amp:ENMISAT_Asc425_LonLatMagMas32160	ENMISAT_Asc425_LonLatMagMas32160
	dint:A228Nyrangono11104_13108	A228Nyrangono11104_13108
	dint:A228Nyrangono11104_18619	A228Nyrangono11104_18619
	dint:A42Nyrangono32160_32661	A42Nyrangono32160_32661
	dint:dint.interfero.f.HH.HH.UTM.5x5	dint.interfero.f.HH.HH.UTM.5x5
	coh:coherence.HH.HH.UTM.5x5	coherence.HH.HH.UTM.5x5
	coh:ENMISAT_Asc425_A42Nyrangono32160_32661_AutoGEOC_VW_LonLatCch_Bp_108_Im_35days_Ha157_7m	ENMISAT_Asc425_A42Nyrangono32160_32661_AutoGEOC_VW_LonLatCch_Bp_108_Im_35days_Ha157_7m
	dem:SR_TM_Rift_28_31_0_3s_shaded85	SR_TM_Rift_28_31_0_3s_shaded85
	geom:Seism_location	Seism_location
	geom:GNSS_station	GNSS_station
	geom:Seismo_station	Seismo_station
	uint:A42Nyrangono32160_43182	A42Nyrangono32160_43182
	uint:unwrappedPhase.HH.HH.UTM.5x5	unwrappedPhase.HH.HH.UTM.5x5

<< < > >> Results 1 to 14 (out of 14 items)

Figure 22: List of layers as shown in GeoServer

4.2.2. Wisdom-volkano layers

After being created in GeoServer, the layers are available in the REST interface and can be added to Wisdom-volkano. This is performed with the administration menu option Create layers (FR10) (Figure 23).

The “Layer workspace and name” drop down option has all layers available from GeoServer (Figure 22) and granted to the current user. When it is the administrator, there is a grant option at the bottom. Once submitted, the layer is shown in a list, where it can be edited or removed. It should be noted that layers are not really created or removed in Wisdom-volkano (this is only possible in GeoServer): create and remove in this context means referencing or dereferencing the layer.

Also, layers can be reordered (FR12) by clicking on “Manage layers” on the left menu, as shown in Figure 24.

The screenshot shows the 'Create layer' form in the Wisdom-volkano administration interface. At the top, there is a navigation bar with links for 'Home', 'Admin', 'Help', and 'Logout'. The main heading is 'Create layer'. Below this, there are three input fields: 'Layer workspace and name' with the value 'amp:ENVISAT_Asc42i5_LonLatMagMas32160', 'Layer type' with the value 'raster', and 'Layer description' with the placeholder text 'enter Layer description'. Below the input fields, there is a section titled 'Grant to these users (admin is always granted)' with three checkboxes: 'admin@admin.com' (checked), 'email@another.com' (unchecked), and 'test@test.com' (unchecked). A 'Submit' button is located at the bottom of the form.

Figure 23: Create layer option in Wisdom-volkano

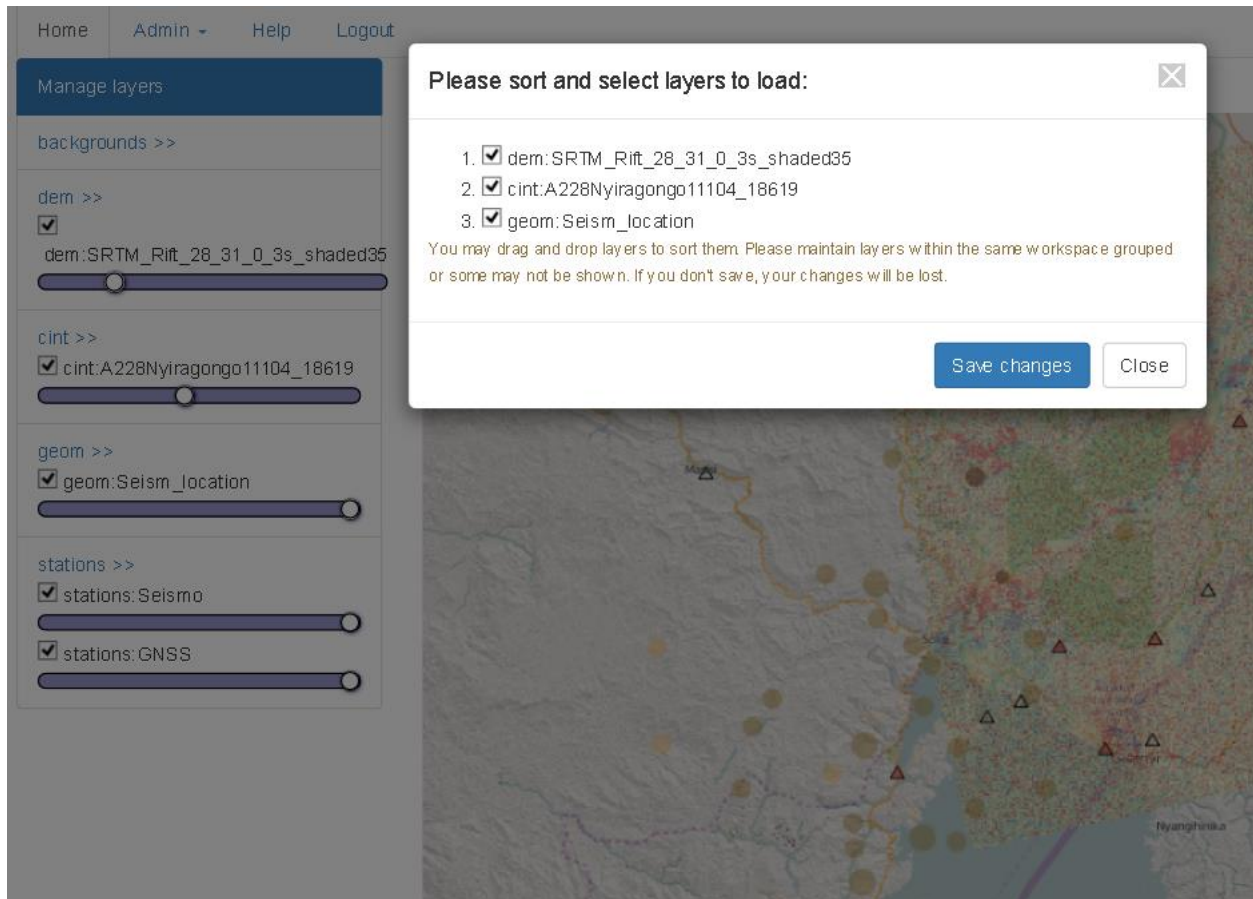


Figure 24: Option to reorder the loaded layers

The interface to work with the maps (FR1) can be seen in Figure 25. It includes a zoom (top left of the map) which modifies accordingly the scale (bottom left of the map), pan (with click and drag of the mouse), background and stations layers (visible on the left panel; these four are hard coded, though they can be disabled and enabled) and the visibility and opacity of all layers.

Moreover, the selection of a point (FR2) is shown in the same Figure 25. This can be done either with a mouse click or by entering the coordinates in the boxes above the map. The result is a white box on the map showing the information stored in that coordinates related to the enabled layers on the left. In the concrete example, there are three:

- Seism location: when selecting the orange spheres shown in the map, there is information related to the seismic location data (GD3) that will be explained later.
- GNSS station: when selecting one of the black triangles, there is a GNSS station which may have a time-series (TS3) loaded – this is not the case in the example of the Figure 25.
- MSBAS time-series: when selecting a point within the limits of a MSBAS time-series (TS1), buttons for each configuration are shown. In this case, there are two, *ew* and *up*.

By clicking in a blue button, Wisdom-volcano will load the time-series configured (FR3). The map in Figure 25 also shows how the seismic events (GD3) and seismic and GNSS stations (GD2 and GD4) are mapped with Wisdom-volcano. The events are classified by magnitude (size) and colour (date, older is lighter). Legend is in Figure 26, as generated by GeoServer with the adapted SLD.

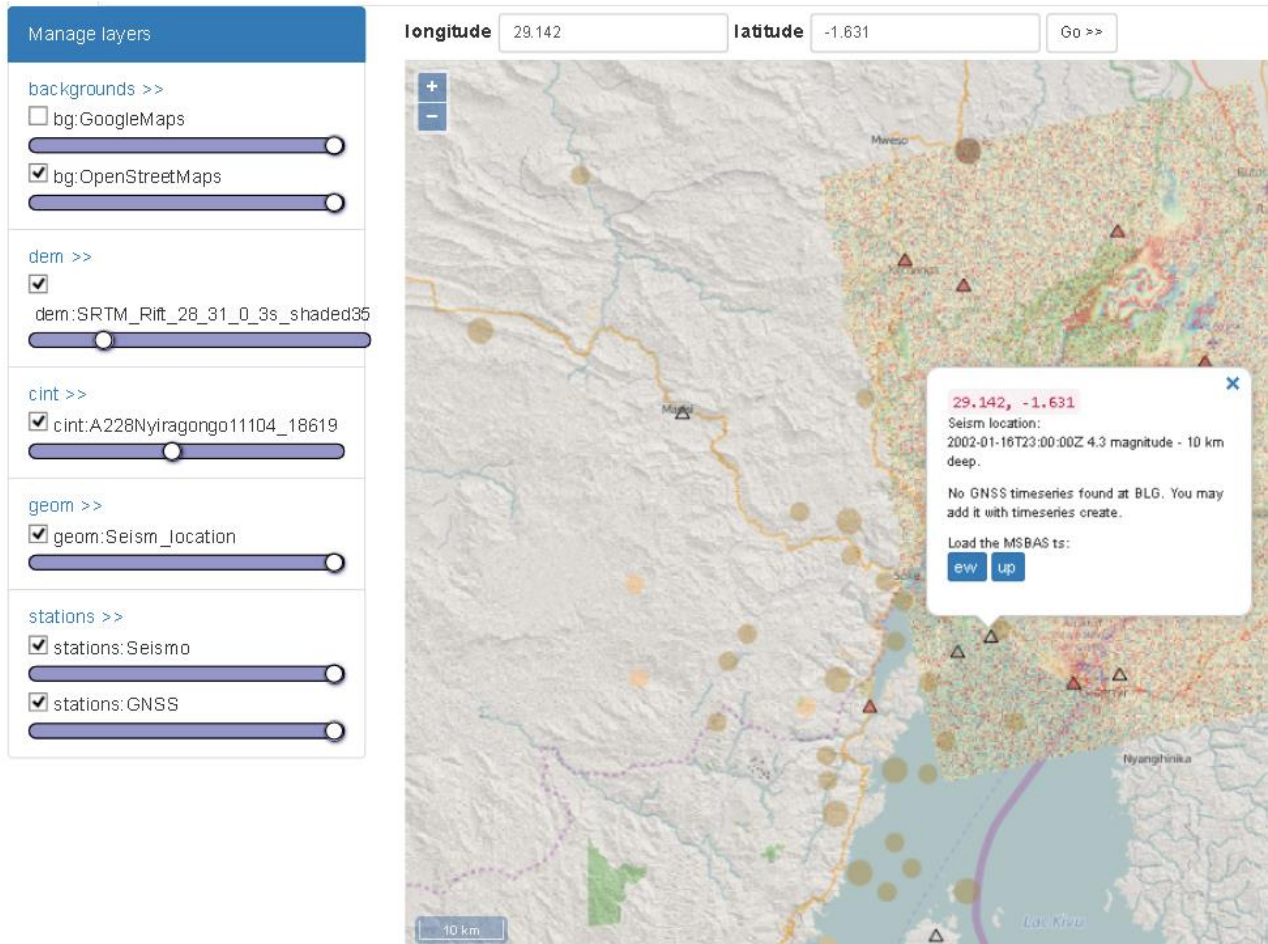


Figure 25: Main screen of layers and map in Wisdom-volcano, with detail after selecting a point

- magnitude 0 to 4, year up to 1995
- magnitude 0 to 4, year from 1995 to 2005
- magnitude 0 to 4, year from 2005
- magnitude 4 to 5, year up to 1995
- magnitude 4 to 5, year from 1995 to 2005
- magnitude 4 to 5, year from 2005
- magnitude from 5, year up to 1995
- magnitude from 5, year from 1995 to 2005
- magnitude from 5, year from 2005

Figure 26: Symbols for seismic localization events, generated by the SLD and previewed in GeoServer

Concerning the stations, also SLD files are created and delivered with the source code. They are shown in Figure 25 as follows:

- Seismic station: red filled triangle: ▲
- GNSS station: outline black triangle: △
- Both fit: where there are two stations in approximately the same place (depending on the zoom), they are shown as a single place.

4.3. Time-series FR and data

When first entering Wisdom-volkano, it appears an empty chart, except for the events loaded from Source code 11 and Source code 12 (Figure 27).

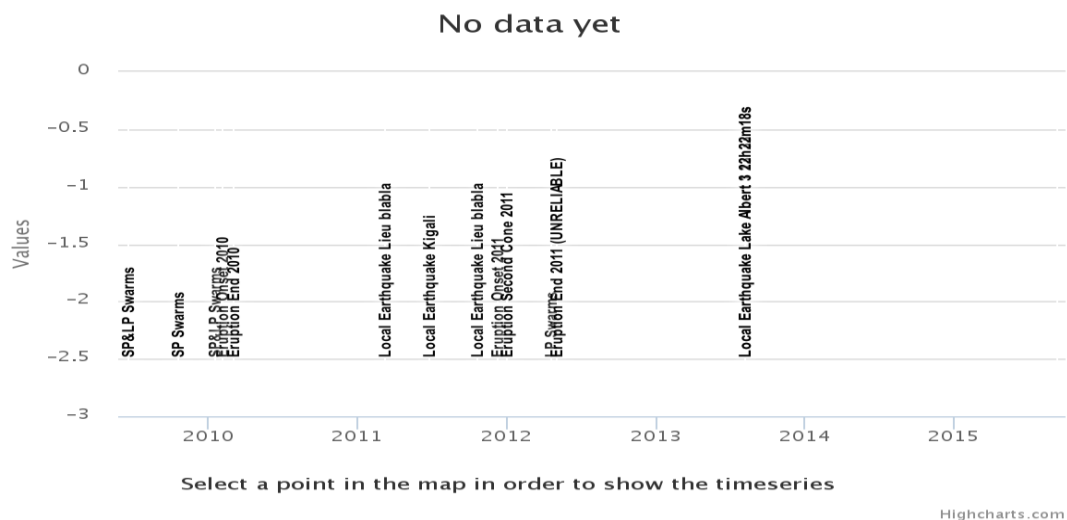


Figure 27: Highcharts chart with only the events generated with Source code 11 and Source code 12

4.3.1. MSBAS time-series chart and favourites dataset

In order to use time-series, first they must be created in the administration menu. For a MSBAS one, the [Figure 28](#) shows the options needed. After setting up the folders in the configuration file, the available time-series will be shown in the drop down option (third field; in the example, it is EW, the other option was UP). When one is chosen, the two file fields will be automatically filled, as “Raster file found” and “Ts file found”.

For the raster stack, Wisdom-volkano will try to identify the date position from the file name and will extract from the header file the coordinates of the top left point, plus the resolution of the pixel. For the time-series part, Wisdom-volkano will try to identify the pixel position from the file name.

The time-series created will be shown in the list, where they can be removed.

After clicking on a position in the Wisdom-volkano map, any time-series configured for the position will be shown. If it is an MSBAS time-series (TS1), the calculation explained in [Figure 15](#) and [Figure 16](#) is performed (FR13), the points are saved for a future use (FR9) and the resulted time-series is loaded via the procedure explained in section 3.6.3.1. Also, in a future release the time-series calculation will allow to take into account surrounding points: this is called multi-looking (FR7).

In [Figure 29](#), a chart of an MSBAS time series is shown, with several points either vertical (UP) or horizontal (EW) from positions around Goma.

The chart allows zooming by clicking on it and dragging left or right. Hovering the mouse shows information about the data. Both are considered to cover the FR4 and are shown in [Figure 30](#).

However, this consideration was not entirely correct. FR4 was about the time-series configuration and indeed, the mock-up ([Figure 14](#)) showed that they should be filtered by date at both ends, and the number of images available for that filter. This is not exactly the same as zooming, which is equivalent to filter just one zone of the chart, and the number of images is the number of points shown. The issue is somewhat mitigated: FR4 was mainly foreseen and needed in order to run the detrending (FR8), which was fully implemented (see section 4.3.4).

The list of MSBAS time-series can be reordered in the same way as layers, disabled (removed) or saved as favourite points from the chart handle present on the top left, what shows the dialog of [Figure 31](#).

The favourite dataset (FR5) is stored in the database and not in GeoServer, while the time-series files are kept in the file system. Once the points are added to it, they can be shown in its list, where they can be edited, added a description, loaded into the current session or removed ([Figure 32](#)).

[Home](#) [Admin](#) [Help](#) [Logout](#)

Create time series

Type

Time series name

Time series file or group folder

Raster file found

Raster filename - date starts at

Example date 20030116

Raster coords - lat top

Raster coords - lon left

Raster coords - lat increment (degrees per pixel)

Raster coords - lon increment (degrees per pixel)

Ts file found

Ts file - coords (NNN_NNN) starts at

Example coords 079_570

Description

Grant to these users (admin is always granted)

- admin@admin.com
- email@another.com
- test@test.com

Figure 28: Options available when creating an MSBAS time-series

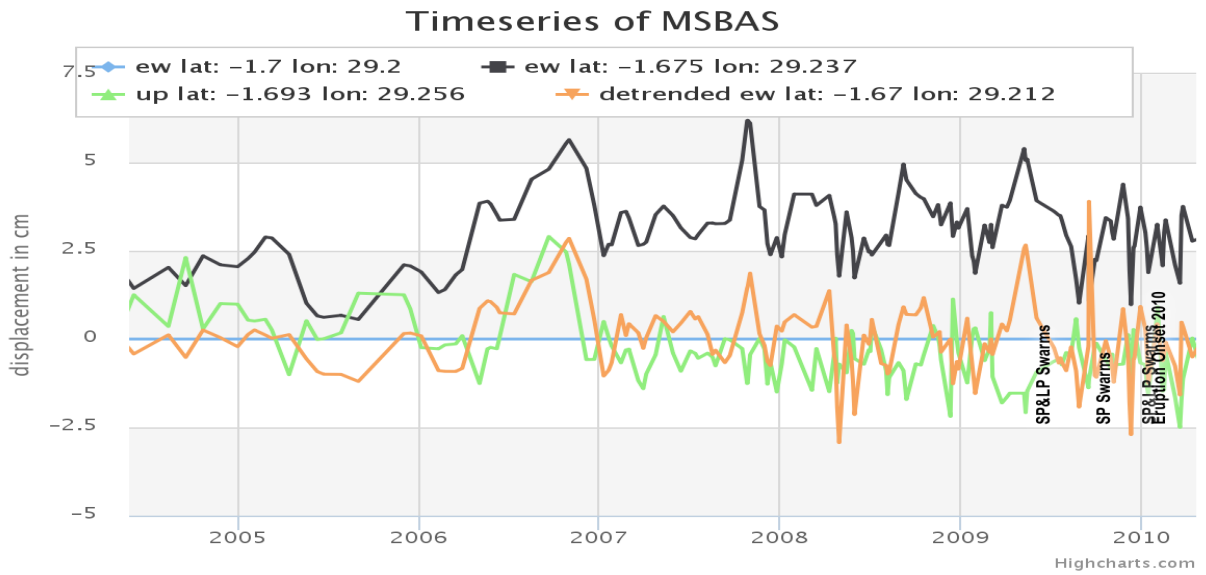


Figure 29: MSBAS time-series calculated from a raster stack of InSAR
Data provided by ECGS/RMCA.

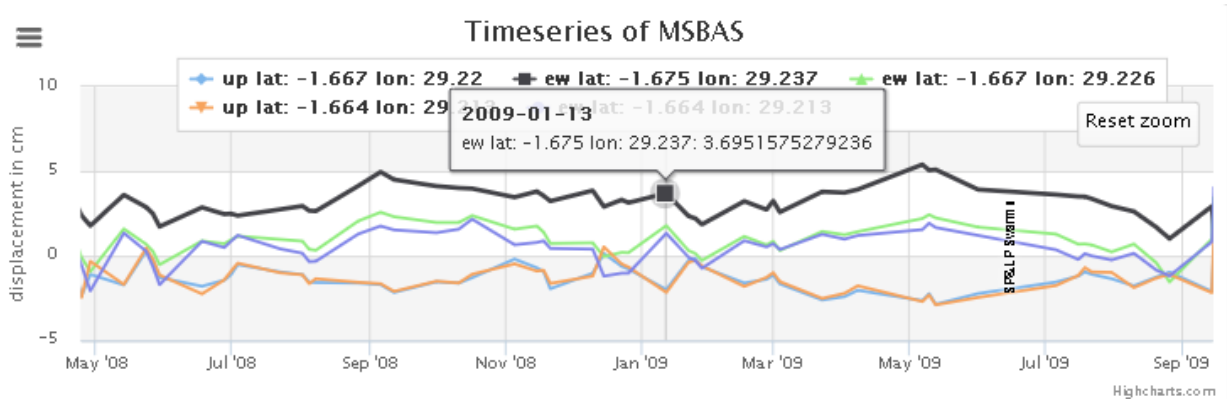


Figure 30: Zoom detail on the MSBAS chart with detail information when hovering a point
Data provided by ECGS/RMCA.

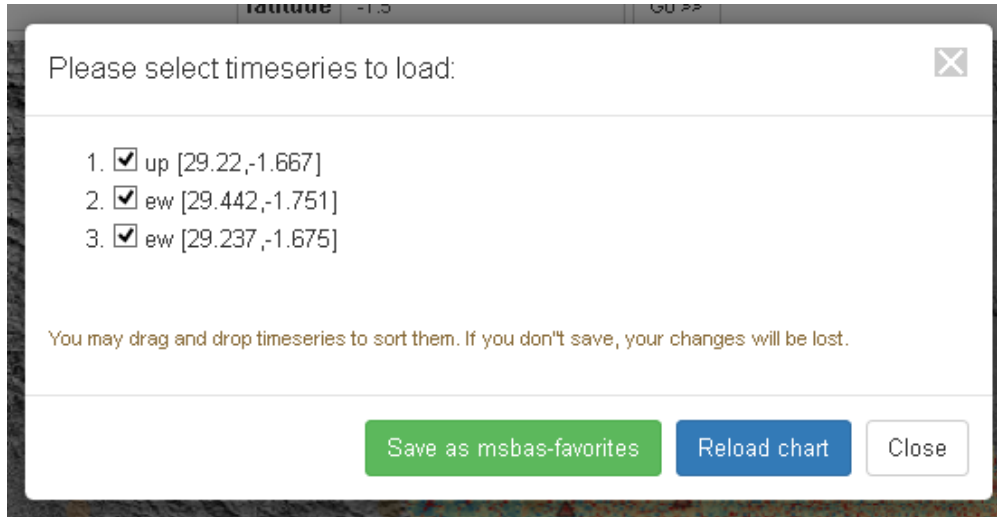


Figure 31: Screen capture of the MSBAS time-series manage modal window

Home | Admin ▾ | Help | Logout

List of favorite MSBAS time series points

MSBAS ts	longitude	latitude	description	action
ew	29.2	-1.7		edit delete load into current session
ew	29.2369	-1.67517	1	edit delete load into current session
ew	29.2199	-1.66694	test	edit delete load into current session
up	29.2369	-1.67511		edit delete load into current session
up	29.2199	-1.66694		edit delete load into current session
up	29.2564	-1.69325		edit delete load into current session

Create favorite point Load all points into current session

Figure 32: Favourite MSBAS points dataset

4.3.2. Histogram time-series chart

The time-series from stations are created in a different way, with single files and not from a group of folders. The key part is writing the correct station name as it was originally in the KML file (Source code 17), see Figure 33.

The time-series of counting seismic events (TS_2) is then shown as a histogram (FR_{14}), as seen in Figure 34. The number of events is shown in thin vertical bars (and its legend axis is on the left), while the accumulated events are the ascending lines (whose axis are on the right).

The zoom and hovering are exactly the same as in the MSBAS chart, but there is one histogram per station. Their handles allow to close them (see [Source code 19](#)) when not needed anymore.

Home Admin ▾ Help Logout

Create time series

Type:

Time series name:

Time series file or group folder:

Seism or GNSS station:
(name must be the same as in KML/KMZ station file)

Description:

Figure 33: Screen capture from Wisdom-volkano on creating a time-series based on seismic stations

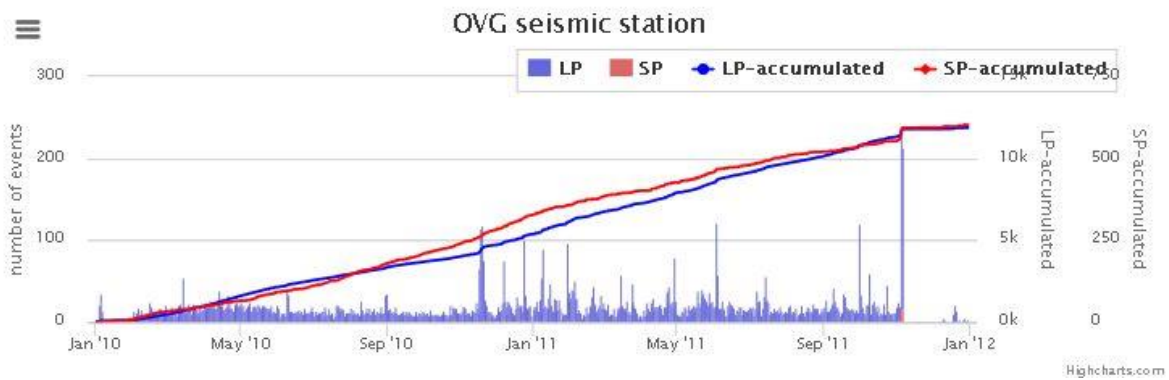


Figure 34: Seismic counting events of OVG station
Data provided by ECGS/RMCA.

4.3.3. GNSS time-series chart

Creating a time-series for a GNSS station source data file ($TS3$) is similar as for the histogram, but the result is as [Figure 35](#). Straight lines show lack of data for those time periods.

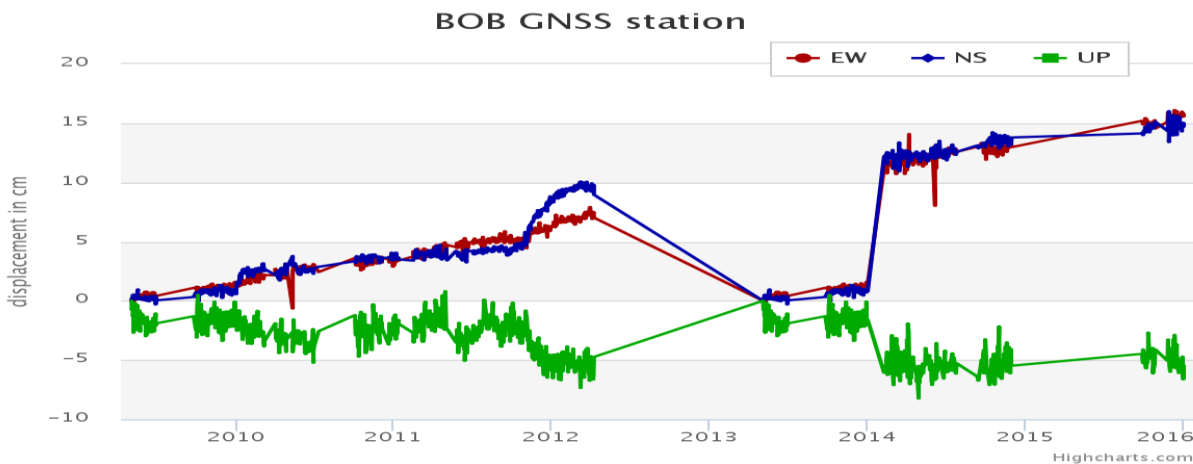


Figure 35: Example of a GNSS time series as plotted in Wisdom-volkano
Data provided by ECGS/RMCA.

4.3.4. Detrending

For both MSBAS and GNSS, the detrending ($FR8$) option is available in their chart handles. For example, in [Figure 35](#), a clear ascending trend is visible in both NS and EW axis between September 2010 and August 2011, so after zooming and selecting the detrend option, the dialog is shown in [Figure 36](#).

In [Figure 37](#) we can see that the NS axis reaches 5 cm at the beginning of 2012, while in [Figure 35](#) it reached 10 cm. The difference corresponds to the natural trending of the terrain, and the 5 cm remaining are really corresponding to the ground volcanic displacement in the few months between October 2011 and January 2012. Actually, as it can be seen in [Figure 38](#), it would be a good idea to detrend also the EW axis.

The EW axis, which had over 15 cm of displacement after seven years in [Figure 35](#), shows no real displacement after detrending in [Figure 38](#), which allows discarding a false signal.

This process can be done also for MSBAS data. The list of all detrended time-series is available from the menu and shown in [Figure 39](#).

When a time-series is detrended, it is used instead of its original (trended) counterpart. It can be removed, and in that case, the original one is used again. Only one detrended can be shown at a time for a given pixel or an axis of a GNSS data station file.

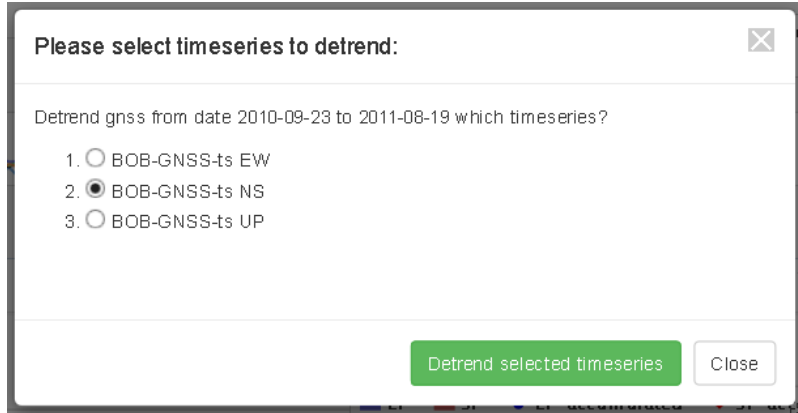


Figure 36: Detrend dialog for the GNSS chart in Figure 35

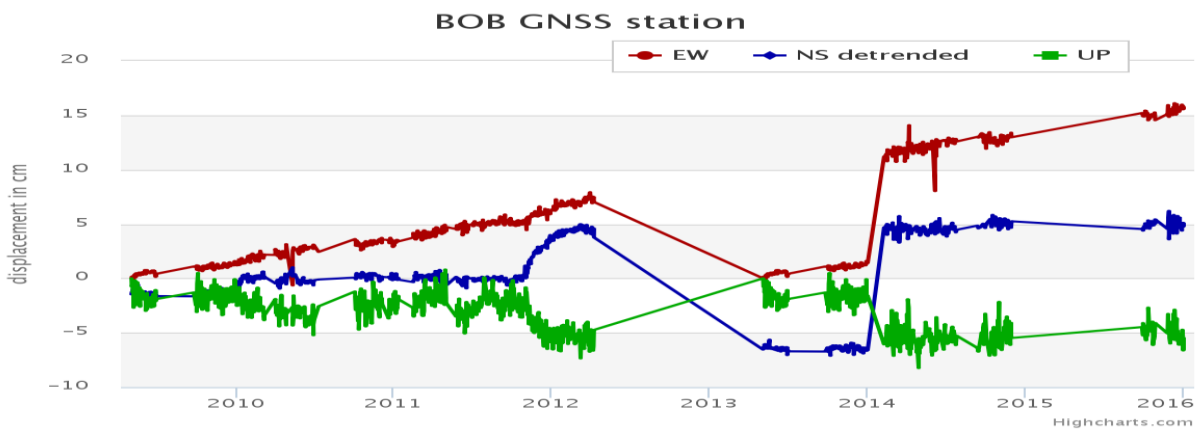


Figure 37: GNSS time-series from Figure 35, with the NS axis detrended

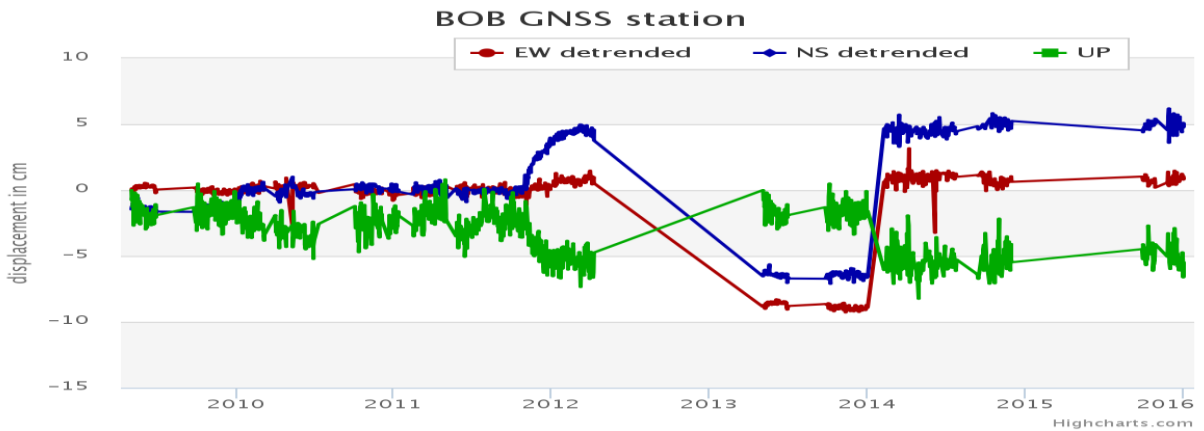


Figure 38: GNSS time-series from Figure 35, with the NS and EW axis detrended

Home Admin ▾ Help Logout

List of detrended time series

type	name	MSBAS lon/lat	GNSS axis	action
gnss	BOB-GNSS-ts		EW	<input type="button" value="delete"/>
gnss	BOB-GNSS-ts		NS	<input type="button" value="delete"/>
msbas	ew	[29.212,-1.67]		<input type="button" value="delete"/>

Figure 39: List of detrended GNSS and MSBAS time-series

4.4. Validation; test with new data

After finishing the Wisdom-volkano third and final iteration, ECGS/RMCA provided a new set of data in order to test the application, covering all data sources above. However, some have their format changed. Details follow.

4.4.1. New InSAR and MSBAS data

This is the list of InSAR product files received:

- Amplitudes: two files from which the interferogram is calculated: `20110415.HH.mod.UTM.5x5.rev` and `20120702.HH.mod.UTM.5x5.rev`
- Coherence: `coherence.HH-HH.UTM.5x5.rev`
- Complex interferogram: `interfero.f.HH-HH.UTM.5x5.rev`
- Unwrapped interferogram: `unwrappedPhase.HH-HH.UTM.5x5.rev`

All were sent with projection UTM 35S, which is focused on the southern hemisphere and in Africa, covering the North-Kivu zone. This is converted to the default projection in GeoServer, as explained in section 3.7. The complex interferogram in Wisdom-volkano is shown in Figure 40.

The new MSBAS files provided were from rasters of the crater of Nyiragongo, like:

- `NyigoCrater_Max100m_50days_ew\20130813u.bin.hdr` and
- `NyigoCrater_Max100m_50days_ew\20130813u.bin`.

However, their data is in meters and not in degrees, which means that the process explained in section 3.2.4 would need to be adapted; the content of the header is shown in Table 16.

The time to implement this adaptation would be long enough not to make part of this project, but of a future development.

In any case, ECGS/RMCA admitted that the MSBAS calculation was being reviewed as of writing this thesis, which will make the format and handling probably even different of this newer batch.

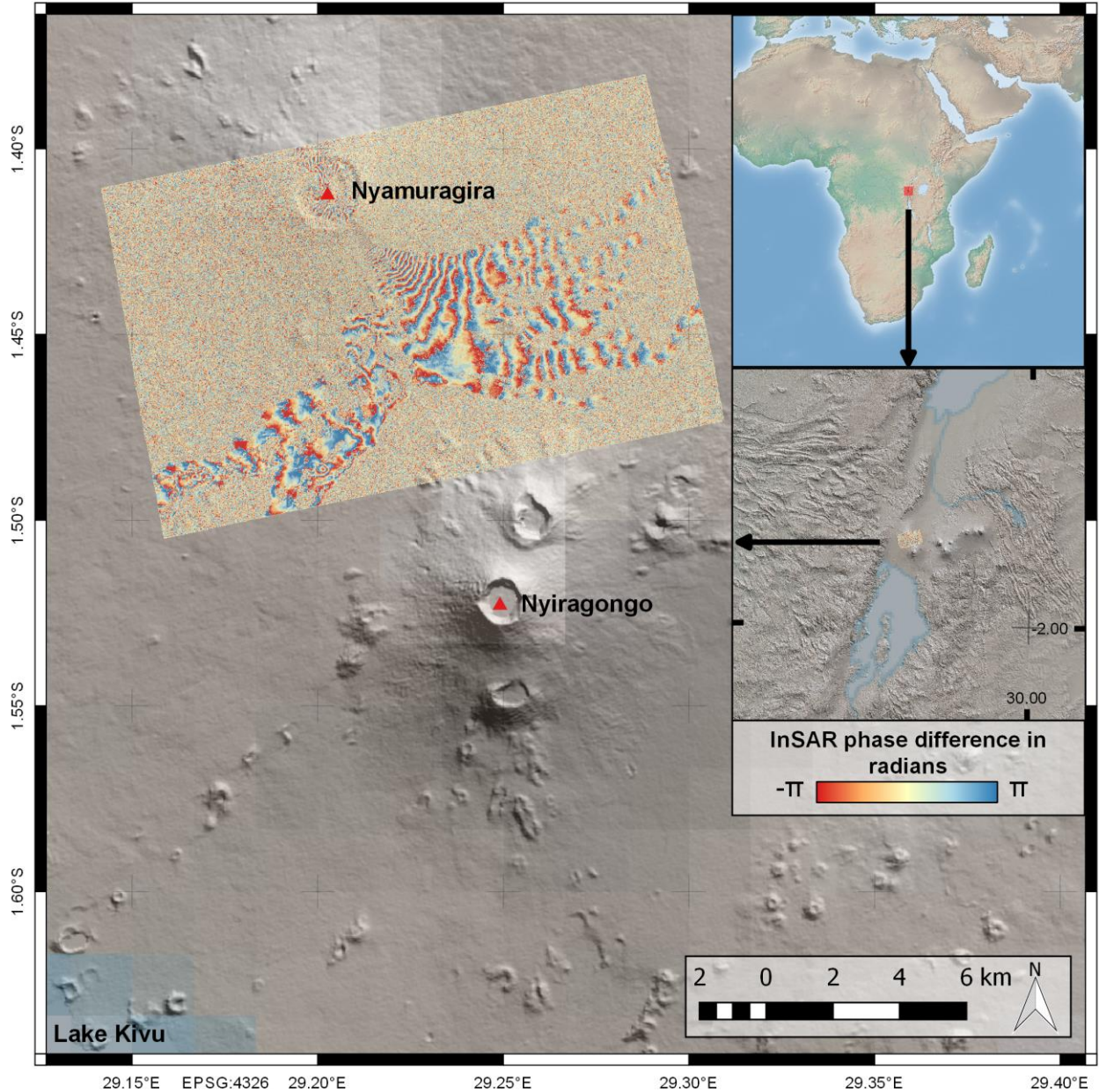


Figure 40: New complex interferogram (April 2011 - July 2012) wrapped on DEM shaded relief
Fringes are here related to the topography. Interferogram and DEM from ECGS/RMCA, background overview from Natural Earth.

Table 16: New MSBAS header data, in meters

```

ENVI
description = {
  Create New File Result Fri Apr  8 17:45:58 CEST 2016}
samples = 502
lines   = 502
bands   = 1
header offset = 0
file type = ENVI Standard
data type = 4
interleave = bsq
sensor type = TSX
byte order = 0
map info = {UTM, 1.000, 1.000, 747999, 9833508, 9, 9, 35, South, WGS-
84, units=Meters}
data ignore value = -32768

```

4.4.2. New seismic data

Two files were received, one for the counting events, `VTNYR-KBT_countperday.txt`, and another for the locations, explained below. The counting file is displayed in Table 17.

They are SP only, and the LP are not included. A future development of Wisdom-volcano might be showing just SP or LP, or both at will, depending on the number of values after the date. This is shown in Table 18.

The file for the seismic location is `virunga_event_list_3Dgrid.txt` (first line has the headers) and shown in Table 19.

This file has 372 rows. The magnitude is defined in the `ML` column, though most of the rows have a value of -9.9 (meaning that the value has not been yet calculated) and only three rows have values over 4.0, which was the threshold for the second class defined in the SLD file for this (see Figure 26). ECGS/RMCA explained that this dataset is being improved with the name of the volcano originating the seismic event, as well as the accuracy in the magnitude.

Table 17: Sample of the new seismic counting events file

```

20151005,6
20151006,14
20151007,13
20151008,14
20151009,13
...

```

Table 18: Improvements for the seismic counting values files

- 1 value after the date: when creating the time-series, ask if the value is SP or LP. Calculate the accumulated.
- 2 values: when creating the time-series, ask if they are SP and LP (and calculate their accumulated); or just one of them, either SP or LP, plus its accumulated.
- 3 values: unlikely to happen, not foreseen.
- 4 values: as designed already in Wisdom-volcano: SP and LP, including accumulates.

Table 19: Sample of the new seismic location file

%	EVTID	Lat[deg]	Lon[deg]	Depth[km]	ML	ERH[km]	ERZ[km]	
minHUnc[km]	maxHUnc[km]	azMaxH[km]	Nphs	Gap[deg]	RMS[s]	MinDist[km]	Origin	
Time [s]								
20140804235532	-1.510	29.190	3.0	-9.9	14.0	5.7	9.1	
19.2	1.6	6	185	0.0854	19.4		2014-08-04_23:55:32.222	
20140809232103	-1.518	29.240	3.0	-9.9	2.1	2.4	1.6	
2.8	162.7	7	149	0.1065	18.2		2014-08-09_23:21:03.000	
20140810223241	-1.737	29.061	0.8	-9.9	2.4	3.0	1.5	
3.3	48.5	8	231	0.1407	6.3		2014-08-10_22:32:41.007	
Etc.								

4.4.3. New GNSS data

Three files were received, all from the Rubavu station in Rwanda:

- RBV_DailySolutionsLatLong.txt,
- RBV_DailySolutionsUTM.txt and
- RBV_DailySolutionsXYZ.txt.

The contents are obviously related not only by the file names, but also all three files have exactly 1500 rows. However, dates are only present in the last file (no headers present) (Table 20).

For the ground displacement, and unlike the previous data, which was already calculated (see Table 12), now the coordinates in meters for Northing, Easting in UTM are given (Table 21).

With Microsoft Excel, both files were integrated into a single table with the differences already calculated in millimetres, assuming that the first row is zero millimetres displacement in all axis. The result is in Table 22.

In Wisdom-volcano, when linked through the station name, RBV, as explained in section 4.3.2, the chart shown is in Figure 41. It can be seen in it that some outlier values prevent the rest to be properly seen. When zoomed, the chart is displayed in Figure 42.

FRO2 was created for removing these kind of outliers, but this depended on the input of a doctorate thesis that was not finished in time. These values may be removed either manually (i.e., editing the file directly) or automatically with a future development, for example, when the change from the previous one would differ in more than a (configurable) percentage.

Table 20: Sample of the new GNSS xyz data file

```

RBV_ 2010.73287671 5.562813517653620E+06 3.118581783291670E+06 -
1.849695995763190E+05 5.10170393038430E-06 2.91882490924690E-06 -9.61122154929870E-
08 2.45743968965820E-06 -5.71237142807000E-08 4.33842795051500E-07
RBV_ 2010.73561644 5.562813523604470E+06 3.118581785120510E+06 -
1.849696009616800E+05 1.46600110598720E-06 7.26308754886550E-07 -1.83054892484520E-
09 5.84999246584870E-07 -1.81407196461880E-08 1.32857460942950E-07
RBV_ 2010.73835616 5.562813520589570E+06 3.118581784282070E+06 -
1.849696001174270E+05 1.99568446408360E-06 1.03196953323260E-06 -3.19733884271350E-
09 9.06865231157280E-07 -5.75634429197770E-09 1.80773942464090E-07
...
    
```

Table 21: Sample of the new GNSS UTM data file

```

RBV_ 753168.9357 9814986.8172 1901.4668 35 0 5.99834E-07 8.51051E-09
0.00000E+00 4.32941E-07 0.00000E+00 6.96038E-06
RBV_ 753168.9344 9814986.8161 1901.4730 35 0 1.76054E-07 -1.48827E-08
0.00000E+00 1.33791E-07 0.00000E+00 1.87406E-06
RBV_ 753168.9350 9814986.8168 1901.4699 35 0 2.86909E-07 -1.41888E-09
0.00000E+00 1.82556E-07 0.00000E+00 2.61392E-06
...
    
```

Table 22: Resulting GNSS file from integrating Table 20 and Table 21

```

2010.73287671 0.00 0.00 0.00
2010.73561644 -1.10 -1.30 6.20
2010.73835616 0.70 0.60 -3.10
2010.74109589 5.20 2.80 12.60
...
    
```

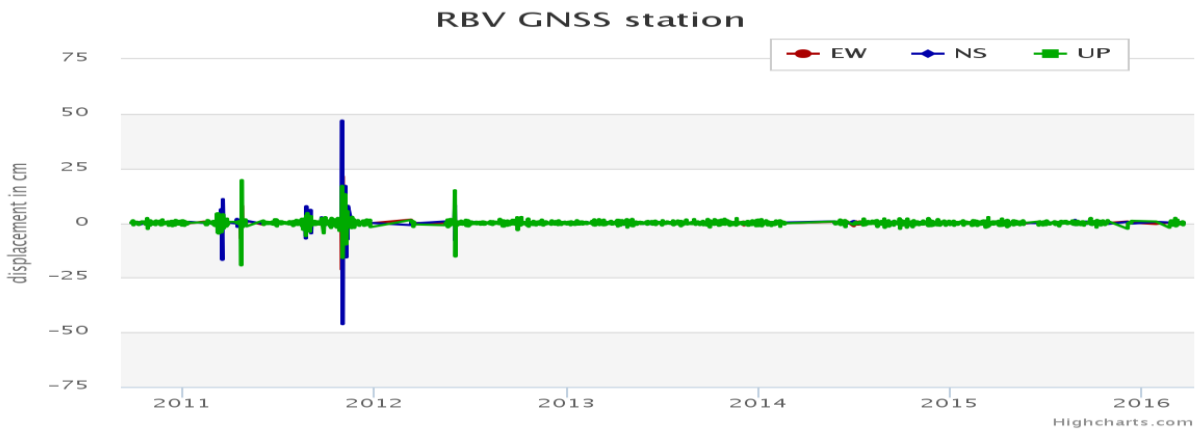


Figure 41: GNSS chart of Rubavu station data, from the file in Table 22

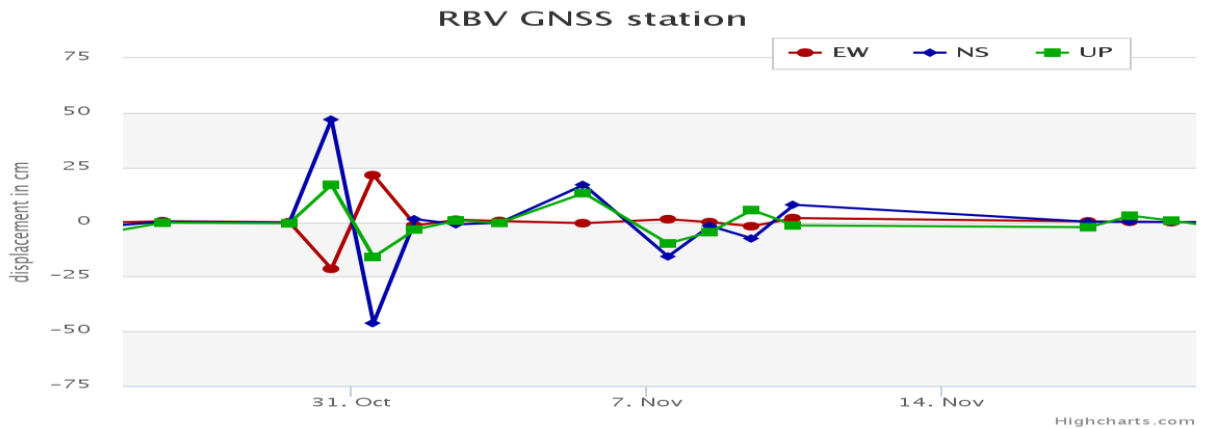


Figure 42: Zoom around second half of 2012 of Figure 41

4.4.4. Validation summary

The maps were shown without problems in Wisdom-volkano.

However, the time-series were a completely different story. Not a single file had the same format, and even when adapted manually, mandatory information was missing (as for the counting seismic events), or the data had outliers that hid other values.

This demonstrates that GeoServer and OpenLayers are able to handle the maps without major issues, while Highcharts and Wisdom-volkano are quite sensitive to the formats and quality of the time-series given.

This page intentionally left blank.

5. DISCUSSION

5.1. *Web GIS and time-series*

Though some advanced commercial tools may be able to present maps and charts together, the enormous amount of data to handle, the different sources of data and their changing formats show the advantage of an ad hoc solution. Implementing open source applications saves time and effort, and allows using the same tools on and offline, even when using a web based application instead of a standalone one. Also, it allows plugging different open sourced projects together, sometimes with some interface adaptations, such as detecting seismic events (Romero et al. 2016).

The standards WMS and WFS were obvious choices since nearly all GIS related applications are based on or allow them. The choice was rather how to use them (for example, with or without tiles) than whether to use them or not. Wisdom-volkano is composed of OpenLayers, GeoServer and Highcharts, an adequate combination for web GIS and time-series. They were proven effective along the process with two validated incremental prototypes.

OpenLayers is probably not as easy to develop with as Leaflet, but much more stable and powerful. During the development of Wisdom-volkano (around one year), more than twenty versions of OpenLayers were released, which were integrated with little or no modifications.

GeoServer is much more intuitive and descriptive than the other map application server considered, MapServer. All the errors are clear and security is strong. Though OpenLayers can work without GeoServer, the problem found with the separated stations demonstrates that they work better together.

Iterations have been perfect for this project, helping to solve problems on the way, while presenting prototype views of the software to the stakeholders. The use of ajax is good to improve the user experience, but costly to develop, test and debug.

The use of well-known background layers as Google Maps or OpenStreetMap with the ability of modifying their visibility gives researchers a fair amount of control over their own images, keeping known points of reference.

The possibility of loading the time-series with simple clicks and without reloading the page, with Highcharts features like zooming or exporting the current image, not only improved the user experience but will certainly help in spotting any trend changes in the data, or discarding false alarms. In order to have even more control on the charts, perhaps D3.js may be used, but in exchange a lot of effort should be invested in programming every single feature.

Wisdom-volkano can be adapted to virtually any format of maps, as far as they are accepted by and can be shown by GeoServer, or at least they can be transformed to a format known by it. In this case, it is no different from many other desktop GIS environments.

Concerning time-series, they ought to be in any kind of format that can be exported or adapted to TSV, a feasible task for big volumes of data with scripts or similar programming.

5.2. *Limitations and opportunities*

Wisdom-volkano is neither a complete statistical analysis tool nor as powerful and featured as a GIS desktop tool. However, it brings them together, even though with a number of known limitations. Concerning the map visualization, the InSAR images are supposed to be in the southern hemisphere, and some programming should be adapted to be used with the northern. Also, no legend is shown, though it could be imported from GeoServer; this was not a requirement for ECGS/RMCA. The points selected for the time-series could be pinned and shown in the map, which in any case was shown in the mock-up (Figure 14). This will be implemented in a future release.

The dependence on the formats of the data can be somewhat overcome by editing them a priori, since getting more coherent (always the same format) data has been proven unlikely. This was only spotted when new time-series stations data was requested, and it is dependent on their sensors availability, and eventual processing done by ECGS/RMCA.

The MSBAS time-series are stored as pixels with three characters, which means InSAR images of 999×999 pixels maximum. This should be increased to at least four (images of up to 9999×9999 pixels). Furthermore, the reason on storing them initially as pixel coordinates was taken by the ECGS/RMCA, while they could be stored as geographic coordinates. Both features will be implemented in a future release.

A known issue of GeoServer is the bulk creation of layers. Though there are (unofficial) guides on how it can be achieved, it is not easy to upload thousands of images at a time. Furthermore, they should be then added or linked in Wisdom-volkano, but once they are exposed in GeoServer, they can be created directly in the database with adapted queries. The same big data problem exists when handling time-series, and can be solved by also editing the database.

Finally, during the third delivery, researchers from the ECGS/RMCA requested some improvements, mostly related to an advanced handling of the charts. Though they are stacked in a column, they are not aligned vertically. This can be solved with a detailed control of the limits and space for the axis legends of each chart, plus a coordinated zoom for all charts at once. Other improvements suggested were the possibility to move the charts up and down, merge and split them at will, or the configuration of lines and points. This must be done with JavaScript code that may be integrated in a future release depending on the ECGS/RMCA new requirements and priorities.

5.3. *Recommendations for the future*

Many other new features may be added in the future to Wisdom-volkano. Two examples already suggested to ECGS/RMCA: getting a time lapse of the changing altitude profile between two points, or showing error bars for the uncertainty data of the GNSS stations.

The formats admitted, shapefiles for features and GeoTIFF for rasters, shall be enough, perhaps only to be complemented with GML (Portele 2012). Increasing the admitted data sources, in Wisdom-volkano, OpenLayers or GeoServer, would be prone to errors and focus the

development away from other requirements such as interoperability or usability, key for final users, or stability, scalability and performance, imperatives in production environments.

The great usability experience given by using ajax, that is, generating the JavaScript code to be evaluated after, has the other side of the medal in the problems to test, debug and validate the results. Perhaps a different approach may be of use, like translating the application to a full JavaScript software environment such as NodeJS (Node.js Foundation 2016).

Unfortunately, there is no standard for time-series other than WaterML. Either in files or in a database, the adoption of a common standard would allow Highcharts to focus on integration with GIS visualization tools, and would greatly ease the development of the above mentioned ajax code.

In the future, all web GIS should also serve time maps, that is, present and past versions of the geospatial information. The standard Memento (Van de Sompel et al. 2013) allows via HTTP headers the content negotiation served through the web. This would also lead to GIS long-term preservation for future generations.

Furthermore, GIS should not only be focused in users, but also provide services from computers to computers in order to automatize discovery, download, sharing or even implement new functionalities. This is called the semantic web (Berners-Lee et al. 2001; Fonseca 2008), where standards must be followed closely, and enough metadata shall be available. Several efforts have been made in this direction in the GIS field, including modelling (Hiramatsu and Reitsma 2004), cataloguing (Athanasidou et al. 2015) and geospatially extending the semantic querying language (Battle and Kolas 2012).

Other improvements may come from fields like security of GIS: WMS are configured open by default in GeoServer; or background layers such as Google Maps or OpenStreetMap can be modified by anyone. And a related issue: how can we trust whoever created or edited a GIS, like a government or a company as an authority? Is more trustable for street data the city council or Google Maps? Who decides on where a political border is? And the correct name of a country or city in a certain language? Standards and authorities shall be defined for trustworthy GIS systems.

This page intentionally left blank.

6. CONCLUSIONS

The spatial dimensions must be integrated with the time, shown together. Almost any field of research will be improved with it. Both GIS and time-series will greatly benefit from a standardization of their relationship. Until then, developers will struggle to integrate different formats, especially of the latter. Other future trends will include the moving the GIS from the semantic web to the Internet of Things (Norris and Snell 2015).

Wisdom-volkano is an open source ad hoc solution that combines maps with time-series data to analyse and find correlations in volcanic data. Based on OGC and ISO standards, it can be integrated in other projects, such as acquiring and examining real time indicators to generate pre-eruptive alerts. With further adaptations, other geospatial and data series may be shown.

Therefore, the initial objective is fulfilled: help identifying correlations and precursor activity in order to recognize pre-eruptive indicators. Also the requirements are met:

1. Show many georeferenced images and time-series, some to be calculated from maps.
Wisdom-volkano shows them while calculating time-series on the fly as needed. Data sources from remote sensing InSAR data and seismic and GNSS receiver stations are integrated. Heat and SO₂ emissions datasets are ready to be integrated in future releases.
2. Allow several users over the world to use the tool or to run it in a laptop on the field.
Wisdom-volkano can be installed as a web server and in a laptop; files must be copied and set up.
3. Follow standards to integrate and reuse the tool within existing and future projects, so the source code shall ideally be open and available for all scientific community, except where explicitly requested by the ECGS/RMCA.
Wisdom-volkano is built with a web GIS architecture based on OGC and ISO standards, and has an open source license itself.
4. Integrate analytical functionalities like detrending.
Wisdom-volkano has detrending implemented and available for any time-series. It may integrate other functions easily such as the outlier detection.

The project will continue its development driven by the ECGS/RMCA requirements. But a project on acquiring and analysing real time data to generate alerts shall absolutely be considered. On the other hand, it may (and probably will) be incorporated in other projects, so its main purpose and even its name may change.

Monitoring volcanoes is crucial since they are still one of the big forces in nature. And we do not fully understand well in advance *when* they are about to trigger their power. While writing this, Popocatepetl in Mexico is erupting, millions of people in Puebla are covered by ashes and airports are closed (Finn 2016), what implies not only personal loses but also a great economic impact worldwide. It is very much worth investing time and resources in further researching volcanic activity.

This page intentionally left blank.

REFERENCES

- Agafonkin, V. 2015. Leaflet - a JavaScript library for interactive maps. Retrieved 8 June 2016, from <leafletjs.com>.
- Aitchinson, A. 2011. The Google Maps/Bing Maps Spherical Mercator Projection. Retrieved 9 April 2016, from <https://alastaira.wordpress.com/2011/01/23/the-google-maps-bing-maps-spherical-mercator-projection>.
- Allard, P., Baxter, P., Halbwachs, M., Kasareka, M., Komorowski, J. C., and Joron, J. L. 2003. The most destructive effusive eruption in modern history: Nyiragongo (RD. Congo), January 2002. *EGS - AGU - EUG Joint Assembly, Abstracts from the meeting held in Nice, France, 6 - 11 April 2003, abstract #11970*.
- Anderson, B., and Deoliveira, J. 2007. WMS Performance Tests! Mapserver & Geoserver (conference presentation). *FOSS4G*. Victoria, Canada: OSGeo.
- von Andrian, J. 2016. jQuery Sortable. Retrieved 8 June 2016, from <johnny.github.com/jquery-sortable>.
- Annoni, A., Luzet, C., Gubler, E., and Ihde, J. 2001. *Map Projections for Europe*. Joint Research Centre. European Union.
- Apple Inc. 2016. Mac - Apple. Retrieved 17 July 2016, from <apple.com/mac>.
- Athanasiou, S., Georgomanolis, N., Patroumpas, K., Alexakis, M., and Stratiotis, T. 2015. TripleGeo-CSW: A middleware for exposing geospatial catalogue services on the semantic web. *CEUR Workshop Proceedings*, 1330: 229–36.
- Baird, K. M., Smith, D. S., and Whitford, B. G. 1979. Confirmation of the currently accepted value 299 792 458 metres per second for the speed of light. *Optics Communications*, 31/3: 367–8. doi: 10.1016/0030-4018(79)90216-5.
- Battersby, S. E., Finn, M. P., Usery, E. L., and Yamamoto, K. H. 2014. Implications of Web Mercator and Its Use in Online Mapping. *Cartographica: The International Journal for Geographic Information and Geovisualization*, 49/2: 85–101. doi: 10.3138/cart0.49.2.2313.
- Battle, R., and Kolas, D. 2012. GeoSPARQL: Enabling a Geospatial Semantic Web. *Semantic Web Journal*, 1–17. doi: 10.3233/SW-2012-0065.
- Bergamaschi, P., Krol, M., Meirink, J. F., Dentener, F., Segers, A., Van Aardenne, J., Monni, S., et al. 2010. Inverse modeling of European CH₄ emissions 2001-2006. *Journal of Geophysical Research: Atmospheres*, 115/22: 1–18. doi: 10.1029/2010JD014180.
- Bernal-Carrera, R. 2014. Final Report Summary - EVOSS (European Volcano Observatory Space Services). *CORDIS - Community Research and Development Information Service*.
- Berners-Lee, T., Hendler, J., Lassila, O., and Others. 2001. The semantic web. *Scientific American*, 284/5: 34–43.
- Bootstrap. 2016. Bootstrap. Retrieved 8 June 2016, from <getbootstrap.com>.
- Bostock, M. 2013. D3.js - Data-Driven Documents. Retrieved 8 June 2016, from <d3js.org>.

- Boutell, T. 1997. PNG (Portable Network Graphics) Specification version 1.0. *IETF RFC 2083*. Retrieved 17 July 2016, from <rfc-editor.org/rfc/rfc2083.txt>.
- British Columbia Institute of Technology. 2016. CodeIgniter Web Framework. Retrieved from <codeigniter.com>.
- Burt, J. E., and Barber, G. M. 1996. *Elementary Statistics for Geographers*. (T. G. Press, Ed.), 2nd editio. New York, New York, USA.
- Canonical Ltd. 2016. Ubuntu. Retrieved 17 July 2016, from <ubuntu.com>.
- Carrara, a, Guzzetti, F., Cardinali, M., and Reichenbach, P. 2000. Use of GIS Technology in the Prediction and Monitoring of Landslide Hazard. *Natural Hazards*, 20: 117–35. doi: 10.1023/A:1008097111310.
- Colditz, R. R., Conrad, C., Wehrmann, T., Schmidt, M., and Dech, S. 2008. TiSeG: A Flexible Software Tool for Time-Series Generation of MODIS Data Utilizing the Quality Assessment Science Data Set. *IEEE Transactions on Geoscience and Remote Sensing*, 46/10: 3296–308. doi: 10.1109/TGRS.2008.921412.
- Le Cozannet, G., Bagni, M., Thierry, P., Aragno, C., and Kouokam, E. 2014. WebGIS as boundary tools between scientific geoinformation and disaster risk reduction action in volcanic areas. *Natural Hazards and Earth System Sciences*. doi: 10.5194/nhess-14-1591-2014.
- Creative Commons. 2015. Attribution-NonCommercial-ShareAlike 4.0 International. Retrieved 8 June 2016, from <<https://creativecommons.org/licenses/by-nc-sa/4.0/>>.
- Crockford, D. 2006. The application/json media type for JavaScript object notation (JSON). *IETF RFC 4627*. Retrieved 17 July 2016, from <tools.ietf.org/html/rfc4627>.
- Currenti, G., Napoli, R., Sicali, A., Greco, F., and Negro, C. Del. 2014. GEOFIM: A WebGIS application for integrated geophysical modeling in active volcanic regions. *Computers & Geosciences*, 70: 120–7. doi: 10.1016/j.cageo.2014.05.001.
- Chen, P. P.-S. 1976. The Entity-Relationship Unified View of Data Model-Toward a Unified View of Dat. *ACM Transactions on Database Systems*, 1/1: 9–36. doi: 10.1145/320434.320440.
- Van Dam, T., Wahr, J., Milly, P. C. D., Shmakin, A. B., Blewitt, G., Lavallée, D., and Larson, K. M. 2001. Crustal displacements due to continental water loading. *Geophysical Research Letters*, 28/4: 651–4. doi: 10.1029/2000GL012120.
- Defense Mapping Agency. 1989. The universal grids: Universal Transverse Mercator (UTM) and Universal Polar Stereographic (UPS) (No. DMA TM 8358.2). Fairfax VA, USA.
- De-la Beaujardiere, J. 2006. OpenGIS Web Map Server Implementation Specification. *Open Geospatial Consortium*. Atlanta.
- ECMA International. 2016. Standard ECMA-262 - ECMAScript 2016 Language Specification 7th edition. Retrieved 17 July 2016, from <ecma-international.org/publications/standards/Ecma-262.htm>.
- Edmunds, B. 2010. Ion Auth. Retrieved 8 June 2016, from <benedmunds.com/ion_auth>.
- Endo, E. T., and Murray, T. 1991. Real-time Seismic Amplitude Measurement (RSAM): a volcano monitoring and prediction tool. *Bulletin of Volcanology*, 53/7: 533–45. doi: 10.1007/BF00298154.

- ESRI. 1998. ESRI Shapefile Technical Description, 34. doi: 10.1016/0167-9473(93)90138-J.
- . 2016a. ArcGIS. Retrieved 8 June 2016, from <arcgis.com>.
- . 2016b. ArcGIS Services Directory - Project Geometries (Geometry). Retrieved 8 June 2016, from <[http://tasks.arcgisonline.com/ArcGIS/rest/services/Geometry/GeometryServer/project?inSR=4326&outSR=3857&geometries={%27geometryType%27:+%27esriGeometryPoint%27,%27geometries%27:+\[%27x%27:+29.100,%27y%27:+-1.500%7D](http://tasks.arcgisonline.com/ArcGIS/rest/services/Geometry/GeometryServer/project?inSR=4326&outSR=3857&geometries={%27geometryType%27:+%27esriGeometryPoint%27,%27geometries%27:+[%27x%27:+29.100,%27y%27:+-1.500%7D)>.
- European Commission. 2015. European Union Public Licence. Retrieved 8 June 2016, from <joinup.ec.europa.eu/software/page/eupl/licence-eupl>.
- European Parliament and Council of the European Union. 2007. Directive 2007/2/EC establishing an Infrastructure for Spatial Information in the European Community (INSPIRE). *Official Journal of the European Union*, L-108: 1–14.
- Fehler, M., and Chouet, B. 1982. Operation of a digital seismic network on Mount St. Helens volcano and observations of long period seismic events that originate under the volcano. *Geophysical Research Letters*, 9/9: 1017–20.
- Ferretti, A., Monti-guarnieri, A., Prati, C., and Rocca, F. 2007. *InSAR Principles: Guidelines for SAR Interferometry Processing and Interpretation*. (K. Fletcher, Ed.). Noordwijk: ESA Publications.
- Fielding, R., Gettys, J., Mogul, J., Frystyk, H., Masinger, L., Leach, P., and Berners-Lee, T. 1999. Hypertext transfer protocol-HTTP/1.1. *IETF RFC 2616*. Retrieved from <ietf.org/rfc/rfc2616.txt>.
- Fielding, R. T., and Taylor, R. N. 2002. Principled Design of the Modern Web Architecture. *ACM Transactions on Internet Technology*, 2/2: 115–50. doi: 10.1145/514183.514185.
- Finn, M. 2016. Mexico Popocatepetl Volcano Eruption Update: Ash Too Dangerous, Can Damage Plane Engines. Retrieved 21 April 2016, from <<http://www.scienceworldreport.com/articles/38520/20160421/mexico-popocatepetl-volcano-eruption-update-ash-too-dangerous-can-damage-plane-engines.htm>>.
- Fonseca, F. 2008. Encyclopedia of GIS. Shekhar S. & Xiong H. (eds) , pp. 388–91. Springer US: Boston, MA. doi: 10.1007/978-0-387-35973-1_513.
- Fowler, M., and Highsmith, J. 2001. The agile manifesto. *Software Development*, 9/August: 28–35. doi: 10.1177/004057368303900411.
- Frain, B. 2012. *Responsive Web Design with HTML5 and CSS3*, 2nd editio. Birmingham: Packt Publishing Ltd.
- Galle, B., Oppenheimer, C., Geyer, A., McGonigle, A. J. ., Edmonds, M., and Horrocks, L. 2003. A miniaturised ultraviolet spectrometer for remote sensing of SO₂ fluxes: a new tool for volcano surveillance. *Journal of Volcanology and Geothermal Research*, 119/1-4: 241–54. doi: 10.1016/S0377-0273(02)00356-6.
- Garrett, J. 2005. Ajax: A New Approach to Web Applications. Retrieved 17 July 2016, from <<http://www.adaptivepath.com/publications/essays/archives/000385.php>>.
- Geirsson, H., D’Oreye, N., Smets, B., Nobile, A., Samsonov, S., De Rauw, D., Mashagiro, N., et al. 2016. Volcano-tectonic deformation in the Kivu Region, Central Africa: Results from multi-year InSAR time series analysis and continuous GNSS observations of the Kivu Geodetic Network (KivuGNet). *EGU General Assembly*, p. 12555. Vienna, Austria.

- GitHub Inc. 2016. GitHub. Retrieved 17 July 2016, from <github.com>.
- Google. 2015. Google Earth Engine. Retrieved 8 June 2016, from <earthengine.google.com>.
- . 2016a. Google Maps. Retrieved 8 June 2016, from <maps.google.com>.
- . 2016b. Google Chrome. Retrieved 11 July 2016, from <google.com/chrome>.
- . 2016c. Google Earth. Retrieved 17 July 2016, from <google.com/earth>.
- Graizer, V., and Kalkan, E. 2008. Response of pendulums to complex input ground motion. *Soil Dynamics and Earthquake Engineering*, 28/8: 621–31. doi: 10.1016/j.soildyn.2007.09.003.
- Hägerstrand, T. 1970. What about people in Regional Science? *Papers of the Regional Science Association*, 24/1: 6–21. doi: 10.1007/BF01936872.
- Hanssen, R. F. 2001. *Radar interferometry: data interpretation and error analysis*. Dordrecht, The Netherlands: Kluwer Academic Publishers.
- Harris Geospatial Solutions. 2016. ENVI Header files. Retrieved 11 July 2016, from <harrisgeospatial.com/docs/ENVIHeaderFiles.html>.
- Highsoft AS. 2016. Interactive JavaScript charts for your webpage | Highcharts. Retrieved 8 June 2016, from <highcharts.com>.
- Hiramatsu, K., and Reitsma, F. 2004. GeoReferencing the Semantic Web: ontology based markup of geographically referenced information. *Joint EuroSDR/EuroGeographics workshop on Ontologies and Schema Translation Services*, 15–6.
- Iacovella, S. 2014. *GeoServer Cookbook*. Birmingham: Packt Publishing Ltd.
- Intel Corp. 2016. Intel | Data Center Solutions, IOT, and PC Innovation. Retrieved 17 July 2016, from <intel.com>.
- International Organization for Standardization. 2005. Open Geospatial Consortium Inc . OpenGIS ® Implementation Specification for Geographic information - Simple feature access - Part 1 : Common - ISO 19125 (No. ISO 19125). Geneva, Switzerland.
- . 2009. Information technology — Database languages — SQL Multimedia and application packages — Part 3: Spatial - ISO 13249-3:2006 (No. ISO 13249-3:2006). Geneva, Switzerland.
- . 2015. ISO 19136-2:2015 - Geographic information -- Geography Markup Language (GML) - Part 2: Extended schemas and encoding rules (No. ISO 19136). Geneva, Switzerland. Retrieved from <http://www.iso.org/iso/home/store/catalogue_tc/catalogue_detail.htm?csnumber=61585>.
- Internet Archive. 2014. Internet Wayback Machine. Retrieved 8 June 2016, from <archive.org/web>.
- ISO/TC 211. 2014. ISO 19115-1:2014 Geographic information - Metadata - Part 1: Fundamentals.
- Janev, M., Delipetrev, B., and Ristova, S. 2015. Performance benchmark of PHP frameworks with database select methods. *International Conference for young researchers, Technical Sciences, Industrial Management*, pp. 38–41. Burgas, Bulgaria.

- Janssens-Maenhout, G., Dentener, F., Van Aardenne, J., Monni, S., Pagliari, V., Orlandini, L., Klimont, Z., et al. 2012. *EDGAR-HTAP: a harmonized gridded air pollution emission dataset based on national inventories*. Luxembourg: Publications Office of the European Union. doi: 10.2788/14102.
- Johnson, E. 2015. Evaluation and Integration of a JavaScript Graphing Library for a Nationwide Honey Bee Hive Scale Network. Allendale, Michigan, United States: Grand Valley State University.
- Kandawasvika, A. M. 2009. On Interoperable Management of Multi-Sensors in Landslide Monitoring Applications, April: 1–172.
- Kervyn, F., D'Oreye, N., Delvaux, D., Barrière, J., Dewitte, O., Celli, G., Jacobs, L., et al. 2015. Remote Sensing and In Situ Detection and Tracking of Geohazards (RESIST). Retrieved 8 June 2016, from <<http://resist.africamuseum.be/>>.
- Khattar, R. K. 2014. A Web Services Based Water Data Sharing Approach using Open Geospatial Standards. Provo, Utah, United States: Brigham Young University.
- Kisangani, E. F. 2012. *Civil Wars in the Democratic Republic of Congo, 1960-2010*. Boulder: Lynne Rienner Publishers.
- Kluge, J., Kargl, F., and Weber, M. 2007. The Effects of the AJAX Technology on Web Application Usability. *International Conference on Web Information Systems and Technologies*, 289–94.
- Korpela, J. 2005. Tab Separated Values (TSV): a format for tabular data exchange. Retrieved 11 July 2016, from <<http://www.cs.tut.fi/~jkorpela/TSV.html>>.
- Kukowski, N. 2013. Encyclopedia of Marine Geosciences. Harff J., Meschede M., Petersen S., & Thiede J. (eds) , pp. 1–2. Springer Netherlands: Dordrecht. doi: 10.1007/978-94-007-6644-0_107-1.
- Linux Kernel Organisation Inc. 2016. The Linux Kernel Archives. Retrieved 17 July 2016, from <kernel.org>.
- Lovelace, R. 2014. Testing web map APIs - Google vs OpenLayers vs Leaflet. Retrieved 20 April 2016, from <<http://robinlovelace.net/software/2014/03/05/webmap-test.html>>.
- Lu, Z. 2007. InSAR imaging of volcanic deformation over cloud-prone areas - Aleutian islands. *Photogrammetric Engineering and Remote Sensing*, 73/3: 245–57.
- Luzi, G. 2010. Ground Based SAR Interferometry: a Novel Tool for Geoscience. *Geoscience and Remote Sensing New Achievements*, pp. 1–27. InTech. doi: 10.5772/9090.
- MapBox. 2016. Mapbox | Design and publish beautiful maps. Retrieved 8 June 2016, from <mapbox.com>.
- Massonnet, D., and Feigl, K. L. 1998. Radar interferometry and its application to changes in the Earth's surface. *Reviews of Geophysics*, 36/4: 441. doi: 10.1029/97RG03139.
- Mavonga, T., Kavotha, S. K., Lukaya, N., Etoy, O., and Durieux, J. 2006. Seismic activity prior to the May 8, 2004 eruption of volcano Nyamuragira, Western Rift Valley of Africa. *Journal of Volcanology and Geothermal Research*, 158/3-4: 355–60. doi: 10.1016/j.jvolgeores.2006.06.021.

- Mavonga, T., Zana, N., and Durrheim, R. J. 2010. Studies of crustal structure, seismic precursors to volcanic eruptions and earthquake hazard in the eastern provinces of the Democratic Republic of Congo. *Journal of African Earth Sciences*, 58/4: 623–33. Elsevier Ltd. doi: 10.1016/j.jafrearsci.2010.08.008.
- McNutt, S. R. 1992. Volcanic Tremor. *Encyclopedia of Earth System Science*, 4: 417–25.
- Mendoza-Rosas, A. T., and De la Cruz-Reyna, S. 2008. A statistical method linking geological and historical eruption time series for volcanic hazard estimations: Applications to active polygenetic volcanoes. *Journal of Volcanology and Geothermal Research*, 176/2: 277–90. doi: 10.1016/j.jvolgeores.2008.04.005.
- Microsoft. 2016a. SQL Server 2016 | Microsoft. Retrieved 8 June 2016, from <microsoft.com/en-us/server-cloud/products/sql-server/>.
- . 2016b. Windows | Microsoft. Retrieved 17 July 2016, from <windows.com>.
- . 2016c. Excel. Retrieved 17 July 2016, from <office.microsoft.com/excel>.
- . 2016d. Bing Maps. Retrieved 8 June 2016, from <bing.com/maps>.
- Moreno-Rivera, J. M., Osann Jochum, A., Calera, A., and Sánchez, J. 2009. SPIDER - An Open GIS application use case for irrigation water management. *1st Open GIS UK Conference*. University of Nottingham.
- Mozilla Foundation. 2016. Mozilla Firefox. Retrieved 11 July 2016, from <mozilla.org/firefox>.
- Murphy, S. W., Filho, C. R. de S., and Oppenheimer, C. 2011. Monitoring volcanic thermal anomalies from space: Size matters. *Journal of Volcanology and Geothermal Research*, 203/1-2: 48–61. Elsevier B.V. doi: 10.1016/j.jvolgeores.2011.04.008.
- National Geospatial Intelligence Agency. 2014. Implementation Practice - Web Mercator Map Projection (No. 1.0.0). Fort Belvoir, Springfield, Virginia, United States.
- National Imagery and Mapping Agency (NIMA). 2000. Department of Defense World Geodetic System 1984. St. Louis MO, USA. Retrieved from <http://earth-info.nga.mil/GandG/publications/tr8350.2/wgs84fin.pdf>.
- Node.js Foundation. 2016. Node.js. Retrieved 8 June 2016, from <nodejs.org>.
- Norris, J., and Snell, J. 2015. Future trends in geospatial information management: the five to ten year vision, Second Edition December 2015. New York, New York, USA.
- OGC and OSGeo. 2011. Open Source and Open Standards. Retrieved 11 July 2016, from <https://wiki.osgeo.org/wiki/Open_Source_and_Open_Standards>.
- Open Geospatial Consortium. 2014. OGC WaterML 2.0: Part 1 - Timeseries. *OGC 10-126r4*, 10-126 revision 4.
- . 2016a. KML | OGC. Retrieved 11 July 2016, from <opengeospatial.org/standards/kml>.
- . 2016b. Geography Markup Language | OGC. Retrieved 11 July 2016, from <opengeospatial.org/standards/gml>.
- . 2016c. Styled Layer Descriptor | OGC. Retrieved 11 July 2016, from <opengeospatial.org/standards/sld>.

- Open Source Geospatial Foundation. 2014. GeoServer. Retrieved 8 June 2016, from <geoserver.org>.
- . 2016a. GeoTIFF. Retrieved 11 July 2016, from <trac.osgeo.org/geotiff/>.
- . 2016b. MapServer. Retrieved 8 June 2016, from <mapserver.org>.
- . 2016c. OpenLayers 3. Retrieved 8 June 2016, from <openlayers.org>.
- . 2016d. GDAL: GDAL - Geospatial Data Abstraction Library. Retrieved 8 June 2016, from <gdal.org>.
- OpenStreetMap. 2016. OpenStreetMap. Retrieved 8 June 2016, from <openstreetmap.org>.
- Oracle. 2015. Database 12c | Oracle. Retrieved 8 June 2016, from <oracle.com/database>.
- . 2016. MySQL. Retrieved 8 June 2016, from <mysql.com>.
- Parker, J., Donnellan, A., Glasscoe, M., Fox, G., Wang, J., Pierce, M., and Ma, Y. 2015. Advantages to Geoscience and Disaster Response from QuakeSim Implementation of Interferometric Radar Maps in a GIS Database System. *Pure and Applied Geophysics*, 172/8: 2295–304. doi: 10.1007/s00024-014-0886-8.
- Patra, S. K. 2014. Data Visualization for Hybrid Application : The Challenges in Choosing an Optimal Library for Line Chart. *International Journal of Emerging Science and Engineering (IJESE)*, 2/10: 12–5.
- Peltier, A., Bianchi, M., Kaminski, E., Komorowski, J. C., Rucci, A., and Staudacher, T. 2010. PSInSAR as a new tool to monitor pre-eruptive volcano ground deformation: Validation using GPS measurements on Piton de la Fournaise. *Geophysical Research Letters*, 37/12: 1–5. doi: 10.1029/2010GL043846.
- Perry, M., and Herring, J. 2012. OGC GeoSPARQL-A geographic query language for RDF data. *OGC Candidate Implementation Standard*, 57.
- Portele, C. 2012. OGC Geography Markup Language (GML) — Extended schemas and encoding rules (No. OGC 10-129r1 v3.3.0).
- QGIS. 2016. QGIS. Retrieved 8 June 2016, from <qgis.org>.
- QlikTech International AB. 2016. Business Intelligence | Data Visualization Tools | Qlik. Retrieved 8 June 2016, from <qlik.com>.
- Refractions Research. 2016. PostGIS - Spatial and Geographic Objects for PostgreSQL. Retrieved 8 June 2016, from <postgis.net>.
- Resig, J. 2016. jQuery. Retrieved 8 June 2016, from <jquery.com>.
- Romero, J. E., Titos, M., Bueno, Á., Álvarez, I., García, L., Torre, Á. de la, and Benítez, M. C. 2016. APASVO: A free software tool for automatic P-phase picking and event detection in seismic traces. *Computers & Geosciences*, 90: 213–20. Elsevier. doi: 10.1016/j.cageo.2016.02.004.
- Roth, R., Donohue, R., Sack, C., Wallace, T., and Buckingham, T. 2013. A Process for Assessing Emergent Web Mapping Technologies. Buchroithner M. F. (ed.) *ICC2013*. Dresden, Germany: ICC.

- Rusangiza, B. K., Mavonga, T., Lesage, P., Kavotha, K. S., Wafula, M., Lukaya, N., and Ciza, A. 2012. About swarms of long - period earthquakes at volcano nyamuragira of the virunga region, Western Rift Valley of Africa (D.R. Congo). *Geographica Pannonica*, 16/1: 10–7.
- Sae-Tang, A., and Ertz, O. 2007. Towards Web Services Dedicated to Thematic Mapping. *OSGeo Journal*, 3/December: 31–4.
- Samra, J. 2015. Comparing Performance of Plain PHP and Four of Its Popular Frameworks. Linnaeus University, Växjö, Sweden.
- Samsonov, S., D'Oreye, N., and D'Oreye, N. 2012. Multidimensional time-series analysis of ground deformation from multiple InSAR data sets applied to Virunga Volcanic Province. *Geophysical Journal International*, 191/3: 1095–108. doi: 10.1111/j.1365-246X.2012.05669.x.
- Sansosti, E., Casu, F., Manzo, M., and Lanari, R. 2010. Space-borne radar interferometry techniques for the generation of deformation time series: An advanced tool for Earth's surface displacement analysis. *Geophysical Research Letters*, 37/20: 1–9. doi: 10.1029/2010GL044379.
- Scharl, A., and Tochtermann, K. 2007. *The Geospatial Web*. London: Springer London. doi: 10.1007/978-1-84628-827-2.
- Schivei Costa, N. 2016. Google Maps Tiles for OpenLayers 3. Retrieved 8 June 2016, from <github.com/schivei/ol-source-gmaps-tms>.
- Shutterstock. 2016. Rickshaw: A JavaScript toolkit for creating interactive time-series graphs. Retrieved 8 June 2016, from <code.shutterstock.com/rickshaw>.
- Van Sickle, J. 2010. *Basic GIS Coordinates*. (CRC Press, Ed.), Second edi. Boca Raton, FL.
- Slocum, T. A., McMaster, R. B., Kessler, F. C., and Howard, H. H. 2010. *Thematic cartography and geovisualization*, Third, Int. Upper Saddle River NJ, USA: Pearson Prentice Hall.
- Smets, B., D'Oreye, N., Kervyn, F., Kervyn, M., Albino, F., Arellano, S. R., Bagalwa, M., et al. 2013. *Detailed multidisciplinary monitoring reveals pre- and co-eruptive signals at Nyamulagira volcano (North Kivu, Democratic Republic of Congo)*. *Bulletin of Volcanology*, Vol. 76. doi: 10.1007/s00445-013-0787-1.
- Smets, B., Kervyn, M., D'Oreye, N., and Kervyn, F. 2015. Spatio-temporal dynamics of eruptions in a youthful extensional setting: Insights from Nyamulagira Volcano (D.R. Congo), in the western branch of the East African Rift. *Earth-Science Reviews*. doi: 10.1016/j.earscirev.2015.08.008.
- Smets, B., Tedesco, D., Kervyn, F., Kies, A., Vaselli, O., and Yalire, M. M. 2010. Dry gas vents ('mazuku') in Goma region (North-Kivu, Democratic Republic of Congo): Formation and risk assessment. *Journal of African Earth Sciences*, 58/5: 787–98. doi: 10.1016/j.jafrearsci.2010.04.008.
- Smets, B., Wauthier, C., and D'Oreye, N. 2010. A new map of the lava flow field of Nyamulagira (D.R. Congo) from satellite imagery. *Journal of African Earth Sciences*, 58/5: 778–86. doi: 10.1016/j.jafrearsci.2010.07.005.
- Smithsonian Institution. 2013. Nyamuragira / Nyiragongo Monthly Reports. Retrieved 11 July 2016, from <http://volcano.si.edu/>.
- Snyder, J. (Usgs). 1997. *Flattening the earth: two thousand years of map projections*. Chicago, Illinois, United States: University of Chicago Press.

- Van de Sompel, H., Nelson, M., and Sanderson, R. 2013. HTTP Framework for Time-Based Access to Resource States -- Memento (No. RFC 7089). ISSN 2070-1721.
- SQL Maestro Group. 2016. PostgreSQL GUI Admin Tool - Postgres manager for Windows by SQL Maestro Group. Retrieved 8 June 2016, from <sqlmaestro.com/products/postgresql/maestro>.
- Steiniger, S., and Hunter, A. J. S. 2012. Free and Open Source GIS Software for Building a Spatial Data Infrastructure. Bocher E. & Neteler M. (eds) *Geospatial free and open source software in the 21st century*, pp. 247–61. Springer-Verlag Berlin Heidelberg: Berlin. doi: 10.1007/978-3-642-10595-1_15.
- Stenberg, C. 2016. curl and libcurl. Retrieved 8 June 2016, from <curl.haxx.se>.
- Stolze, K. 2003. SQL/MM Spatial - The Standard to Manage Spatial Data in a Relational Database System. *Datenbanksysteme für Business, Technologie und Web*, pp. 247–64. Leipzig, Germany: Gesellschaft für Informatik - GI (German Computer Society).
- Tableau Software. 2016. Business Intelligence and Analytics | Tableau Software. Retrieved 8 June 2016, from <tableau.com>.
- Tait, S., and Ferrucci, F. 2013. A Real-Time, Space Borne Volcano Observatory to Support Decision Making during Eruptive Crises: European Volcano Observatory Space Services. *2013 UKSim 15th International Conference on Computer Modelling and Simulation*, pp. 283–9. IEEE. doi: 10.1109/UKSim.2013.121.
- Tanaka, M. 2014. C3.js | D3-based reusable chart library. Retrieved 8 June 2016, from <c3js.org>.
- Tedesco, D., Vaselli, O., Papale, P., Carn, S. A., Voltaggio, M., Sawyer, G. M., Durieux, J., et al. 2007. January 2002 volcano-tectonic eruption of Nyiragongo volcano, Democratic Republic of Congo. *Journal of Geophysical Research*, 112/B9: B09202. doi: 10.1029/2006JB004762.
- The PHP Group. 2016. PHP: Hypertext Preprocessor. Retrieved 17 July 2016, from <php.net>.
- The PostgreSQL Global Development Group. 2016. PostgreSQL: The world's most advanced open source database. Retrieved 8 June 2016, from <postgresql.org>.
- Theeten, F. 2011. Creating a tiled raster image (pyramid) with Geoserver + OpenLayers. *Cybertaxonomy Portal, Royal Museum for Central Africa, Tervuren*. Retrieved 6 April 2016, from <http://cybertaxonomy.africamuseum.be/node/49>.
- Tonini, R., Sandri, L., and Anne Thompson, M. 2015. PyBetVH: A Python tool for probabilistic volcanic hazard assessment and for generation of Bayesian hazard curves and maps. *Computers & Geosciences*, 79: 38–46. doi: 10.1016/j.cageo.2015.02.017.
- Tuszynski, J., and Khachatryan, H. 2015. Package 'caTools'. Retrieved 3 June 2016, from <http://cran.r-project.org/package=caTools>.
- Upton, D. 2007. *Codeigniter for Rapid Php Application Development. Image Rochester NY*. Birmingham: Packt Publishing Ltd.
- Vicari, A., Bilotta, G., Bonfiglio, S., Cappello, A., Ganci, G., Hérault, A., Rustico, E., et al. 2011. LAV@HAZARD: a web-GIS interface for volcanic hazard assessment. *Annals of Geophysics*. doi: 10.4401/ag-5347.

- Vizzuality. 2016. CartoDB - Predict through location. Retrieved 8 June 2016, from <cartodb.com>.
- W3C. 1998. Extensible Markup Language (XML). Retrieved 17 July 2016, from <w3.org/XML>.
- . 2009. Web addresses in HTML5. Retrieved 17 July 2016, from <w3.org/html/wg/href/draft#url>.
- . 2014. HTML5. Retrieved 11 July 2016, from <w3.org/TR/html5/>.
- . 2016. Cascading Style Sheets. Retrieved 11 July 2016, from <w3.org/CSS>.
- Wauthier, C., Cayol, V., Kervyn, F., and D'Oreye, N. 2012. Magma sources involved in the 2002 Nyiragongo eruption, as inferred from an InSAR analysis. *Journal of Geophysical Research: Solid Earth*, 117/B5: 1–20. doi: 10.1029/2011JB008257.
- Wauthier, C., Cayol, V., Smets, B., D'Oreye, N., and Kervyn, F. 2015. Magma pathways and their interactions inferred from InSAR and stress modeling at Nyamulagira Volcano, D.R. Congo. *Remote Sensing*, 7/11: 15179–202. doi: 10.3390/rs71115179.
- van Wijk, J. J. 2008. Unfolding the Earth: Myriahedral Projections. *Cartographic Journal, The*, 45/1: 32–42. doi: 10.1179/000870408X276594.
- Wooster, M. J., and Rothery, D. A. 1997. Thermal monitoring of Lascar volcano, Chile, using infrared data from the along-track scanning radiometer: a 1992-1995 time series. *Bulletin of Volcanology*, 58/7: 566–79. doi: 10.1007/s004450050163.
- Wright, D. J., O'Dea, E., Cushing, J. B., Cuny, J. E., and Toomey, D. R. 2003. Why Web GIS May Not Be Enough: A Case Study with the Virtual Research Vessel. *Marine Geodesy*, 26/1-2: 73–86. doi: 10.1080/01490410306701.
- Yourdon, E. 1989. *Modern structured analysis*. Upper Saddle River NJ, USA: Prentice Hall.

APPENDIX: Source codes

Source code 1: Reading a pixel value from an ENVI header raster file

Code inspired in (Tuszynski and Khachatryan 2015) and its Python implementation in Spectral Python (Boggs, T., <github.com/spectralpython/spectral/blob/master/spectral/io/envi.py>) package.

```
01 public function get_pixel( $binfile, $col, $row )
02 {
03   $file = fopen( $binfile, "rb" );

04   // goes to the offset: file and column where the pixel is
05   $offset = $this->headerOffset
06             + $row * $this->nCol * $this->dataType
07             + $col * $this->dataType;
08   fseek( $file, $offset );

09   //reads a number of bytes depending on the dataType
10   $bytes = fread( $file, $this->dataType );
11   fclose( $file );

12   //if local comp encodes as little endian, must be reversed
13   $v = unpack('S', "\x01\x00");
14   $ieee = ( $v[1] === 1 ) ? 0 : 1;
15   $endian = ( $ieee == $this->byteOrder
16             || $this->byteOrder < 0 ) ? "big" : "little";
17   if( $endian == "little" )
18     $bytes = strrev( $bytes );

19   // the read value is unpacked to an array and returned
20   $val = unpack( "f*", $bytes );
21   return $val[1];
22 }
```

Source code 2: PHP to exec cURL in order to get the list of workspaces from GeoServer REST

```
1 $curl = 'curl -u '
2     . $this->config->item( 'geoserver_userpwd' )
3     . ' -v -XGET -H "Accept: text/xml" '
4     . ' http://geoserver_name:8080/geoserver/workspaces/ ';
5 $out = shell_exec( $curl );
6 // With cURL we call the GeoServer REST for the workspaces' list
7 $xml = simplexml_load_string( $out );
8 // The response is XML, which must be decoded
9 if( $xml instanceof SimpleXMLElement ) {
10   foreach( $xml as $workspace ) {
11     // do something with the $workspace name
12   }
13 }
```

Source code 3: REST calls to get the list of rasters or layers from GeoServer

```
4     . ' http://geoserver_name:8080/geoserver/cint/coveragestores/ ';
4     . ' http://geoserver_name:8080/geoserver/cint/datastores/ ';
```

Source code 4: JavaScript using OpenLayers library to access the GeoServer WMS of a complex interferogram

```
// Connecting to GeoServer WMS to get a complex interfero
1  new ol.layer.Tile({
  // This is the name given in GeoServer
2  title: 'cint:A228Nyiragongo11104_18619',
  // Connection from OpenLayers to GeoServer WMS
3  source: new ol.source.TileWMS({
4    url: 'http://geoserver_name:8080/geoserver/cint/wms',
5    params: { 'LAYERS': 'cint:A228Nyiragongo11104_18619',
  // Tiled WMS request will save bandwidth and speed the visualization
6      'TILED': true
7    }
8  }),
```

Source code 5: OpenLayers JavaScript code to add the two station layers from KML files

```
20  new ol.layer.Vector({
21    source: new ol.source.Vector({
22      url: "/assets/data/stations/Seismos.kml",
23      format: new ol.format.KML()
24    })
25  }),
26  new ol.layer.Vector({
27    source: new ol.source.Vector({
28      url: "/assets/data/stations/GPS.kml",
29      format: new ol.format.KML()
30    })
31  })
```

Source code 6: OpenLayers JavaScript code to add the two station layers from GeoServer

Workspace and layer names in lines 25 and 34 are hard coded.

```
20  new ol.layer.Image({
21    title: "gnss",
22    source: new ol.source.ImageWMS({
23      url: 'http://geoserver_name:8080/geoserver/geom/wms',
24      params: {
25        'LAYERS' : 'geom:GNSS_station'
26      }
27    })
28  }),
29  new ol.layer.Image({
30    title: "seismo",
31    source: new ol.source.ImageWMS({
32      url: 'http://geoserver_name:8080/geoserver/geom/wms',
33      params: {
34        'LAYERS' : 'geom:Seismo_station'
35      }
36    })
37  })
```

Source code 7: JavaScript for loading via OpenLayers the background layers, Google Maps and OpenStreetMap

```
    // Connecting from OpenLayers to Google Maps (needs API key)
 9   new ol.layer.Tile({
10     title: "gmaps",
11     source: ol.source.GMapsTMS({layer: 'satellite'})
12   }),
    // Connecting from OpenLayers to OpenStreetMap
13   new ol.layer.Tile({
14     title: "bg-osm",
15     source: new ol.source.OSM()
16   })
```

Source code 8: JavaScript for preparing and performing an asynchronous JavaScript and XML (ajax) call to get information on the selected point for all layers

```
    // The clicked point coordinates are "coords", in WGS 84 or EPSG:4326
    // So they must be reprojected to Web Mercator or EPSG:3857
01 var coord3857=ol.proj.transform( coords, 'EPSG:4326', 'EPSG:3857' );
    // Then one or more layer(s) information is loaded, here is 1
02 var srcLayer1 = listLayers[ i ].getSource();
03 var urlLayer1 = srcLayer1.getGetFeatureInfoUrl(
04   coord3857, viewResolution, view.getProjection(),
05   {'INFO_FORMAT': 'application/json'});
(...)
    // Point + all layers loaded sent to GeoServer, to find out...
    // which of those layers can be found at that point?
10 $.ajax({type: "POST",
11   url: "/index.php/geoserver/ajaxGetFeatInfo/",
12   data: { url1: urlLayer1
13     //, url2: urlLayer2...
14   },
15   success: function(result){ // construct and show the response
```

Source code 9: PHP code to execute the ajax call from Source code 8

```
1 $curl = 'curl -u -v '
2   . $this->config->item( 'geoserver_userpwd' )
3   . $urlLayer1;
4 $out = shell_exec( $curl );
5 $json = json_decode( $out );
6 if( count( $json['features'] ) {
7   // echo data available to return
8   else echo '';
```

Source code 10: URL created by the call in Source code 8 and response generated in JavaScript Object Notation (JSON)

```
// URL query from line 12 in Source code 8, run in line 4 in Source code 9
http://127.0.0.1:8080/geoserver/geom/wms?SERVICE=WMS&VERSION=1.3.0&REQUEST=GetFeatureInfo&FORMAT=image%2Fpng&TRANSPARENT=true&QUERY_LAYERS=geom%3AGNSS_station&LAYERS=geom%3AGNSS_station&INFO_FORMAT=application%2Fjson&FEATURE_COUNT=50&I=50&J=50&CRS=EPSG%3A3857&STYLES=&WIDTH=101&HEIGHT=101&BBOX=3231677.042227458%2C-174718.4536097248%2C3247117.3219410637%2C-159278.1738961192
```

```
// Response in JSON, decoded in line 5 in Source code 9
// and returned in line 15 in Source code 8
{"type":"FeatureCollection","totalFeatures":"unknown","features":[{"type":"Feature","id":"GNSS_station.7","geometry":{"type":"Point","coordinates":[29.01308599002924,-1.706252935240847]},"geometry_name":"the_geom","properties":{"Name":"BOB","Description":""}}],"crs":{"type":"name","properties":{"name":"urn:ogc:def:crs:EPSG::4326"}}}
```

Source code 11: JavaScript code to declare the events used as background in the MSBAS chart

```
01 var ar = [];
02 ar[ Date.UTC(2009, 5, 15) ] = "SP&LP Swarms";
03 ar[ Date.UTC(2009, 9, 15) ] = "SP Swarms";
04 ar[ Date.UTC(2009, 12, 15) ] = "SP&LP Swarms";
05 ar[ Date.UTC(2010, 1, 2) ] = "Eruption Onset 2010";
06 ar[ Date.UTC(2010, 1, 27) ] = "Eruption End 2010";
Etc.
30 var baseY = -2.5; // base Y-axis for the labels, can be negative
31 for( var i in ar )
32 { dataH[ z++ ] = [ parseInt( i ), baseY ]; }
```

Source code 12: JavaScript Highcharts code to load the events data from Source code 11

```
1 $('#chart0').highcharts({
2   chart: { type: 'column', zoomType: 'x' },
3   title: { text: 'No data yet' },
4   xAxis: { type: 'datetime' },
5   series: [{
6     name: 'Select a point in the map in order to show the
timeseries',
7     // dataH has the list of events loaded
8     data: dataH
9   }
10  ]});
```

Source code 13: PHP code to generate the MSBAS time-series boundaries from the interferogram data

```
1 $data[ 'left' ] = $ts->ts_coord_lon_left;
2 $data[ 'right' ] = $ts->ts_coord_lon_left
3   + $ts->ts_coord_lon_inc * $enviheader->get_value( "nCol" );
4 $data[ 'top' ] = $ts->ts_coord_lat_top;
5 $data[ 'down' ] = $ts->ts_coord_lat_top
6   - $ts->ts_coord_lat_inc * $enviheader->get_value( "nRow" );
```

Source code 14: JavaScript and PHP code to check if the clicked point is within MSBAS time-series boundaries

```

1  if( type == 'msbas'
2    && coord[0] >= <?php echo $left; ?>
3    && coord[0] <= <?php echo $right; ?>
4    && coord[1] <= <?php echo $stop; ?>
5    && coord[1] >= <?php echo $down; ?> ) // coord[1] is negative

```

Source code 15: PHP code to generate the JavaScript code for MSBAS time-series

```

// Generates a Javascript line per each MSBAS time-series to be read
01 for( $i = 0; $i < $totMsbas; $i ++ ) {
03   echo "tsv".$i.".done( function( csv".$i.") {           \n" .
04     "   if(csv".$i."=='false') return 'Data not found'; \n" .
05     "   else {                                           \n";
06 }
// And will load the time-series into a variable
07 for( $i = 0; $i < $totMsbas; $i ++ ) {
08   echo "var data".$i."=[]; // [ dates, values ]         \n";
09 }

// Will split every time-series line to get each pair: date, value
20 for( $i = 0; $i < $totMsbas; $i ++ ) {
21   echo "lines=csv".$i.".split('\n');                   \n" .
22     "$.each(lines, function( lineNo, line ) {         \n" .
23     "   items=line.split('\t');                       \n" .
// Date is in decimal format, must be decoded
24     "   fecha=tick2Date(items[0]);                     \n" .
// And value is a float. Loads date, value in an array
25     "   data".$i.".push([fecha,parseFloat(items[1])]); \n" .
26     "});                                               \n";
27 }
// Name for the time-series "name, lat, lon"

30 echo "name: '". $det." ".trim($ts_msbas[$i]->ts_name )
31     . "   lat: ".$lat[$i]." lon: ".$lon[$i]."',         \n"
32     . "showInLegend: true,                             \n"
33     . "enableMouseTracking: true,                      \n"
// the data array is linked with the chart
34     "data: data".$i."                                   \n"
Etc.

```

Source code 16: JavaScript to execute the Source code 15

```

1  success: function(result){
2    //console.log( result ); // uncomment to debug the ts code
3    try {
// this single line makes that the generated Javascript code "result"
// is actually executed after being returned (echoed in ajax)
4      eval(result);
5    } catch (e) {
6      if (e instanceof SyntaxError) {console.log(e.message);}

```

Source code 17: KML code for a station

```

<Placemark>
  <name>BOB</name>
  <LookAt>
    <longitude>29.01415579435389</longitude>
    <latitude>-1.706567298803349</latitude>
    <altitude>0</altitude>
    <heading>16.09102427818585</heading>
    <tilt>0</tilt>
    <range>469.3413698331368</range>
    <gx:altitudeMode>relativeToSeaFloor</gx:altitudeMode>
  </LookAt>
  <styleUrl>#msn_placemark_circle0</styleUrl>
  <Point>
    <coordinates>29.01308599002924,-
1.706252935240847,0</coordinates>
  </Point>
</Placemark>

```

Source code 18: JavaScript to generate HTML code to keep every chart time-series station

```

1 var newdiv;
2 for( var i = 1; i <= ( ts_seism_num + ts_gnss_num ); i++ ) {
3   newdiv = '<div class="chart" id="chart' + i + '">';
4   // The following jQuery code appends the HTML div above
5   // to the div below "#container"
6   $( newdiv ).appendTo( $('#container') );
7 }

```

Source code 19: PHP code to generate the JavaScript code to unload the time-series and remove the chart

```

1 echo "text: 'remove timeseries', \n" .
2   "onclick: function() { \n" .
3   // It locates the station in the Javascript array of time-series
4   " var i=ts_seism_data.indexOf('".$seism_station."');\n" .
5   // Removes the station from the Javascript array
6   " ts_seism_data.splice( i, 1 ); \n" .
7   // Removes the div for this station, created in Source code 18
8   " $('#chart" . $nth . "').remove(); \n" .
9   " ts_seism_num --; \n" .
10  // And destroys the Highcharts object to unload it from memory
11  " this.destroy(); \n" .

```

Source code 20: PHP to calculate the trend or regression parameters, based on a zoomed region

```

// Implementation of equation (6)
01 $n = count($x);
02 $x_sum = array_sum($x);
03 $y_sum = array_sum($y);
04 $xx_sum = 0; $xy_sum = 0;
05 for($i = 0; $i < $n; $i++) {
06   $xy_sum+=$x[$i]*$y[$i];
07   $xx_sum+=$x[$i]*$x[$i];
08 }
09 $b=(( $n*$xy_sum)-($x_sum*$y_sum))/(( $n*$xx_sum)-($x_sum*$x_sum));
// Implementation of equation (7); many calculations are done
10 $a=($y_sum-($b*$x_sum))/ $n;

```

Source code 21: PHP to calculate the theoretical trend for the whole time-series

```
20 for( $i = 0; $i < count( $x ); $i++ )
21     $ytrend[$i] = ( $x[$i] * $b ) + $a;
```

Source code 22: PHP to remove the trend of the whole time-series

```
30 for( $i = 0; $i < count( $yreal ); $i++ )
31     $ydetrend[$i] = $yreal[$i] - $ytrend[$i] + $offset;
```

Source code 23: JavaScript for showing the OpenLayers projection in the console log and result

```
console.log('projection: '+map.getView().getProjection().getCode());
> projection: EPSG:3857
```

Source code 24: JavaScript for rounding to a maximum of three decimals of WGS 84 geographical coordinates

```
var hdms = ol.coordinate.toStringXY( coord, 3 );
```

Source code 25: PHP code to log the use grant of a layer to a user by another

```
log_message( 'info', '[Wisdom-volkano] Layer '. $layer_name
. ' granted to ' . $user_email
. ' by ' . $this->session->userdata( 'email' ) );
```

This page intentionally left blank.

Series from Lund University

Department of Physical Geography and Ecosystem Science

Master Thesis in Geographical Information Science

1. *Anthony Lawther*: The application of GIS-based binary logistic regression for slope failure susceptibility mapping in the Western Grampian Mountains, Scotland. (2008).
2. *Rickard Hansen*: Daily mobility in Grenoble Metropolitan Region, France. Applied GIS methods in time geographical research. (2008).
3. *Emil Bayramov*: Environmental monitoring of bio-restoration activities using GIS and Remote Sensing. (2009).
4. *Rafael Villarreal Pacheco*: Applications of Geographic Information Systems as an analytical and visualization tool for mass real estate valuation: a case study of Fontibon District, Bogota, Columbia. (2009).
5. *Siri Oestreich Waage*: a case study of route solving for oversized transport: The use of GIS functionalities in transport of transformers, as part of maintaining a reliable power infrastructure (2010).
6. *Edgar Pimiento*: Shallow landslide susceptibility – Modelling and validation (2010).
7. *Martina Schäfer*: Near real-time mapping of floodwater mosquito breeding sites using aerial photographs (2010).
8. *August Pieter van Waarden-Nagel*: Land use evaluation to assess the outcome of the programme of rehabilitation measures for the river Rhine in the Netherlands (2010).
9. *Samira Muhammad*: Development and implementation of air quality data mart for Ontario, Canada: A case study of air quality in Ontario using OLAP tool. (2010).
10. *Fredros Oketch Okumu*: Using remotely sensed data to explore spatial and temporal relationships between photosynthetic productivity of vegetation and malaria transmission intensities in selected parts of Africa (2011).
11. *Svajunas Plunge*: Advanced decision support methods for solving diffuse water pollution problems (2011).
12. *Jonathan Higgins*: Monitoring urban growth in greater Lagos: A case study using GIS to monitor the urban growth of Lagos 1990 - 2008 and produce future growth prospects for the city (2011).
13. *Mårten Karlberg*: Mobile Map Client API: Design and Implementation for Android (2011).
14. *Jeanette McBride*: Mapping Chicago area urban tree canopy using color infrared imagery (2011).
15. *Andrew Farina*: Exploring the relationship between land surface temperature and vegetation abundance for urban heat island mitigation in Seville, Spain (2011).
16. *David Kanyari*: Nairobi City Journey Planner An online and a Mobile Application (2011).

17. *Laura V. Drews*: Multi-criteria GIS analysis for siting of small wind power plants - A case study from Berlin (2012).
18. *Qaisar Nadeem*: Best living neighborhood in the city - A GIS based multi criteria evaluation of ArRiyadh City (2012).
19. *Ahmed Mohamed El Saeid Mustafa*: Development of a photo voltaic building rooftop integration analysis tool for GIS for Dokki District, Cairo, Egypt (2012).
20. *Daniel Patrick Taylor*: Eastern Oyster Aquaculture: Estuarine Remediation via Site Suitability and Spatially Explicit Carrying Capacity Modeling in Virginia's Chesapeake Bay (2013).
21. *Angeleta Oveta Wilson*: A Participatory GIS approach to *unearthing* Manchester's Cultural Heritage 'gold mine' (2013).
22. *Ola Svensson*: Visibility and Tholos Tombs in the Messenian Landscape: A Comparative Case Study of the Pylian Hinterlands and the Soulima Valley (2013).
23. *Monika Ogden*: Land use impact on water quality in two river systems in South Africa (2013).
24. *Stefan Rova*: A GIS based approach assessing phosphorus load impact on Lake Flaten in Salem, Sweden (2013).
25. *Yann Buhot*: Analysis of the history of landscape changes over a period of 200 years. How can we predict past landscape pattern scenario and the impact on habitat diversity? (2013).
26. *Christina Fotiou*: Evaluating habitat suitability and spectral heterogeneity models to predict weed species presence (2014).
27. *Inese Linuza*: Accuracy Assessment in Glacier Change Analysis (2014).
28. *Agnieszka Griffin*: Domestic energy consumption and social living standards: a GIS analysis within the Greater London Authority area (2014).
29. *Brynja Guðmundsdóttir*: Detection of potential arable land with remote sensing and GIS - A Case Study for Kjósarhreppur (2014).
30. *Oleksandr Nekrasov*: Processing of MODIS Vegetation Indices for analysis of agricultural droughts in the southern Ukraine between the years 2000-2012 (2014).
31. *Sarah Tressel*: Recommendations for a polar Earth science portal in the context of Arctic Spatial Data Infrastructure (2014).
32. *Caroline Gevaert*: Combining Hyperspectral UAV and Multispectral Formosat-2 Imagery for Precision Agriculture Applications (2014).
33. *Salem Jamal-Uddeen*: Using GeoTools to implement the multi-criteria evaluation analysis - weighted linear combination model (2014).
34. *Samanah Seyedi-Shandiz*: Schematic representation of geographical railway network at the Swedish Transport Administration (2014).
35. *Kazi Masel Ullah*: Urban Land-use planning using Geographical Information System and analytical hierarchy process: case study Dhaka City (2014).
36. *Alexia Chang-Wailing Spitteler*: Development of a web application based on MCDA and GIS for the decision support of river and floodplain rehabilitation projects (2014).
37. *Alessandro De Martino*: Geographic accessibility analysis and evaluation of potential changes to the public transportation system in the City of Milan (2014).

38. *Alireza Mollasalehi*: GIS Based Modelling for Fuel Reduction Using Controlled Burn in Australia. Case Study: Logan City, QLD (2015).
39. *Negin A. Sanati*: Chronic Kidney Disease Mortality in Costa Rica; Geographical Distribution, Spatial Analysis and Non-traditional Risk Factors (2015).
40. *Karen McIntyre*: Benthic mapping of the Bluefields Bay fish sanctuary, Jamaica (2015).
41. *Kees van Duijvendijk*: Feasibility of a low-cost weather sensor network for agricultural purposes: A preliminary assessment (2015).
42. *Sebastian Andersson Hylander*: Evaluation of cultural ecosystem services using GIS (2015).
43. *Deborah Bowyer*: Measuring Urban Growth, Urban Form and Accessibility as Indicators of Urban Sprawl in Hamilton, New Zealand (2015).
44. *Stefan Arvidsson*: Relationship between tree species composition and phenology extracted from satellite data in Swedish forests (2015).
45. *Damián Giménez Cruz*: GIS-based optimal localisation of beekeeping in rural Kenya (2016).
46. *Alejandra Narváez Vallejo*: Can the introduction of the topographic indices in LPJ-GUESS improve the spatial representation of environmental variables? (2016).
47. *Anna Lundgren*: Development of a method for mapping the highest coastline in Sweden using breaklines extracted from high resolution digital elevation models (2016).
48. *Oluwatomi Esther Adejoro*: Does location also matter? A spatial analysis of social achievements of young South Australians (2016).
49. *Hristo Dobrev Tomov*: Automated temporal NDVI analysis over the Middle East for the period 1982 - 2010 (2016).
50. *Vincent Muller*: Impact of Security Context on Mobile Clinic Activities A GIS Multi Criteria Evaluation based on an MSF Humanitarian Mission in Cameroon (2016).
51. *Gezahagn Negash Seboka*: Spatial Assessment of NDVI as an Indicator of Desertification in Ethiopia using Remote Sensing and GIS (2016).
52. *Holly Buhler*: Evaluation of Interfacility Medical Transport Journey Times in Southeastern British Columbia (2016).
53. *Lars Ole Grottenberg*: Assessing the ability to share spatial data between emergency management organisations in the High North (2016).
54. *Sean Grant*: The Right Tree in the Right Place: Using GIS to Maximize the Net Benefits from Urban Forests (2016).
55. *Irshad Jamal*: Multi-Criteria Analysis for School Site Selection in Gorno-Badakhshan Autonomous Oblast, Tajikistan (2016).
56. *Fulgencio Sanmartín*: Wisdom-volkano: A novel tool based on open GIS and time-series visualization to analyse and share volcanic data (2016).